

Field Survey Report: Marine Resources Offshore Ellwood California

Infauna

Epifauna

Seawater Properties

Seafloor Features

Sediment Chemistry

Sediment Grain Size

Marine Research Specialists
3140 Telegraph Road, Suite A
Ventura, CA 93003-3238

20 February 2008

Submitted to:

California State Lands Commission
County of Santa Barbara
City of Goleta

TABLE OF CONTENTS

1.0 BACKGROUND.....	1
1.1 GEOGRAPHIC EXTENT	3
1.1.1 Existing Pipeline Corridor.....	3
1.1.2 Ellwood Marine Terminal	3
1.1.3 Alternative Offshore Pipeline Corridor	5
1.1.4 Brant Debris Field	6
1.2 SCOPE OF SAMPLING	7
1.3 SUMMARY OF FINDINGS.....	11
1.4 ORGANIZATION OF THE REPORT.....	12
2.0 PHYSICAL OCEANOGRAPHY	13
2.1 DATABASE	13
2.2 FLOW FIELD.....	13
2.3 SEAWATER PROPERTIES.....	14
2.3.1 Euphotic Zone.....	15
2.3.2 Temporal Variability	17
2.3.3 Pipeline Corridor.....	17
2.3.4 Offshore EMT.....	21
2.3.5 Shane Seep Discharge	24
2.4 EQUIPMENT AND PERSONNEL, AND METHODS	26
2.4.1 Vessel	26
2.4.2 Personnel	26
2.4.3 Navigation	26
2.4.4 Ancillary Observations	27
2.4.5 CTD Instrumentation Package	27
2.4.6 Analysis of Seawater Properties.....	27
3.0 SEAFLOOR SEDIMENTS	29
3.1 SEDIMENT DATABASE	29
3.1.1 Samples Analyzed.....	29
3.1.2 Sample Collection	33
3.1.3 Chemistry Sample Processing	33
3.1.4 Infaunal Sample Processing	34
3.1.5 Moisture Content.....	35
3.1.6 Grain-Size Analysis	35
3.1.7 TPH Analysis	36

TABLE OF CONTENTS

(Continued)

3.2	PHYSICOCHEMICAL PROPERTIES.....	37
3.2.1	Physical Properties.....	37
	<i>Inherent Sampling Variability.....</i>	<i>38</i>
	<i>Grain-Size Characterization.....</i>	<i>40</i>
	<i>Cross-Shore and Seep Influences.....</i>	<i>43</i>
	<i>Along-Shore Trends.....</i>	<i>46</i>
	<i>Moisture Variability.....</i>	<i>46</i>
3.2.2	Chemical Properties.....	47
3.3	BENTHIC INFAUNAL BIOLOGY.....	49
3.3.1	Univariate Analyses.....	50
	<i>Organism Density.....</i>	<i>52</i>
	<i>Species Diversity.....</i>	<i>56</i>
	<i>Species Evenness.....</i>	<i>57</i>
	<i>Species Dominance.....</i>	<i>58</i>
	<i>Species Richness.....</i>	<i>58</i>
3.3.2	Multivariate Analyses.....	59
	<i>Inherent Sampling Variability.....</i>	<i>59</i>
	<i>Temporal Changes.....</i>	<i>64</i>
	<i>Environmental Factors.....</i>	<i>69</i>
	<i>Grain Size, Sorting, and Water Depth.....</i>	<i>70</i>
	<i>Hydrocarbons.....</i>	<i>71</i>
	<i>Influential Taxa.....</i>	<i>71</i>
4.0	SEAFLOOR FEATURES.....	74
4.1	INVENTORY.....	75
4.2	ANTHROPOGENIC DEBRIS.....	77
4.3	SEAFLOOR EQUIPMENT.....	77
4.4	NATURAL AND ARTIFICIAL REEFS.....	77
4.5	SEEPS.....	82
5.0	BIBLIOGRAPHY.....	83

LIST OF FIGURES

Figure 1. Geographic Setting of the Offshore Survey Region.....	1
Figure 2. Regional Map showing the Seafloor Survey Areas, Water Quality and Sediment Sampling Sites, and Other Features of Interest	2
Figure 3. Map of Three Principal Survey Areas	4
Figure 4. Photograph of Gas Boil at the Sea Surface above the Shane Seep	5
Figure 5. ROV Photograph of Ceramic Sink from the M/V Brant. Laser Scaling Benchmarks are separated by 15 cm.	6
Figure 6. ROV Photograph of the Steel Hull from the M/V Brant peeled back by an explosion.	7
Figure 7. ROV Photograph of <i>Metridium Giagantium</i> thriving on the M/V Brant Debris Field. A Population of Finfish and the Yellow ROV Umbilical can be seen in the background.....	8
Figure 8. Locations of the 14 Benthic Stations where Seafloor Sediment Samples were collected on 30 January 2007	10
Figure 9. Locations where the 48 Vertical Profiles of Seawater Properties were collected between 22 January and 31 January 2007	11
Figure 10. Surface Currents at 11:00 PST on 31 January 2007 during the Seawater Quality Leg of the Offshore Survey	14
Figure 11. Locations of Vertical Profiles of Seawater Properties near the Project Area	16
Figure 12. Comparison of Secchi Depth Measurements along the Pipeline Corridor and the EMT	17
Figure 13. Sound-Velocity Profiles Recorded during the Bathymetric Leg of the Offshore Survey.....	18
Figure 14. Cross-Shore Vertical Sections of Salinity, Temperature, and Density Collected on 31 January 2007 along the Platform Holly Pipeline Corridor	19
Figure 15. Cross-Shore Vertical Sections of Transmissivity, Dissolved Oxygen, and pH collected on 31 January 2007 along the Platform Holly Pipeline Corridor	20
Figure 16. Longitudinal Vertical Sections of Salinity, Temperature, and Density Collected on 31 January 2007 within the Offshore Portion of the EMT	22
Figure 17. Longitudinal Vertical Sections of Transmissivity, Dissolved Oxygen, and pH Collected on 31 January 2007 within the Offshore Portion of the EMT	23

LIST OF FIGURES

(Continued)

Figure 18. Vertical Profiles of Six Seawater Properties Measured within the Shane Seep (in Red) compared to Properties Measured at other Locations within the EMT (in Blue) on 31 January 2007	25
Figure 19. Locations of the Sediment Sampling Sites	30
Figure 20. Photograph of the Sediment Grab Sampler and Support Frame	33
Figure 21. Photograph of an Infaunal Sample on the 1-mm Sieve	34
Figure 22. Original Hydrocarbon Datasheet for the 14 Benthic Samples Collected on 31 January 2007	37
Figure 23. Cumulative Grain-Size Distribution of Duplicate Analyses a) with and b) without Coarse Fractions	39
Figure 24. Ternary Diagram of Grain-Size Properties with Coarse Fractions	41
Figure 25. Ternary Diagram of Grain-Size Properties without Coarse Fractions	43
Figure 26. Spatial Distribution of Sediment Sorting	44
Figure 27. Grain-Size Distributions Categorized by Water Depth	44
Figure 28. Cross-Shore Grain-Size Distributions along the Pipeline Corridor between Platform Holly and the EOF	45
Figure 29. Grain-Size Distributions along the Alternative Pipeline Corridor between Platform Holly and LFC	46
Figure 30. Relationship between Sediment Sample Moisture and Mud Fraction	46
Figure 31. Spatial Distribution of Sediment TPH Concentrations	48
Figure 32. Distribution of Infaunal Abundance	55
Figure 33. Sixteen-Year History of Mean Abundance in the GSD Benthic Samples (Aquatic Bioassay & Consulting Laboratories, Inc, 2007)	56
Figure 34. Scatter Plot of the Relationship between Shoreline Distance and a) Infaunal Diversity and b) Infaunal Dominance	57
Figure 35. Upper Portion of the Dendrogram showing the Similarity in Infaunal Communities among 99 Replicate Sediment Samples	61
Figure 36. Lower Portion of the Dendrogram showing the Similarity in Infaunal Communities among 99 Replicate Sediment Samples	62
Figure 37. Ordination of Benthic Infaunal Samples	65

LIST OF FIGURES

(Continued)

Figure 38. Dendrogram Displaying the Relationship Among Infaunal Communities in Sediment Samples Collected from the Same Site on Four Different Occasions.	68
Figure 39. Joint Plot of the Ordination of MRS Samples and its Relationship to Environmental Properties.....	69
Figure 40. Joint Plot of the Ordination of MRS Samples and the Taxa that Differentiate the Three Major Groups.....	72
Figure 41. Location of Seafloor Slides Offshore of the Study Region [Adapted from Green et al (2006)].....	75
Figure 42. Locations of the Bathymetric Tracklines	76
Figure 43. Swath Bathymetric Images of a) the Locations of Seafloor Features within the EMT Mooring Area, and b) the Acoustic Signature of the Shane Seep.....	78
Figure 44. Multibeam Image of Offshore Rocky Reef Structure along the Alternative Pipeline Corridor	79
Figure 45. Pier Debris Adjacent to the Pipeline Landing near the EOF.....	80
Figure 46. Kelp Stands Associated with Pier Debris Adjacent to the Pipeline Landing near the EOF	81
Figure 47. Map of the Seep Field near Coal Oil Point.....	82

LIST OF TABLES

Table 1.	Ancillary Measurements collected during the Water-Quality Leg on 31 January.....	15
Table 2.	Instrumental Specifications for CTD Profiler	28
Table 3.	Inventory of Sediment Samples Collected in the Study Region	31
Table 4.	Percent of Total Weight for each Grain-Size Fraction within Subsamples collected from Seafloor Sediments on 31 January 2007 as part of the Ellwood Marine Survey	38
Table 5.	Weights used in the Grain-Size Analyses, Percent Summary for Major Size Classifications, and Moisture Content for All Sediment Subsamples	40
Table 6.	Grain-Size Distributional Parameters.....	41
Table 7.	Narrative Classification of Grain-Size Distributions sorted by Water Depth	42
Table 8.	Sediment Hydrocarbon Concentrations and Related Sediment Properties Offshore Ellwood and Goleta.....	47
Table 9.	Average Infaunal Community Indices	53
Table 10.	Five most Indicative Taxa of the Three Major Benthic Surveys	66

1.0 BACKGROUND

This document summarizes data collected during a marine survey conducted offshore southern California (Figure 1) between 21 January and 3 February 2007 by Marine Research Specialists (MRS). The survey provided site-specific baseline information on marine resources in four offshore subareas that could be potentially impacted by the proposed Project to expand oil development from Platform Holly off the coast of Ellwood California, and to install a new pipeline from Platform Holly to Las Flores Canyon (Figure 2).





Figure 2. Regional Map showing the Seafloor Survey Areas, Water Quality and Sediment Sampling Sites, and Other Features of Interest

1.1 GEOGRAPHIC EXTENT

Most of the marine-resource survey was encompassed within a 14 km² region that was the focus of high-resolution swath bathymetric soundings. The four main subareas within the survey region included:

- 1) The existing cross-shore pipeline corridor from Platform Holly,
- 2) The Ellwood barge-loading marine terminal (EMT),
- 3) An alternative offshore pipeline corridor to Las Flores Canyon (LFC), and
- 4) The debris field associated with the M/V Brant shipwreck.

Some sampling components of the marine-resource survey extended beyond the boundaries of the four principal bathymetric survey's subareas (Figure 2). These included sound-velocity profiles, water-quality profiles, and benthic (seafloor) sediment box-core samples.

1.1.1 Existing Pipeline Corridor

As shown in Figure 3, the primary survey area extended shoreward from Platform Holly along the pipeline corridor to the Ellwood Onshore Facility (EOF). As part of the proposed Project, a new power cable would be installed within this corridor, additionally; a cross-shore section of the existing utility line would be replaced. An existing oil-water emulsion pipeline and a gas pipeline currently transport hydrocarbons produced on Platform Holly to the EOF. Increased production on Platform Holly resulting from the proposed Project would increase the emulsion pipeline's throughput, thereby increasing the potential size of a spill due to an accidental breach of the pipeline. In addition to the existing pipeline infrastructure associated with Platform Holly, gas collected in tents overlying a natural hydrocarbon seep to the east of the platform is currently transported along another pipeline to the EOF within the corridor (refer to Figure 3).

Because of potential impacts to the marine environment from constructions activities associated with the seafloor-cable installation and pipeline repair, or from an accidental oil spill along the pipeline corridor, several data collection activities were conducted within the existing pipeline corridor. These included cross-shore transects of water-quality measurements and benthic sediment sampling. Seafloor features of potential cultural, biological, or geotechnical (hazard) interest were identified from the high-resolution swath bathymetry data collected within the corridor. A remotely operated vehicle (ROV) was used to photodocument seafloor features of particular interest. Similarly, the distribution of sensitive kelp habitat shown in Figure 3 was delineated using aerial photographs. The seafloor survey of the existing pipeline corridor covered an area of 7.4 km², or more than half of the entire seafloor survey area. The same data collection techniques were used for the other three subareas.

1.1.2 Ellwood Marine Terminal

As shown in Figure 3, a smaller area surrounding the offshore portion of the EMT, where barge loading takes place, was also surveyed. The swath bathymetric survey encompassed an area of 0.8 km², which is approximately 6 percent of the overall seafloor survey area. The barge-loading area contains an irregular six-point mooring system, a pipeline, and sub-sea hoses. The proposed Project would remove the moorings and sub-sea hoses, while the pipeline would be abandoned in

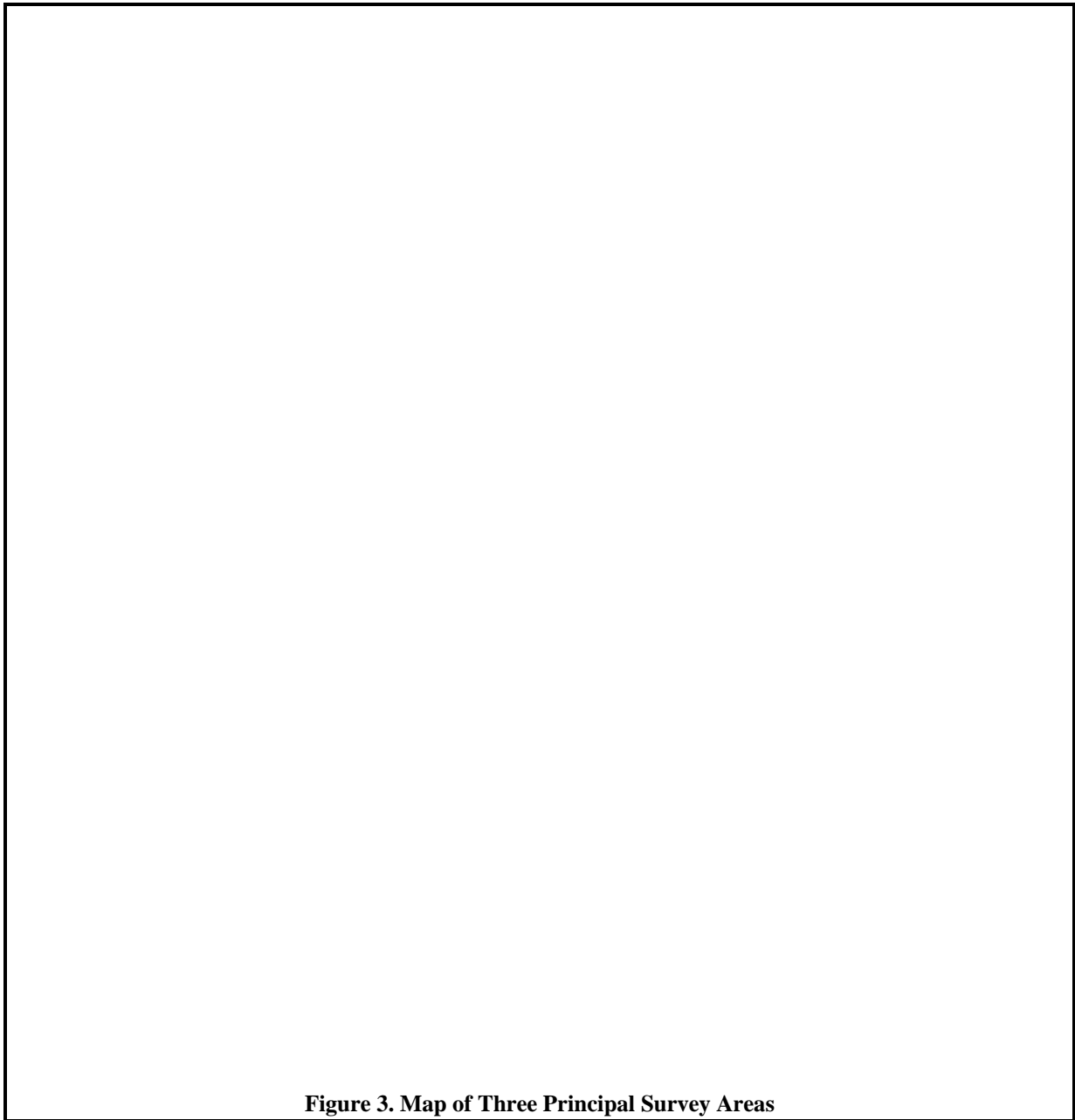


Figure 3. Map of Three Principal Survey Areas

place. Abandonment activities associated with the EMT could potentially impact sensitive marine habitat consisting of hard substrate and kelp that lie adjacent to the loading area.

Additionally, an active and well-studied seep, known as the Shane Seep, is located within the offshore EMT mooring area, where it influences seawater properties in a variety of ways (Figure 4). The Shane Seep modifies water quality by saturating the water contained within the bubble plume with methane (Leifer, Clark, & Chen, Modifications of the local environment by a natural marine hydrocarbon seep, 2000). The transfer of gas to the atmosphere from seeps is potentially a significant source of atmospheric methane, one of the most important greenhouse gases. Methane is at least twenty times more effective in radiant heating than carbon dioxide. The seafloor expression of Shane Seep is distributed over an area of approximately 100 m² and

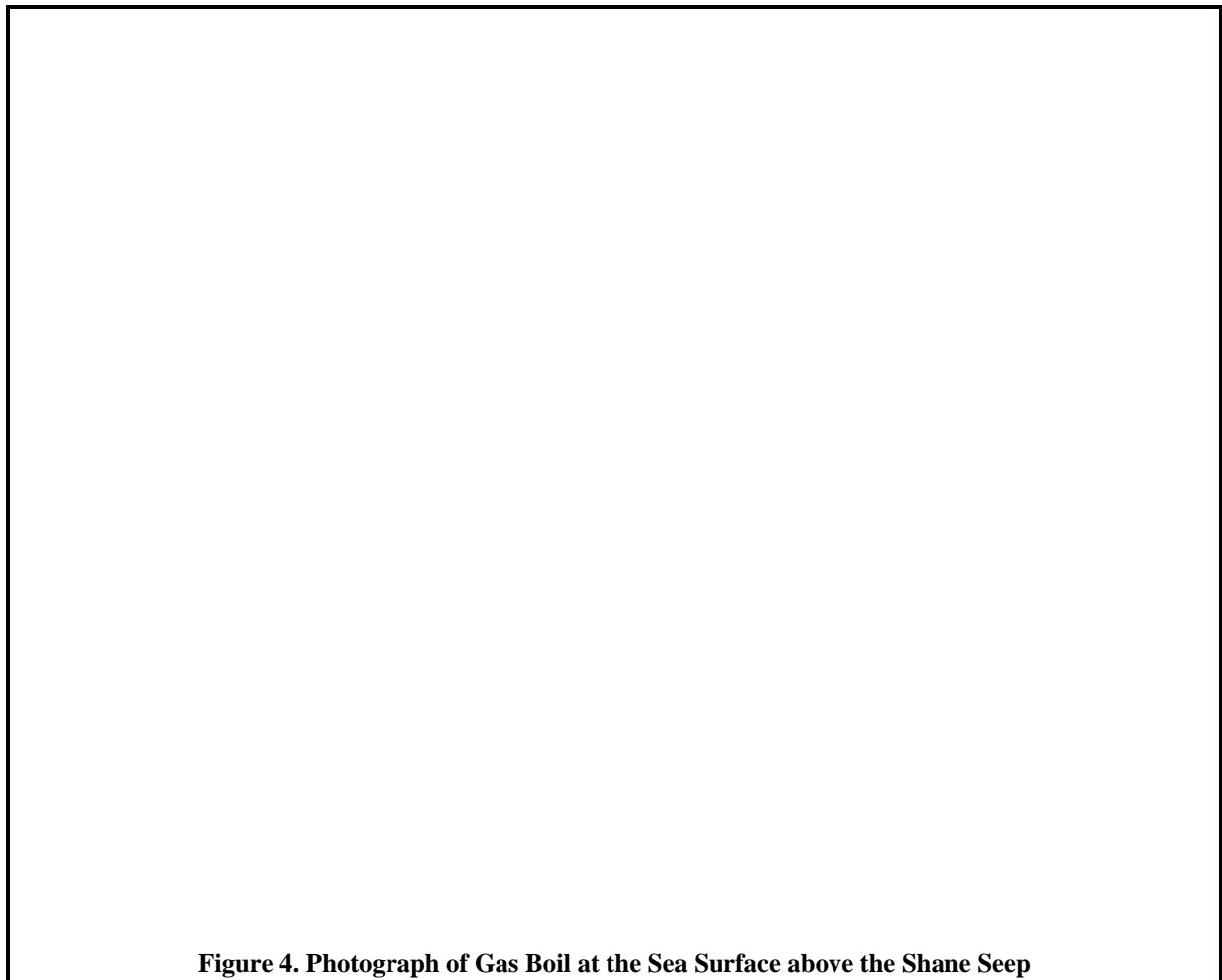


Figure 4. Photograph of Gas Boil at the Sea Surface above the Shane Seep

consists of numerous small vents surrounding two larger tar and mud volcanoes. Each volcano has a diameter of approximately 3 m, rising 1 m above the seafloor.

1.1.3 Alternative Offshore Pipeline Corridor

The proposed Project is for transport of oil along an onshore pipeline to the Los Flores Canyon (LFC) facility. A potential viable alternative to the onshore pipeline is an offshore oil pipeline from Platform Holly to the LFC facility. One representative offshore route was also surveyed for seawater properties and seafloor features to determine whether there could be environmental constraints that would preclude consideration of the offshore pipeline alternative. As shown in Figure 2, the alternative oil pipeline would transport oil offshore from Platform Holly, for approximately 16 km, in a northwestward direction, directly to the LFC. This alternative would replace the proposed onshore pipeline from the EOF to the LFC and would transport hydrocarbons produced on Platform Holly directly to the LFC for processing. The seafloor survey area associated with the alternative pipeline corridor encompassed 5.2 km², or approximately 38 percent of the total survey area.

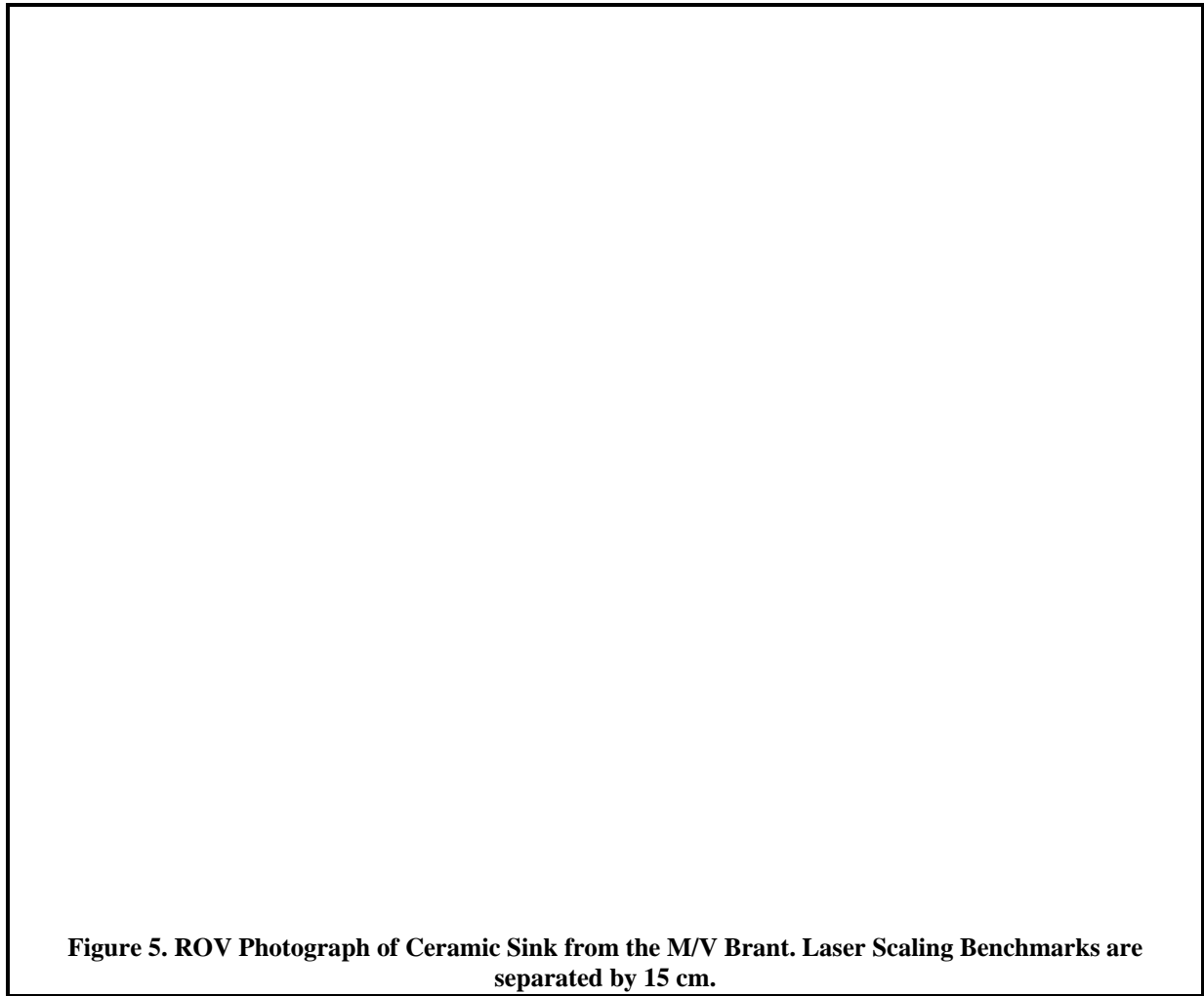


Figure 5. ROV Photograph of Ceramic Sink from the M/V Brant. Laser Scaling Benchmarks are separated by 15 cm.

1.1.4 Brant Debris Field

The marine-resource survey included a small area (0.28 km²), approximately 1.1 km to the east of the shoreline crossing of the alternative pipeline corridor, where a search was conducted for the wreck of the M/V Brant (Figure 2). The seafloor debris field associated with the wreck was the only well-documented shipwreck within the survey area, thereby warranting an evaluation of its potential cultural significance. The ROV dive on 3 February 2007 collected photographs and video that confirmed the seafloor debris was of modern origin, and probably from the M/V Brant, rather than from some more ancient shipwreck (Figure 5 and **Figure 6**). Cultural significance notwithstanding, the M/V *Brant* debris field provides a high-quality artificial reef habitat populated by a well-established, diverse hard-substrate community that is sensitive to mechanical disturbance and increased turbidity (Figure 7).

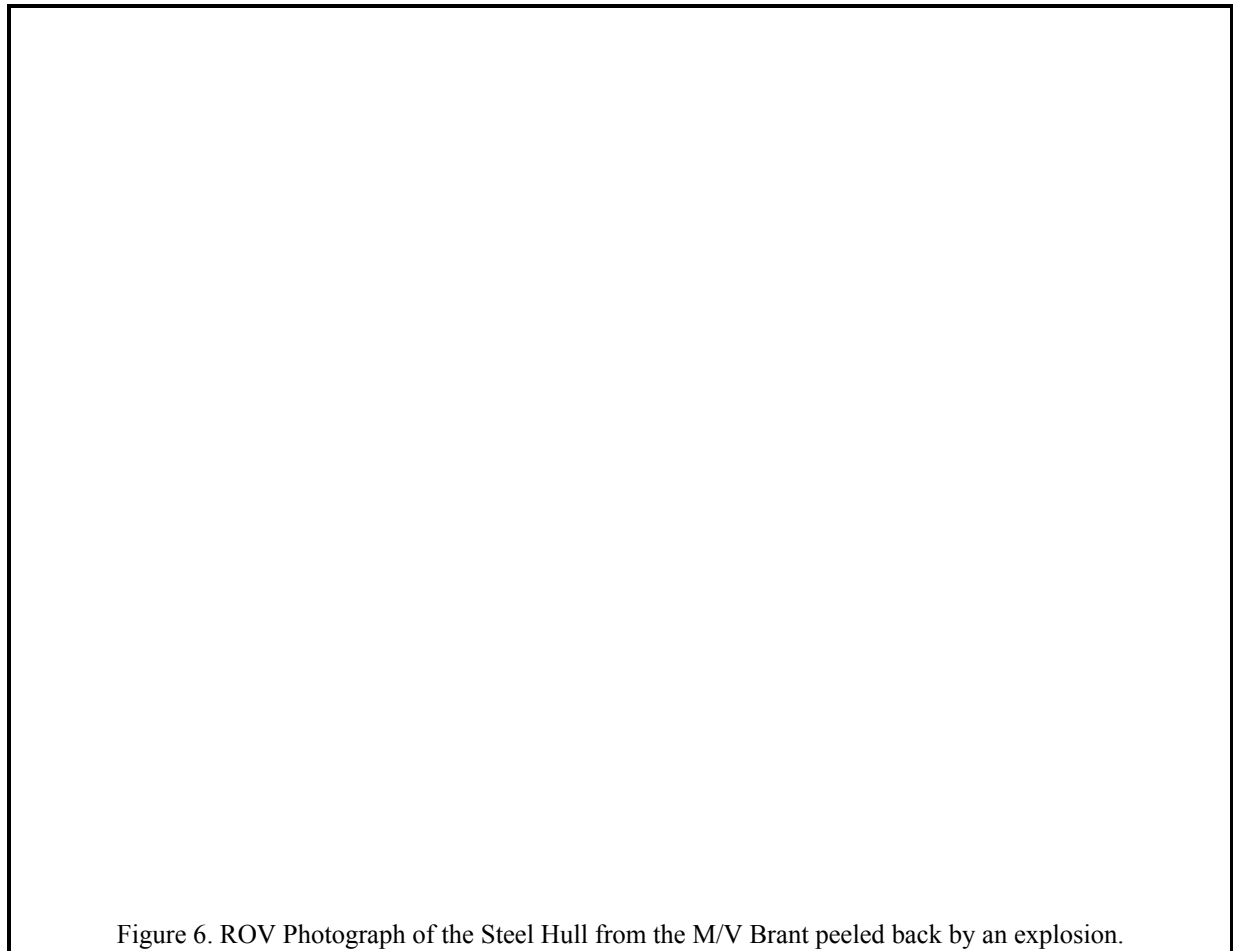


Figure 6. ROV Photograph of the Steel Hull from the M/V Brant peeled back by an explosion.

1.2 SCOPE OF SAMPLING

A wide variety of site-specific data were collected during the marine-resource survey. These data provide a comprehensive and definitive examination of marine resources in the vicinity of the existing pipeline corridor, along the alternative pipeline corridor, and at the EMT.

- The biological and cultural significance of seafloor features were investigated using high-resolution swath bathymetry, a magnetometer, a fathometer, and an ROV.¹
- Seafloor sediments were collected using a grab sampler and were analyzed for grain-size, infauna, and chemical constituents.
- In situ seawater properties were determined using a CTD instrument package.²

¹ See Appendix C for a description of the sampling equipment.

² Conductivity, Temperature, and Depth (CTD) are the basic measurements collected by this standard oceanographic instrument package, but the system used in this survey also included dissolved oxygen, transmissivity, and pH probes.

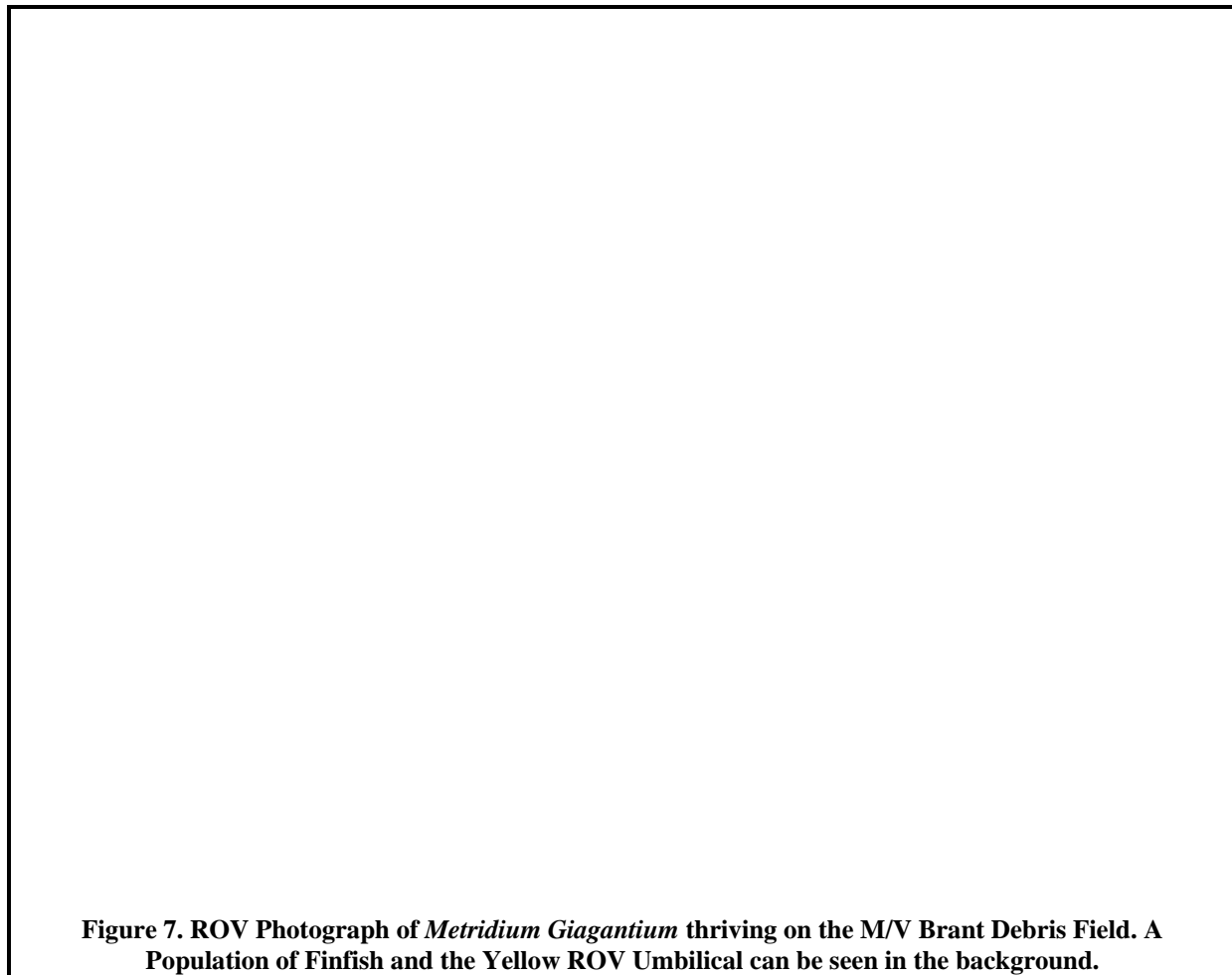


Figure 7. ROV Photograph of *Metridium Gigantium* thriving on the M/V Brant Debris Field. A Population of Finfish and the Yellow ROV Umbilical can be seen in the background.

- The oceanic flow field was determined from available real-time surface current maps provided by the Southern California Coastal Ocean Observing System (SCCOOS) for the Santa Barbara Channel.

The offshore survey spanned 21 days. Benthic sampling equipment was mobilized onboard the 38-ft F/V *Bonnie Marietta* on 16 and 17 January 2007 in Morro Bay, California, which is the survey vessel's home port. On 18 and 19 January, the vessel transited to Ventura Harbor. On 20 January, the CTD, magnetometer, and ROV were mobilized from the local MRS office. The ROV's associated equipment was configured and tested, including the topside control station, high-resolution still and video feeds, navigation, and the digital multi-frequency imaging sonar. On 21 January, the survey vessel transited to Santa Barbara Harbor and the multibeam transducer head was mounted on the port side of the vessel. Sea trials for the multibeam sonar system were conducted offshore Santa Barbara on Monday, 22 January, and included calibration of the position and orientation system, a ping test at the dock, and a patch test for reconciling bathymetric readings collected along various headings.

Bathymetric surveying was conducted continuously for four consecutive days from 23 January through 26 January 2007. The purpose of the bathymetric survey was to map the seafloor habitat within the four subareas of interest, and to identify features of potential biological, cultural, or geohazard significance. The high-resolution bathymetry data was collected primarily to support the environmental assessment for the proposed Project and an offshore pipeline alternative, rather than for site-clearance purposes as a precursor to abandonment of the offshore portion of the EMT. Nevertheless, the high-resolution bathymetric data gathered during this offshore environmental assessment, along with the interpretation of seafloor features based on ROV dives, can be used to guide and focus a future site-clearance survey.

Nearly all of the seafloor within the 14 km² survey area was covered by high-resolution bathymetric data. Trackline separations within most of the surveyed area provided 100 percent overlap of data collected on adjacent tracklines. Only some small nearshore areas within the northern portion of the existing pipeline corridor could not be surveyed due to heavy kelp forestation (Figure 3 on Page 4). In total, the 167 tracklines captured reliable bathymetric data along 211km of linear tracklines that were run during the 22 hours of bathymetric surveying that was conducted at an average vessel speed of 2.6 m/s. From this bathymetric dataset, 592 seafloor features were identified within the survey area.

In contrast to the favorable weather conditions experienced during the bathymetric leg of the survey, weather became a significant limiting factor for the benthic, water quality, and ROV legs of the survey. Not only did unsettled sea states result in four onshore standby days, but low visibility and high current velocities limited ROV operations on other days. Originally, the survey had been scheduled to occur in September 2006 when weather and sea state conditions were more likely to favor offshore sampling. However, delays unrelated to the offshore mobilization, prevented the survey from occurring until the winter months of early 2007.

After the bathymetric equipment was demobilized on January 26th, a passing winter storm prevented offshore sampling on three consecutive days from January 27th through the 29th. Despite unsettled wind and wave conditions in the wake of this rainstorm, benthic sediment samples were collected at 14 stations on 30 January (Figure 8). The primary benthic sampling occurred along the existing pipeline corridor, which provided a cross-shore transect consisting of seven stations extending from the shoreline crossing (Station MRS11) to Platform Holly (MRS06). The Platform Holly Station (MRS06) also provided the anchor point for the five along-shore benthic stations that assessed variation along the alternative pipeline corridor (Stations MRS02 through MRS06). Three other stations (MRS01, MRS17, and MRS18) were located near and within the offshore EMT. Sediment subsamples from all of these stations were analyzed in the MRS laboratory for infaunal taxonomy, physical properties, and hydrocarbon concentration. As described in Section 3.0 on Page 29, the interpretation of these data were augmented with an analysis of data from 85 other benthic samples collected in the area over the last three decades.

Water-quality measurements were collected on the morning of 31 January 2008, just prior to the passage through the Santa Barbara Channel of another severe winter storm that occurred later that afternoon. A severe winter storm warning, small craft advisory, and special marine warning for waterspouts was issued during the rough 1.5-hour transit from the survey area back to Santa Barbara Harbor. Despite sustained high winds during the morning, 31 vertical profiles of


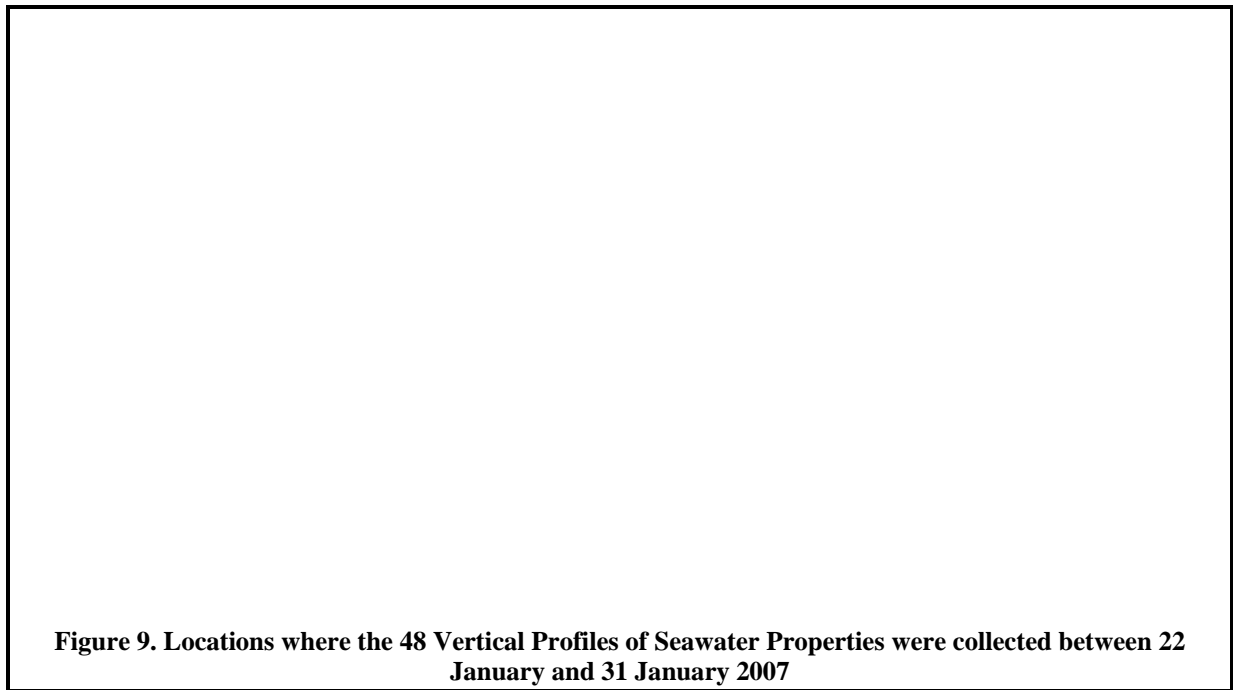


Figure 8. Locations of the 14 Benthic Stations where Seafloor Sediment Samples were collected on 30 January 2007

seawater properties were measured (Figure 9 on Page 11). Ten of these profiles were located along the pipeline corridor as shown by the ■ symbols. These were used to produce cross-shore vertical sections of seawater properties. Also on 31 January 2007, a longitudinal transect of 18 closely spaced water-quality profiles was measured within the offshore EMT (◆ symbols). Three additional vertical profiles of water-quality data were also collected directly over a seep discharge in the southern portion of the EMT region. This active seep, known as Shane Seep, is particularly well studied. The remaining 18 profiles of seawater properties were measured at a wide range of locations throughout the five-day swath bathymetry leg survey to establish sound velocity profiles (✕ symbols). Sound velocity profiles were used to correct the acoustic ray paths of the sonar pings.

The ROV leg of the survey was conducted on February 2nd and 3rd, after a standby day due to poor offshore weather conditions, particularly water clarity. Preliminary processing of bathymetric data was conducted during the four weather standby days, during the three-hour transit to and from the survey area on field days, and during the evening after the vessel was secured. Based on the results of this preliminary processing, 16 seafloor features of potential interest were selected from the 592 features that were eventually identified during final processing. Preference was given to features near the existing pipeline corridor and that were near the shoreline where most of the proposed Project's construction activities were anticipated to occur. During the ROV leg, most of these seafloor features of interest were scanned with a single-beam echosounder to precisely locate the feature and assess its hardness from the amplitude of the return signal. For some features, whose character and origin was still in question, namely, they were not readily identifiable crab pots, the ROV was deployed for exploratory video and photographic documentation.



Upon returning to Santa Barbara Harbor in the late evening of February 3rd, most of the equipment was demobilized. With an impending further decline in weather conditions, the survey vessel immediately left for her home port, arriving in Morro Bay Harbor on the morning of February 4th, at which point, the remaining equipment was demobilized and the three-week offshore survey was concluded.

1.3 SUMMARY OF FINDINGS

The marine-resource field survey provided a wide array of site-specific baseline information on the marine environment surrounding the offshore portion of the proposed Project, and along a possible alternative offshore pipeline corridor to LFC. Together, this wide array of data accurately characterized the marine resources present in the region at the time of the survey. Consequently, the findings presented in this report are based largely on a synthesis of data collected during this survey alone, which may not be representative of future conditions. Exceptions to the temporal focus of this report's results are the analysis of benthic sediments and seafloor features. The benthic sediments analysis incorporated data collected during other surveys conducted in the region (Chambers Group, 1987; Aquatic Bioassay & Consulting Laboratories, Inc., 2006). Additionally, seafloor features are not expected to change significantly over time. In contrast, while the seawater properties measured in the January 2007 survey were site-specific, they spanned a limited time and thus, provide only a synoptic snapshot of some of the physical processes that prevail in the region. However, many recent comprehensive descriptions of the distribution of seawater properties and the mechanisms that drive those distributions are available for the region (Auad & Hendershott, 1997; Auad, Hendershott, & Winant, 1999; Beckenbach, 2004; Breaker, 2003; Dever & Winant, 2002; Dever, Hendershott, & Winant, 1998; Dever, Johnson, Wang, Winant, & Oey, 2004) (Dorman & Winant, 2000; Harms

& Winant, 1998; Hendershott & Winant, 1996; Oey, Wang, Hayward, Winant, & Hendershott, 2001; Cudaback, Washburn, & Dever, 2005).

The marine-resource survey revealed an offshore environment containing only a few, highly localized sensitive marine resources that could potentially be affected by the proposed Project, or by the alternative installation of an offshore pipeline to LFC. Some of the more biologically sensitive offshore areas that could be affected by the proposed Project are the extensive series of artificial and natural reefs that reside in shallow water where the pipelines currently cross the shoreline near the EOF. These low-relief hard-substrate features support a thriving kelp habitat.

The rest of the seafloor in the study area consists largely of a sparsely populated sand seafloor containing a relatively uniform infaunal community typical of soft-substrate subtidal environments throughout the southern California region. This soft-substrate seafloor habitat is occasionally punctuated by isolated hard-substrate features with marine communities of increased diversity. Most of these hard-substrate features are associated with anthropogenic (“human-derived”) debris that was discarded on the seafloor. Except for the M/V *Brant*, these targets do not appear to be of cultural significance.

For the most part, the offshore portions of the EMT and the pipeline corridors, including the alternative pipeline route to LFC, are free of sensitive habitats and objects of potential cultural significance. However, where the existing pipeline route approaches the shoreline, low-relief hard-substrate habitats become more prevalent. In some areas shoreward of the 20 m isobath, the substrate supports a kelp forest habitat that has historically been considered a sensitive marine habitat. Because of this, and particularly if extensive turbidity is generated by the installation of utility and power lines, the use of horizontal directional drilling (HDD) could mitigate impacts to the kelp beds and associated marine organisms.

The influence of naturally occurring hydrocarbon seeps in the study area is important for the evaluation of potential environmental impacts from the proposed Project and its alternatives. Most regulatory standards used to evaluate the significance of potential impacts are cast in terms of excursions beyond the inherent natural variability in the ocean environment of the region. In most nearshore areas of the California coast, the ambient variability is relatively limited, and largely dictated by seasonal variations rather than spatial differences. This is not the case for the Ellwood study area because naturally occurring hydrocarbon seeps are distributed throughout the region, and strongly influence oceanic conditions within localized areas, as well as throughout the region. As a result, the seeps introduce significant natural variability and mask anthropogenic impacts that would normally be evident against the backdrop of ambient seasonal variability.

1.4 ORGANIZATION OF THE REPORT

Each of the remaining major sections of this report describes a separate type of marine data.

- Section 2 (Physical Oceanography) describes the physical measurements of seawater properties.
- Section 3 (Seafloor Sediments) presents data on the chemical and physical (grain size) properties of benthic sediments and the infauna that reside within them.
- Section 4 (Seafloor Features) describes hard-substrate habitats that were found in the survey area. These features were initially surveyed by a fathometer or magnetometer. If

warranted, they were photo-documented with still and video images collected by ROV. Seafloor features can be of potential cultural, biological, or geotechnical significance.

2.0 PHYSICAL OCEANOGRAPHY

Accurate determination of the physicochemical properties of seawater is important for the assessment of potential impacts from the proposed Project and its alternatives for at least two reasons. First, the vertical structure, or stratification, of the water column dictates the disposition of discharges from the seafloor, such as might occur during an accidental breach of a seafloor crude-oil pipeline. The second reason ambient seawater properties are important is that they can be used to assess the relative importance of potential impacts from the removal of offshore equipment and pipelines associated with the EMT decommissioning, construction activities near the shoreline along the existing pipeline corridor, and installation of an offshore pipeline to LFC associated with the proposed Project. These construction impacts are likely to arise primarily from increased turbidity caused by the re-suspension of ambient sediments. For point-source discharges, the California Ocean Plan (COP) assesses the severity of most impacts by comparing their amplitude with the inherent variability in background seawater properties (State Water Resources Control Board, 2006). Data collected on ambient seawater properties as part of this marine-resource survey, and as part of other surveys, lends insight into the degree of natural variability and stratification that exists in the study area. This information can be used to gauge the significance of Project-related changes to seawater quality.

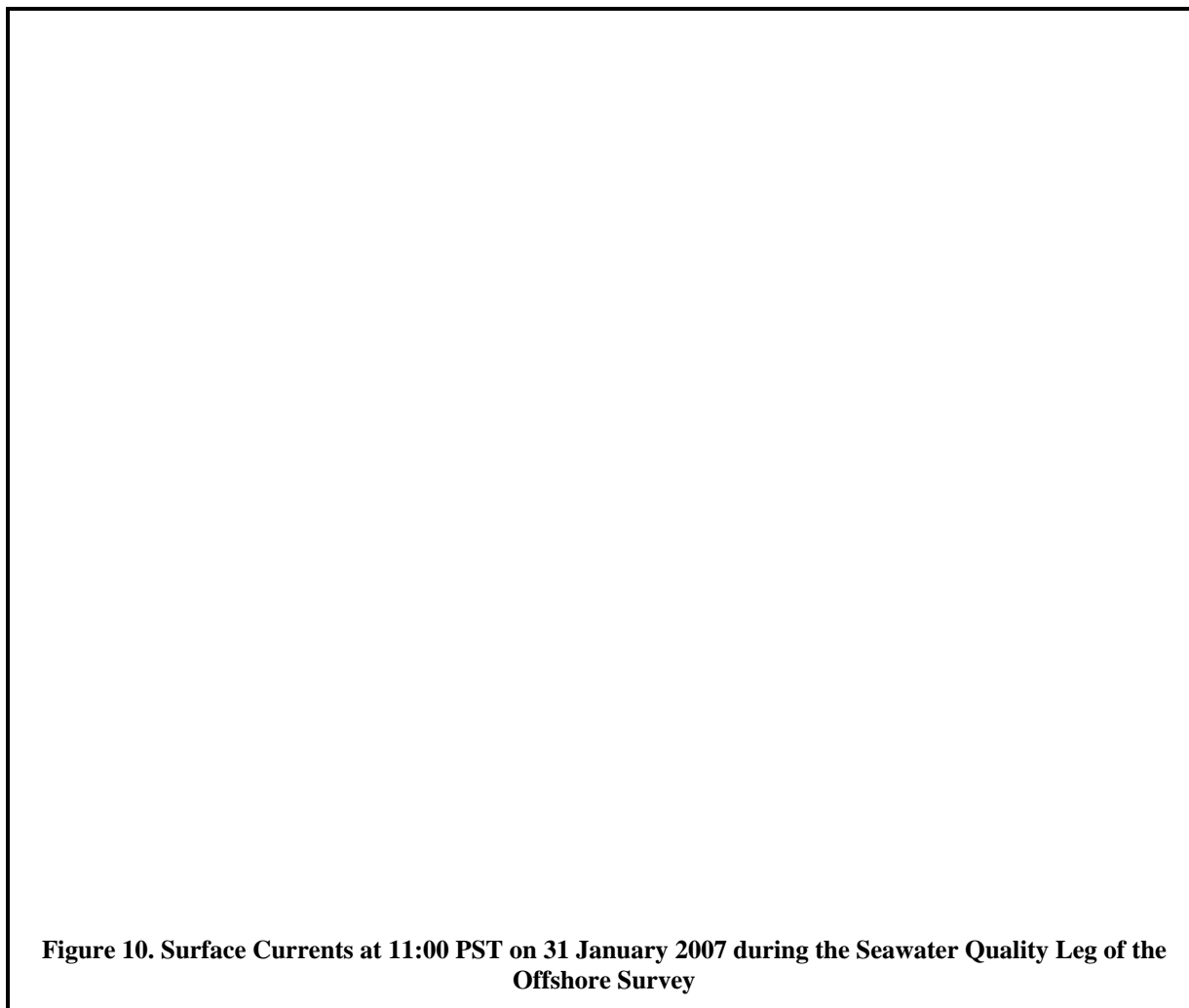
2.1 DATABASE

Physical and chemical properties of seawater within the survey area were characterized on 31 January 2007 by *in situ* measurements collected along three transects. These were comprised of one cross-shore section within the existing pipeline corridor between Platform Holly and the EOF, and two along-shore transects within a possible alternative pipeline route to LFC, and within the EMT mooring area (Figure 9 on Page 11). In addition, sound velocity profiles were collected throughout the bathymetric survey at locations where the depth soundings were being collected. Although the sound-velocity profiles were collected largely to correct acoustic ray paths measured during the bathymetric leg of the survey, they also lend valuable information about the degree of water-column stratification in the area, and how it changes over time.

In total, 33,513 water-quality measurements were recorded during the survey. Of these, 14,017 high-resolution measurements were the most useful because they were recorded during CTD downcasts. These data were averaged into 0.5-m vertical bins to yield a total of 2,842 observations, in 48 vertical profiles, collected on six separate days.

2.2 FLOW FIELD

The oceanographic flow conditions at the time of the seawater-property survey were atypical, and probably affected the resulting property distributions. As described earlier, the water-quality leg of the offshore survey was squeezed within a very brief weather window; after an extended winter rainstorm, and shortly before a severe weather event that impinged on the Santa Barbara Channel. The turbulent wind conditions caused an unsettled sea state and imposed significant



complexity to the surface flow as shown in the average radar-derived flow pattern that was recorded near the conclusion of the survey (Figure 10).

Strong westerly winds³ prevailed during the early portions of the seawater quality leg of the survey, and a severe weather advisory was issued for marine waters near the end of this leg. As a result, the surface flow pattern exhibited a number of localized eddies and flow convergences. In response to strong local winds, the surface current flow was toward the east within the survey area, as opposed to the westward flow that normally occurs within this section of the coastline along the northern portion of the Santa Barbara Channel.

2.3 SEAWATER PROPERTIES

A variety of qualitative and semi-quantitative observations of water quality and weather conditions were recorded in addition to the precision instrumental measurements provided by the CTD package. These included air temperature, Secchi depth, cloud cover, and wind speed and

³ Westerly winds are from the west and directed toward the east.

direction. Observations of beneficial use in the survey region, such as the presence of recreational fishing vessels and workboat traffic, were also noted.

Table 1. Ancillary Measurements collected during the Water-Quality Leg on 31 January

Location			Shoreline	Sample	Air	Cloud	Wind			Secchi
			Distance	Time	Temp	Cover	Avg	Max	From	Depth
Station	Latitude	Longitude	(km)	(PST)	(°C)	(%)	(kt)	(kt)	(°T)	(m)
W20	34° 24.476' N	119° 53.607' W	1.03	08:52:50	13.0	30	11.5	17.5	270	7.0
W25	34° 24.464' N	119° 53.422' W	0.69	09:04:21	13.4	25	11.9	17.8	270	7.0
W27	34° 24.454' N	119° 53.356' W	0.63	09:08:32	13.0	20	13.2	17.8	270	—
W30	34° 24.450' N	119° 53.257' W	0.58	09:14:40	12.9	20	14.5	18.2	270	7.0
W34	34° 24.426' N	119° 53.140' W	0.39	09:21:30	13.0	15	13.0	16.1	270	7.0
W35	34° 24.420' N	119° 53.115' W	0.38	09:23:01	13.0	10	14.3	16.5	270	—
W38	34° 24.365' N	119° 53.429' W	0.86	09:41:09	13.4	10	10.4	14.1	270	7.0
W39	34° 25.491' N	119° 54.901' W	0.48	10:25:23	13.3	5	12.1	13.7	270	4.0
W40	34° 25.402' N	119° 55.010' W	0.70	10:32:15	13.4	5	10.4	13.5	270	4.7
W41	34° 25.303' N	119° 55.142' W	0.98	10:39:23	13.5	5	9.6	12.2	270	6.0
W42	34° 25.135' N	119° 55.186' W	1.25	10:45:52	13.4	2	10.9	13.4	270	6.5
W43	34° 24.938' N	119° 55.138' W	1.47	10:53:11	13.2	2	17.3	19.9	260	6.5
W44	34° 24.686' N	119° 55.116' W	1.81	11:01:36	13.2	2	14.6	17.8	260	7.0
W45	34° 24.402' N	119° 55.074' W	2.21	11:11:04	13.3	0	15.7	19.5	260	9.0
W46	34° 24.101' N	119° 54.981' W	2.62	11:20:58	13.4	0	15.2	18.6	260	11.0
W47	34° 23.823' N	119° 54.878' W	3.01	11:47:22	13.7	50	13.1	15.0	270	12.0
W48	34° 23.391' N	119° 54.624' W	3.35	12:01:10	13.5	100	12.8	15.9	260	12.0

Table 1 lists the quantitative results for those stations where ancillary measurements were recorded during the water-quality leg of the survey on 31 January. The locations of these stations, and the other stations where only CTD hydrocasts were recorded, are shown in Figure 11.

2.3.1 Euphotic Zone

Secchi depths were measured with a Secchi disk that was lowered through the water column to determine its depth of disappearance. The depth of disappearance is inversely proportional to the average amount of organic and inorganic suspended material along a line of sight immediately below the sea surface. Because Secchi depth measurements provide a visual measure of the penetration of ambient light in the upper water column, they directly address the turbidity objective in the COP, which states that “*Natural light shall not be significantly reduced at any point outside the initial dilution zone as the result of the discharge of waste.*” Although this objective strictly applies to point-source discharges, it implies that turbidity increases are less of concern if they occur below the euphotic zone, where the penetration of ambient light is negligible.

Secchi depth measurements provide a visual measure of the penetration of ambient light in the upper water column. As such, they define the approximate depth of the euphotic zone, where ambient light is sufficient for photosynthesis. The cross-shore installation of the power cable and installation of the water line associated with the proposed Project, and the decommissioning and removal of offshore EMT components could cause temporary increases in water column

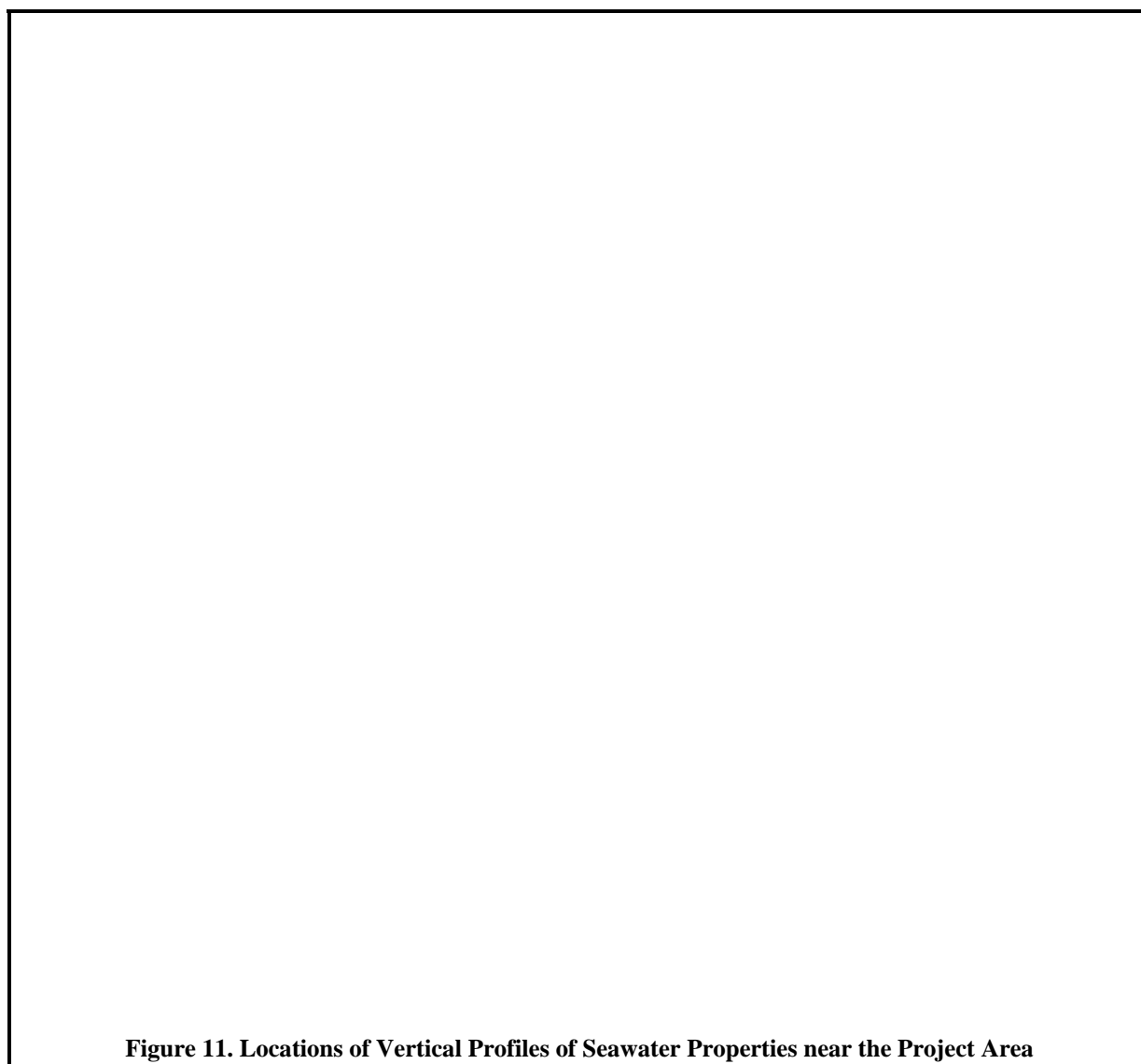


Figure 11. Locations of Vertical Profiles of Seawater Properties near the Project Area

turbidity. To some degree, the significance of these impacts will depend on the depth of the euphotic zone relative to overall water depth at the time of the installation or removal. The lower limit of the euphotic zone can be inferred from the Secchi disk measurements, which mark the depth of the mid-point of the euphotic zone.

Several conclusions concerning the offshore environment during the water-quality leg of the survey can be discerned from the table and map. As discussed below, these inferences are supported by the high-resolution CTD measurements. For example, within 1 km of the shoreline, the EMT had higher water clarity than the nearshore portions of the pipeline corridor. This is apparent from the uniformly higher Secchi depths observed at Stations W20 through W38, which all reached 7 m at those locations where measurements were recorded (Table 1). All five of these measurements were recorded within the EMT area (Figure 11). In contrast, Secchi depths within the nearshore portion of the existing pipeline corridor ranged from 4 m to 6 m within 1 km of the shoreline. Thus, because the euphotic zone reaches to twice the water depth, and water depths

were less than 20 m close to shore, the euphotic zone reached nearly to the seafloor within the EMT, while natural light penetration was restricted to the upper water column with the pipeline corridor out to a distance of 1.8 km (Station W44 in 40 m of water depth). Increased turbidity within the pipeline corridor probably arose because the veneer of nearshore sediments was thicker and more widespread than in the EMT area.

Also of note, the 7 m Secchi depth measured within the gas-bubble plume associated with the Shane Seep (Station W38) was consistent with the other measurements within the EMT, indicating that the seep discharge has little influence on ambient water clarity.

Finally, the Secchi depths consistently increased with increasing distance offshore along the existing pipeline corridor (Figure 12). Close to shore, Secchi depths were only 4 m, while ambient light penetration near Platform Holly increased to 12 m, as measured by the Secchi disk. This trend reflects the increased turbidity associated with the resuspension of surficial sediments in the nearshore region. Oscillatory motions associated with shoaling gravity waves preferentially resuspend surficial sediments in the nearshore region as compared to deeper waters where surface gravity waves do not impact the benthic boundary layer.

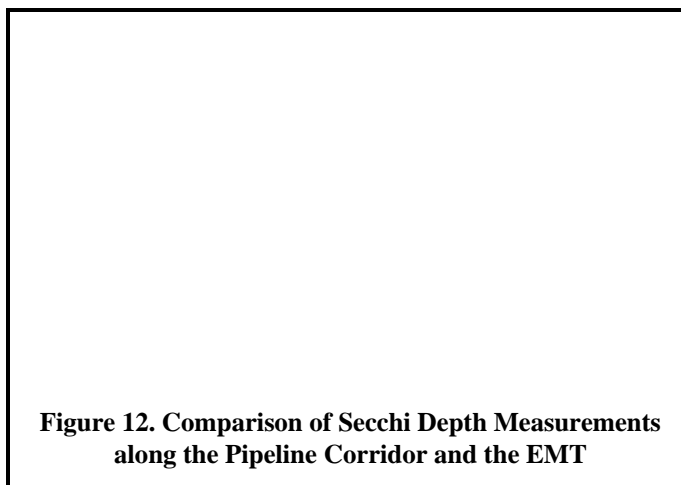


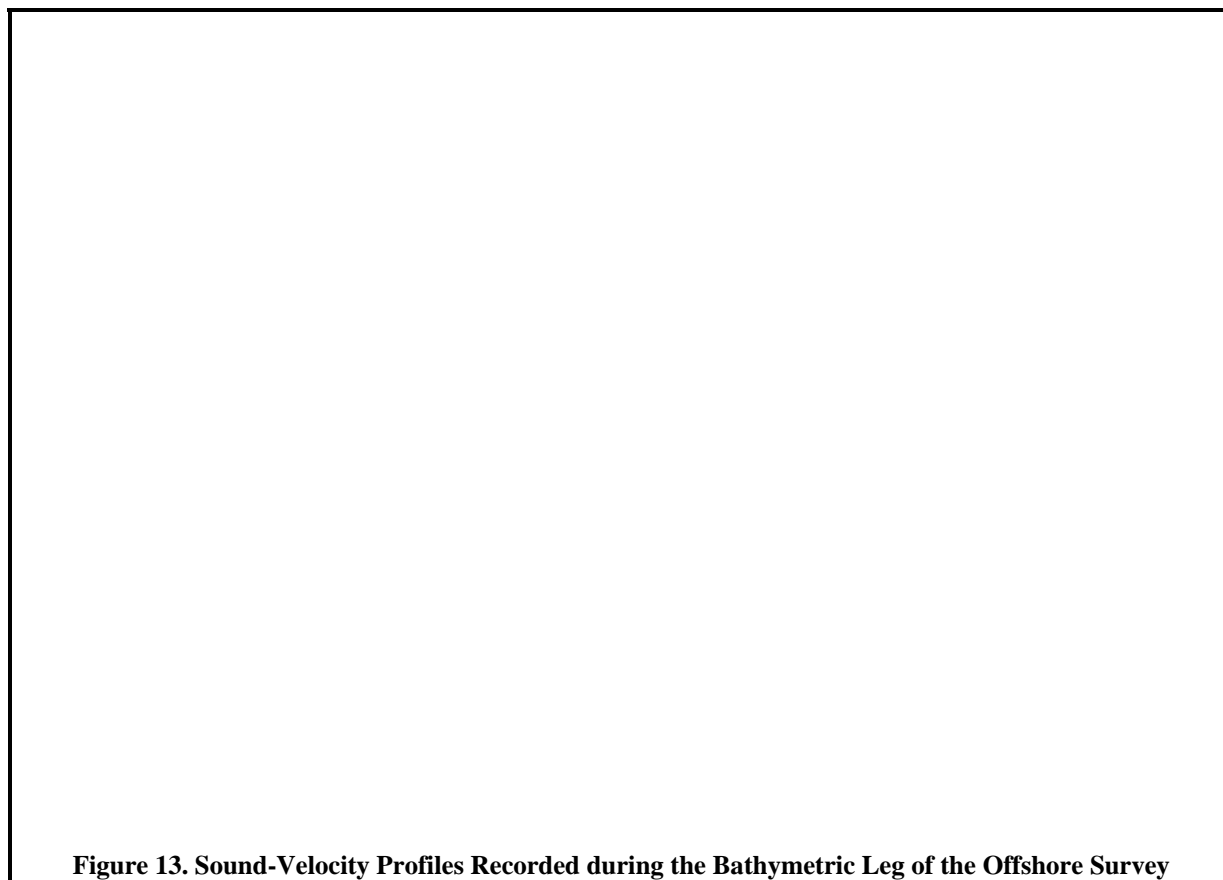
Figure 12. Comparison of Secchi Depth Measurements along the Pipeline Corridor and the EMT

2.3.2 Temporal Variability

The vertical structure of seawater properties varied significantly during the offshore survey. This variability is apparent in the presence or absence of a shallow mixed layer within the upper water column as reflected in the sound velocity profiles recorded during the bathymetric survey (Figure 13 on Page 18). Even within the same day, for example on 22, 24, and 25 January 2007, profiles collected in the morning did not exhibit a shallow mixed layer, while profiles collected in the afternoon exhibited a sharp pycnocline just below the sea surface. Presumably, the sharply defined surface layer formed from insolation as the sun rose during the day and heated the sea surface. Regardless of the mechanism that caused these short-term changes in vertical structure, the overall large variability in the time series of sound-velocity profiles demonstrated the importance of regular corrections to the acoustic ray paths used in the bathymetric survey.

2.3.3 Pipeline Corridor

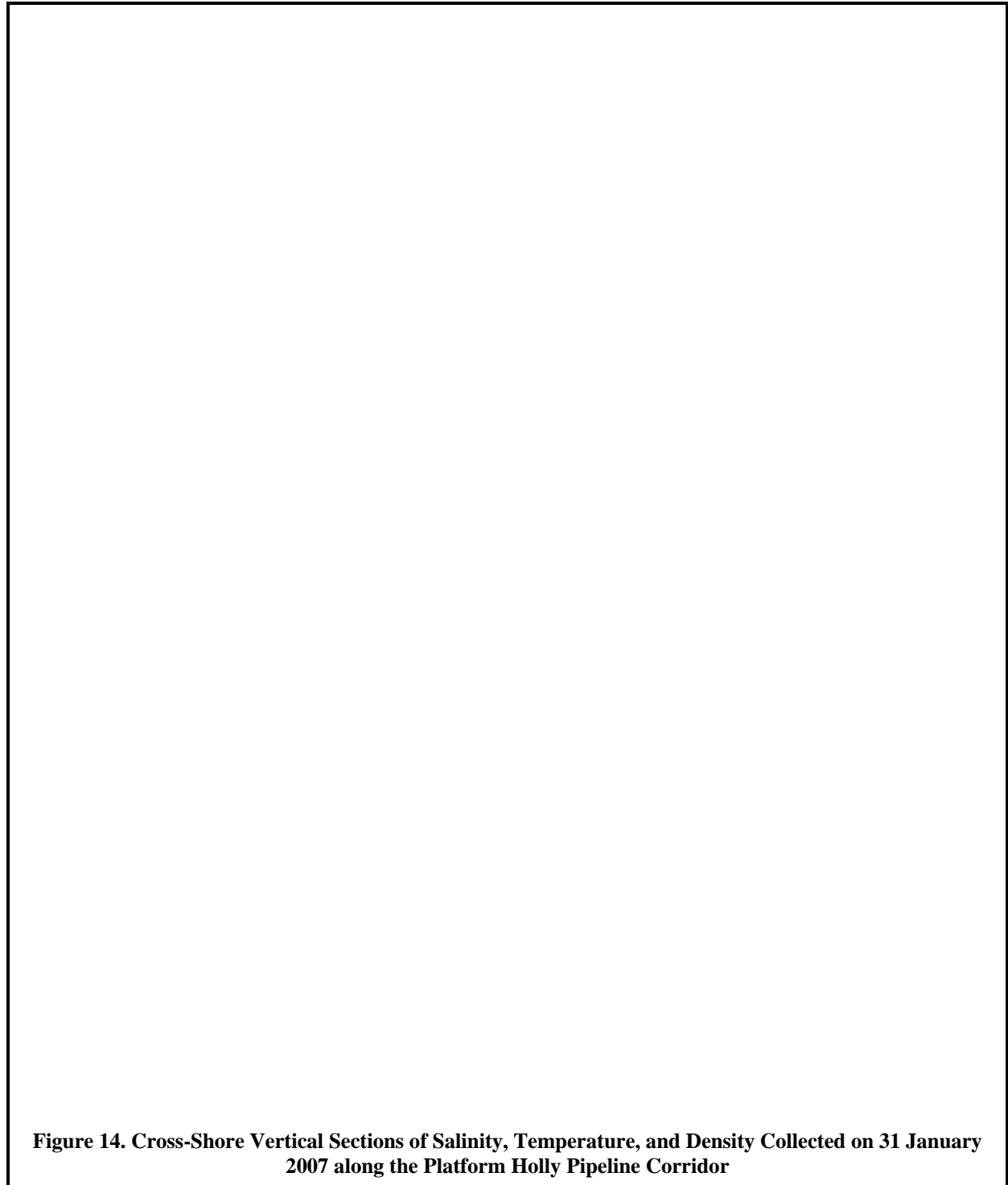
The vertical sections shown in Figure 14 and Figure 15 provide a synoptic view of the vertical and lateral distributions of six seawater properties along the existing pipeline corridor between Platform Holly and the shoreline near the EOF. The downcast positions of the 10 vertical profiles that were used to construct the sections are shown as Stations W39 through W48 in Figure 11.



Note that this cross-shore transect was not perfectly perpendicular to the shoreline; rather, it tracked the configuration of the pipeline bundle.

Note also from the distribution of individual observation points shown in Figure 14 that the CTD instrumentation package moved laterally as it was lowered through the water column. This offshore movement was caused by vessel drift that resulted in part, from residual momentum of the survey vessel as it approached each station from an onshore direction. The drift resulted because the CTD casts were conducted by live-boating (dynamic positioning) rather than by anchoring at each station. For example, during the four-minute duration of the 60 m downcast at the deepest station (W48), the vessel drifted 100 m. However, almost all of that drift was toward the east, in a direction perpendicular to the vertical section, and thus, it is not fully reflected in the figures. This eastward vessel drift was caused by the strong eastward winds and currents that prevailed at the time of the water-quality leg of the survey. As discussed in Section 2.2 on Page 13, wind and current conditions were unusual because of an approaching storm.

The cross-shore vertical sections of the six seawater properties exhibit some features that are fairly typical of offshore conditions in the regions, and some that are related to the rainy conditions which prevailed immediately prior to the survey. For example, a pool of fresh, cool, low density water is apparent shoreward of 2 km (Station W44) in Figure 14. The seawater properties of this nearshore watermass were probably influenced by onshore runoff from rainfall during the extended period of stormy weather that preceded the survey.



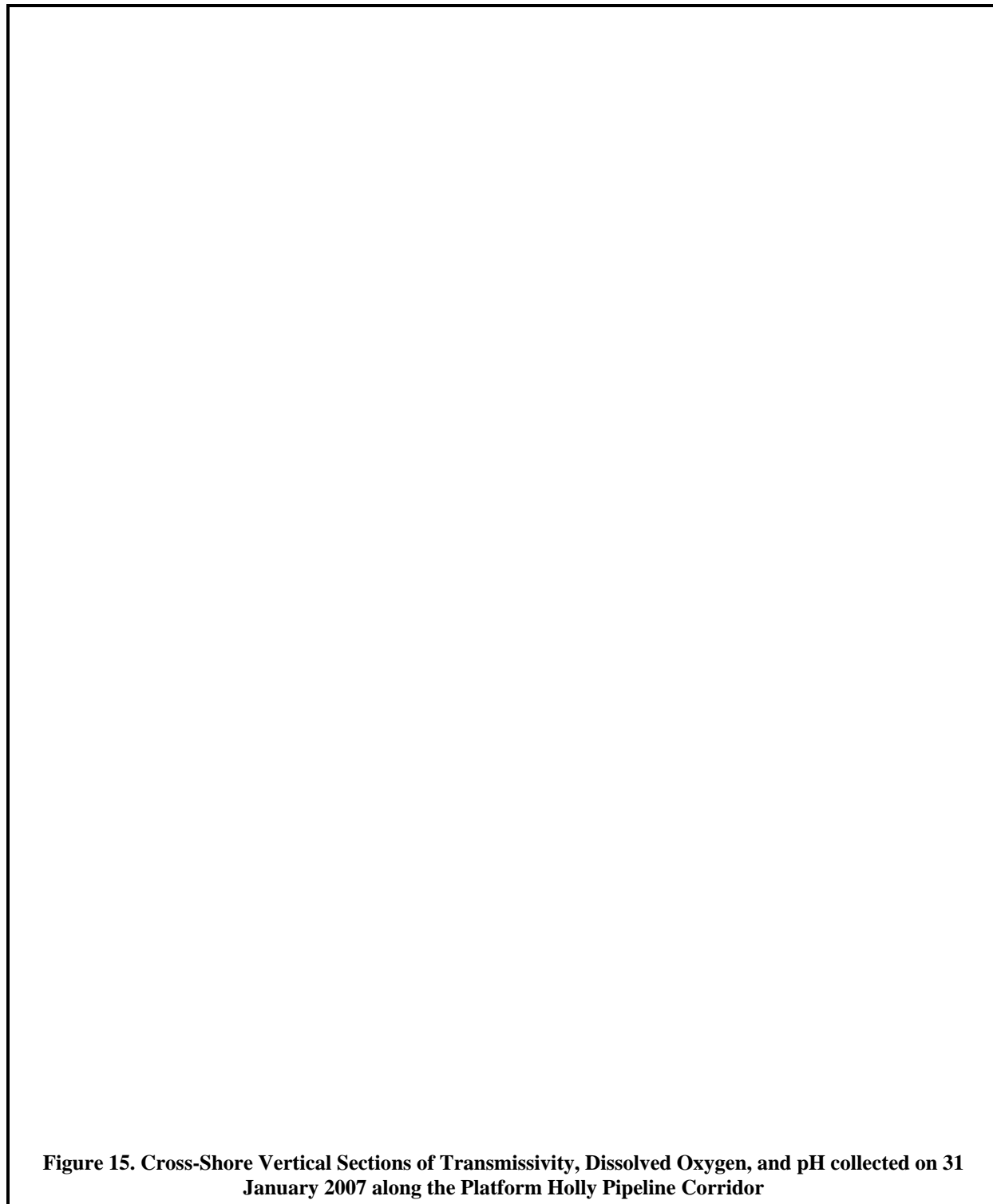


Figure 15 shows that this nearshore watermass was also turbid, being as much as 12 percent lower in transmissivity, and had low dissolved oxygen (DO) concentrations. However, these differences may not have been related solely to the onshore origin of the runoff. For example, transmissivity steadily increases with distance from the shoreline as shown in the top frame of Figure 15. This contrasts with the uniform distribution of low salinity within the nearshore watermass that is delineated in blue in the top frame of Figure 14. Instead, wave-induced resuspension of surficial sediments near the shoreline was probably responsible for the observed reduction in water clarity. Similarly, the DO distribution shown in the middle frame of Figure 15 contained marked vertical structure, quite unlike the salinity field.

Farther offshore, beyond the frontal region, near 2 km, where isopleths of most seawater properties were vertically aligned, the property distribution was more typical of general oceanographic conditions in the region. In particular, density stratification (bottom frame of Figure 14) was driven largely by a deep thermocline near 45 m (middle frame), which was often present in the area, as shown by the velocity profiles in Figure 13. Although seawater at depth was more saline, as delineated in red in the top frame of Figure 14, the salinity differences did not play a significant role in determining the vertical density structure.

Dissolved oxygen concentrations (middle frame of Figure 15) and pH (bottom frame) exhibited a general decline with depth in this offshore region. Declines with increasing depth in these seawater properties usually result from an increase in the ratio of respiration to photosynthesis that naturally occurs below the oceanic mixed layer. Without recent direct atmospheric exchange, biotic respiration and decomposition slowly deplete DO levels at depth. Respiration and decomposition of organic detritus also increases the concentration of dissolved CO₂ (carbonic acid), which results in a reduction in pH (more acidic) with increasing depth.

Lastly, the mid-depth maximum in transmissivity, delineated in light blue in the top frame of Figure 15, is also commonly observed as a result of natural processes. Near the seafloor, water clarity is naturally reduced even at depths beyond the influence of oscillatory motions associated with surface gravity waves. Instead, reductions in water clarity above a deep seafloor are caused by the presence of a bottom nepheloid layer, which is a widespread phenomenon on continental shelves. The decreased clarity within the layer is caused by a suspension of naturally occurring particulates formed from light-weight flocs of detritus. In the Figure, reduced offshore water clarity near the seafloor is apparent as a layer with transmissivity below 84 percent, as delineated by dark-blue shading. Similarly, near the sea surface, primary productivity within the euphotic zone reduces water clarity because of the increased abundance of phytoplankton. The near-surface and seafloor reductions in water clarity create a localized mid-depth maximum in measured transmissivity.

2.3.4 Offshore EMT

The vertical sections shown in Figure 16 and Figure 17 provide a synoptic view of the vertical and lateral distributions of six seawater properties within the offshore portion of the EMT. Eighteen closely spaced vertical profiles were collected along a longitudinal transect that traversed 900 m of the EMT area. The downcast positions are shown as Stations W18 through W35 in Figure 11. Note that, because the local isobaths and the adjacent coastline trends southeast toward Coal Oil Point, the transect was not perfectly parallel to the local shoreline.

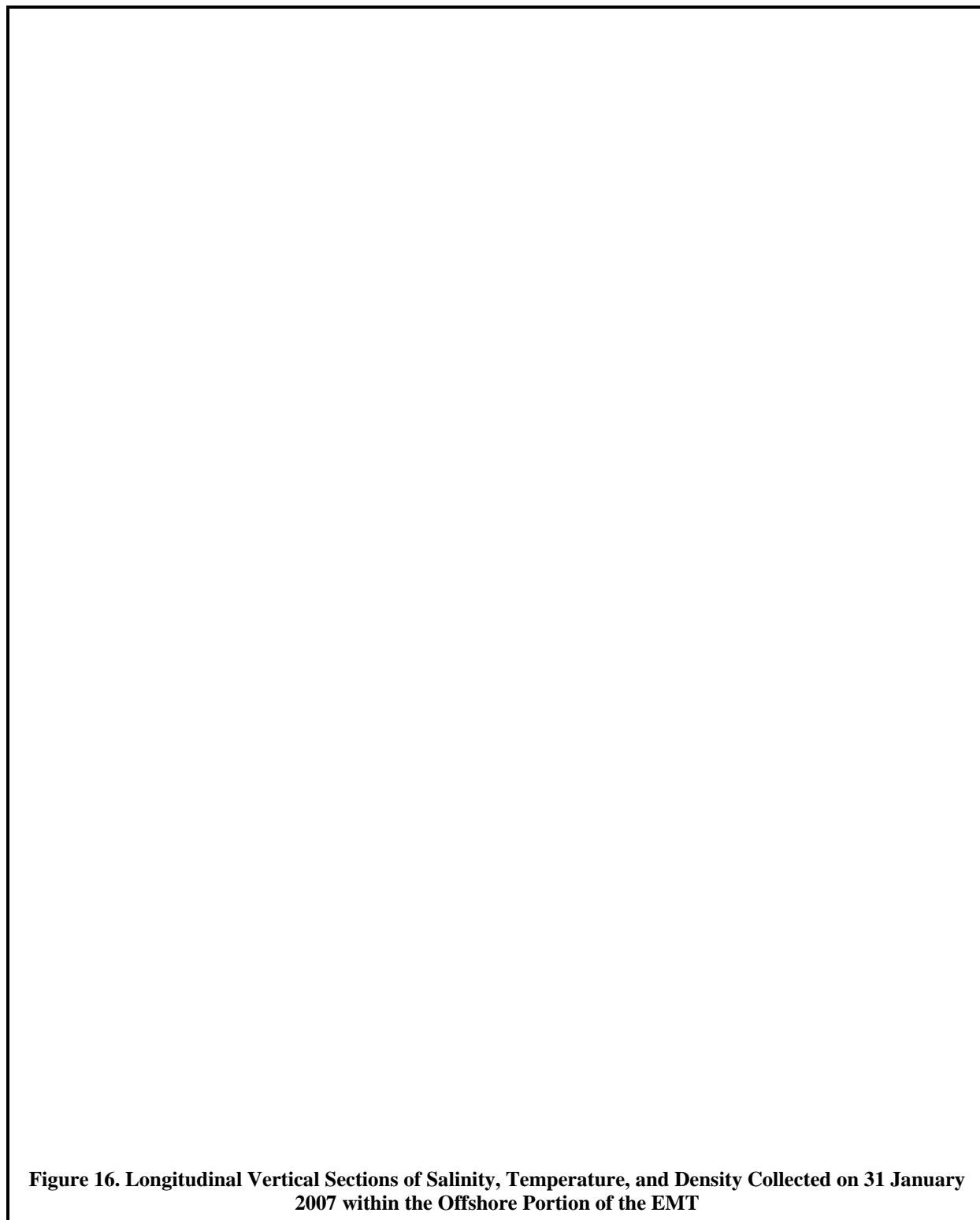




Figure 17. Longitudinal Vertical Sections of Transmissivity, Dissolved Oxygen, and pH Collected on 31 January 2007 within the Offshore Portion of the EMT

Nevertheless, it represents an along-shore transect relative to the shoreline along most of the northern Santa Barbara Channel. As with the cross-shore transect along the pipeline corridor, the CTD instrumentation package moved laterally as it was lowered through the water column within the EMT as shown by the individual observations in Figure 16 and Figure 17. The hydrocasts at the first three Stations (W18, W19, and W20) did not reach the seafloor, and the location of the resulting data gap is shown in the vertical sections.

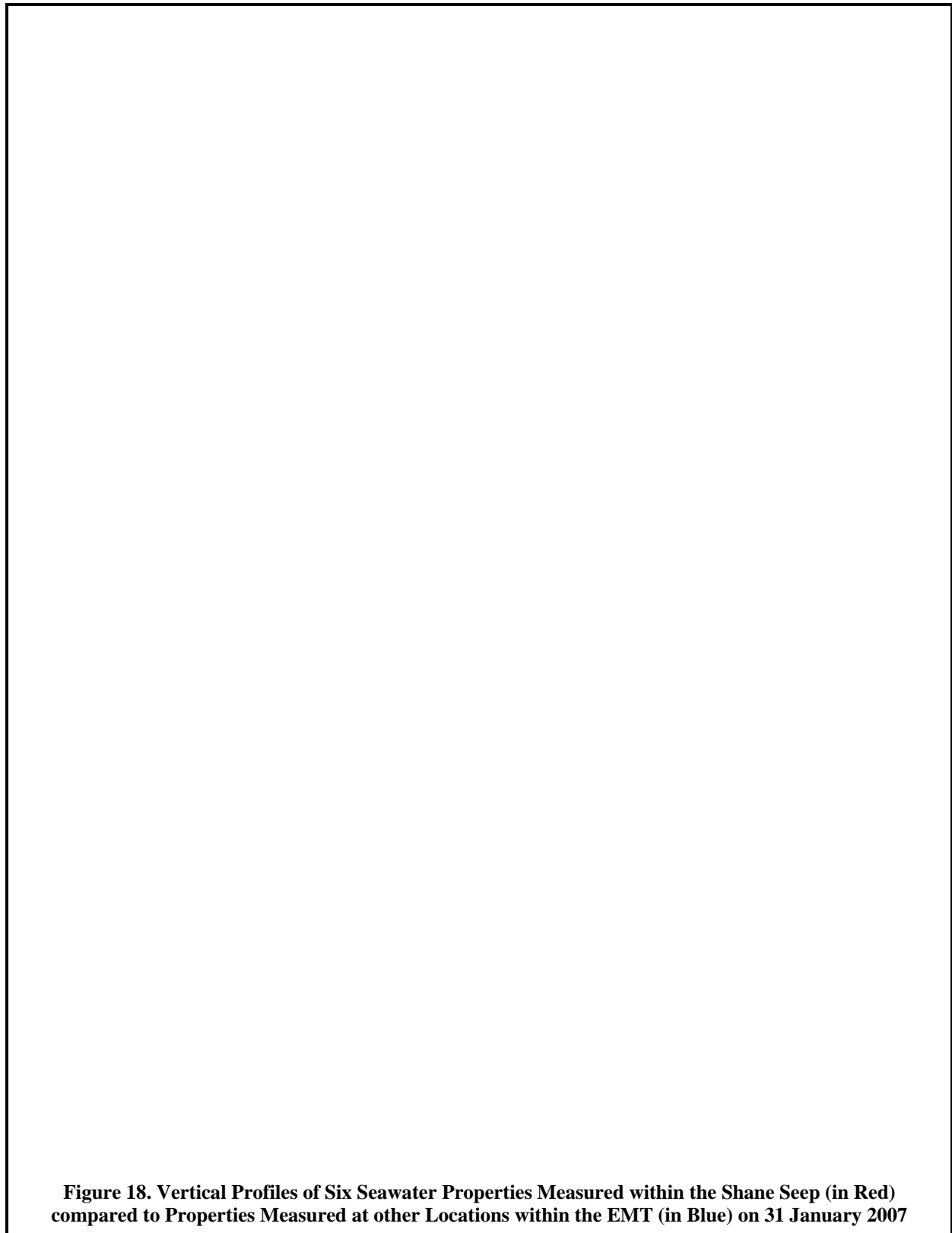
There are several features of interest in the distribution of properties along the EMT transect. For example, a sharp halocline 5 m above the seafloor separates a deep, saline water mass, delineated in red, from a fresher watermass, delineated in blue, that covers most of the water column (top frame of Figure 16). In contrast, there was little thermal stratification (middle frame), so the salinity distribution dictated the density field (bottom frame). Normally, thermal variations are more influential in the seawater equation of state, but in this case, as in the case of the nearshore portion of pipeline-corridor transect, it is likely that freshwater runoff influenced the nearshore seawater properties and over-rode the influence of temperature on vertical stratification.

The fresher watermass was also associated with slightly decreased water clarity, as delineated by red shading in the upper frame of Figure 17, and slightly increased DO (light blue in the middle frame). Decreased water clarity is consistent with contributions from terrigenous particulates carried into the ocean by turbid onshore runoff. However, the decreased clarity was very small, and resulted in only a two percent reduction in light transmittance in the upper water column in the eastern portion of the transect. The two percent reduction in near-surface transmissivity along the transect was too small for the lower precision Secchi-disk measurements to resolve. Instead, all five of the Secchi depths measured within the EMT reached 7 m (Stations W20, W25, W30, W34, and W38 in Table 1 on Page 15).

Despite the slight reduction in nearshore transmissivity, overall transmissivity was high within the EMT, exceeding 77 percent. In the eastern portion of the EMT, where water depths were less than 14 m, the base of the euphotic zone, which is approximately twice the Secchi depth, reached the seafloor. This contrasts with the nearshore transmissivity measured along the pipeline corridor, which dropped below 70 percent. Secchi-depth measurements were capable of discerning a difference in water clarity of that magnitude, and nearshore Secchi depths measured along the pipeline corridor were as much as 3 m shallower than those measured within the EMT (Station W39 in Table 1).

2.3.5 Shane Seep Discharge

Three vertical CTD profiles were collected within the discharge of Shane Seep during the water-quality leg of the offshore survey on 31 January 2007. These three profiles, designated W36, W37, and W38, were recorded 150 m due south of the center of the EMT transect (Figure 11 on Page 16). Prior to the downcast, the vessel was repositioned so that the CTD instrumentation package was deployed in the center of the seep's gas boil on the sea surface (Figure 4). These additional measurements were collected to assess whether the seep was significantly altering the ambient water quality within the region surrounding the EMT.



Five of the six seawater properties measured within the seep plume fell within the range of measurements recorded along the EMT transect. The water-quality profiles associated with the seep casts (highlighted in red in Figure 18) generally fell in the center of the profiles recorded within the EMT transect that were recorded on the same day (shown in blue). Only the oxygen saturation profile recorded within the seep extended beyond the range in properties measured within the EMT transects. The increased gaseous dissolution was undoubtedly related to the release of pressurized gas within the seafloor seep. Accordingly, the associated rapid vertical transport reduced the degree of vertical stratification in the water column near the seep.

2.4 EQUIPMENT AND PERSONNEL, AND METHODS

2.4.1 Vessel

The 38-ft F/V *Bonnie Marietta*, owned and operated by Captain Mark Tognazzini of Morro Bay, provided vessel support for all legs of the offshore survey. The F/V *Bonnie Marietta* is a single-screw, diesel powered vessel, with molded fiberglass construction, and a fully enclosed wheelhouse. It has an open fly bridge with dual engine control (third throttle control located at the stern), a fully enclosed galley, head, engine room, and storage with four berths in the foc'sle. The hull was built by Channel Island Boat Works in 1981 and underwent a major retrofit in 2002. The hull's beam is 13'6" and depth is 4'6" with a gross displacement of 21 tons.

The vessel was equipped with a modified H-frame, and an 8-inch aluminum mast with a 1000-pound capacity boom and hydraulic winch. A stern mounted swim platform with T-ladder facilitated diver support. Electronics equipment included a Ritchie compass; a Sitex™ Kodon T-180 radar; a Sitex™ Kodon T-185 radar; a ComNav™ 1101 autopilot, with steering stabilizer and ComNav™ 101 remote; and a Sitex™ CVS 211 video fathometer/plotter.

2.4.2 Personnel

Captain Mark Tognazzini supervised vessel operations, while Mr. Mike Lindley acted as marine technician on all legs of the offshore survey. Dr. Douglas Coats of MRS was chief scientist on all legs of the survey. Ms. Bonnie Luke, also of MRS, was second science officer on the water-quality leg of the survey that is described in this section.

2.4.3 Navigation

Offshore navigation aboard the survey vessel was supplied by a Furuno™ GPS 30 coupled to a FBX2 differential beacon receiver. Global positioning satellite (GPS) navigational fixes were recorded digitally at 1-second intervals. Prior to the survey, all computers and chronometers were synchronized with the GPS. Post-processing of the navigation log provided precise positions of the offshore samples by aligning the time stamps. Navigational errors inherent in standard GPS reading are greatly reduced with the Differential GPS (DGPS) system that was first implemented by the U.S. Coast Guard. DGPS incorporates a second signal from a nearby land-based beacon. Because the beacon is fixed at a known location, the position error in the reading from the GPS satellites can be precisely calculated. This correction is continuously transmitted to the DGPS receiver and results in extremely accurate offshore navigation, typically with position errors of less than 2 m.

2.4.4 Ancillary Observations

Standard observations for weather, seas, water clarity/coloration, Secchi depth, and the presence of any odors and floating debris were recorded during the surveys. Wind speeds and air temperatures were measured with a Kestrel® 2000 Thermo-Anemometer.

2.4.5 CTD Instrumentation Package

Vertical water-column profiling was conducted using an electronic instrument package equipped with a number of probes and sensors. A Sea Bird Electronic SBE-19 Seacat CTD (Conductivity-Temperature-Depth) module was used to collect profiles of conductivity, salinity, temperature, light transmittance, DO, pH, density, and pressure at each station. A submersible pump on the CTD flushed water through the conductivity cell and oxygen sensor at a constant rate, independent of the CTD's motion through the water column. Prior to the surveys, the transmissivity, DO, and pH sensors were calibrated. The pre-cruise calibration for DO was conducted by immersing the CTD in an aerated temperature-controlled calibration tank. In addition to this oxygen reading at full saturation, a zero-oxygen calibration point was determined by filling the oxygen-sensor plenum with an 8 percent solution of sodium sulfite (Na_2SO_3). Oxygen calibration coefficients were determined by regression analysis of sensor membrane current and temperature as recommended by the manufacturer (Sea-Bird Electronics, Inc, 1993).

Calibration coefficients for the pH (alkalinity) sensor were determined from a linear regression of output voltage after immersion in three separate buffered solutions of known pH. Buffering solutions with a pH of 4 ± 0.01 , 7 ± 0.01 , and 10 ± 0.02 were used to bracket the range of *in situ* measurements. The Sea-tech transmissometer was air calibrated by fitting the voltages recorded with and without blocking the light transmission path in air, as recommended by the manufacturer (Sea-Bird Electronics, Inc., 1989). The revised calibration coefficients determined prior to each survey were used in the algorithms that convert sensor voltage to engineering units when processing the field data from each individual survey.

The last full factory calibration of the entire CTD package was conducted in October 2001. All factory calibrations confirmed the continued accuracy of the temperature, pressure, and conductivity sensors as well as the operational integrity of the transmissometer, oxygen, and pH probes. The DO and pH sensors were again returned to the factory in May 2003 and June 2006 for testing and recalibration. The aging DO probe was replaced with a new DO probe on both occasions. The new DO probe and existing pH probe were factory calibrated prior to being returned to MRS.

2.4.6 Analysis of Seawater Properties

Six seawater properties were used to assess water quality during the field survey. They were derived from the continuously recorded output from the electronic probes and sensors on the CTD. Depth limitations on the combination oxygen/pH sensor confined the CTD to depths less than 200 m, which is well beyond the maximum depth of the deepest station (Table 2). The precision and accuracy of the various probes, as reported in the manufacturer's specifications, are also listed in Table 2. Salinity (‰) was calculated from conductivity (Siemens/m) measurements. Density was derived from contemporaneous temperature (°C) and salinity data. It was expressed as 1,000 times the specific gravity minus one, which is a unit of sigma-T (σ_t). All three of these

Table 2. Instrumental Specifications for CTD Profiler

Component	Depth ⁴	Units	Range	Accuracy	Resolution
Housing	600	—	—	—	—
Pump	3400	—	—	—	—
Pressure	680	psia	0 to 1000	± 5.0	± 0.5
Depth	—	meters	0 to 690	± 3.0	± 0.3
Conductivity	600	Siemens/m	0 to 6.5	± 0.001	± 0.0001
Salinity	600	‰	0 to 38	± 0.006	± 0.0006
Temperature	600	° C	–5 to 35	± 0.01	± 0.001
Transmissivity	2000	%	0 to 100	± 0.1	± 0.025
Dissolved Oxygen	200	Mg/L	0 to 21.5	± 0.14	± 0.014
Acidity/Alkalinity	200	pH	0 to 14	± 0.1	± 0.006

physical parameters (salinity, temperature, and density) were used to determine the lateral extent of seawater perturbations. Additionally, they defined the layering (vertical stratification) of the ambient seawater, which defines the behavior and dynamics of future discharges from the proposed Project discharges as they mix with ambient seawater.

Data on the three remaining seawater properties were used to further characterize ambient seawater conditions. They include light transmittance (water clarity), hydrogen ion concentration (acidity/alkalinity – pH), and dissolved oxygen (DO). Light transmittance was measured as a percentage of the transmitted beam of light detected at the opposite end of a 0.25-m path. Increased transmittance indicates increased water clarity and decreased turbidity.

Before deployment at the initial station, the CTD package was held below the sea surface for a three-minute to seven-minute equilibration period. Subsequently, the CTD was raised to within 0.3 m of the sea surface and profiling commenced. The CTD was lowered at a continuous rate of speed to the seafloor. Multiple stations were collected during each deployment by towing the CTD package below the water surface while transiting between adjacent stations. Upon retrieval of the CTD, the profile data were downloaded to a portable computer.

Profile plots and data for each parameter were checked for accuracy and completeness in the field. During the surveys, no obvious irregularities were found that would suggest a malfunctioning sensor. CTD casts were deemed satisfactory, based on the range-acceptability criteria prescribed for waters of the mainland shelf of Southern California (Table 2 in (SCBPPFCT, 1995). The locations of the seawater measurements were determined by aligning the time stamps on the internally recording CTD data with the digital navigation log downloaded from the DGPS system. The layback position of the CTD instrument package relative to the DGPS antenna on the survey vessel was determined for each half-second measurement from the measured amount of line out and the depth recorded by the CTD package.

⁴ Maximum depth limit in meters

3.0 SEAFLOOR SEDIMENTS

Both the physicochemical and biological properties of the benthos are described in this Section. The character of seafloor sediments reflects the influence of a wide variety of oceanographic and biological processes. The physical properties of the surficial sediments lend insight into the relative strength of competing depositional and erosional processes as they vary throughout the survey area. In combination with sediment chemistry, these properties reveal the localized influence of natural hydrocarbon seeps. Sedimentary properties also yield information about the marine ecosystem as a whole because the benthos act as a sink for organic and inorganic matter introduced to the water column. Infauna residing within seafloor sediments serve as indicators of the health of the marine environment because of their limited mobility and well-defined responses to pollution. Numbers of species, abundance, biomass, and other parameters of infaunal community composition can indicate contaminant-caused stresses if, for example, gradients extending from a pollutant source to distant unaffected areas are observed.

3.1 SEDIMENT DATABASE

A wide variety of physical, chemical, and biological analyses were conducted on the 28 sediment samples collected during the benthic leg of the field survey. This section examines these parameters to establish ambient conditions within seafloor sediments throughout the proposed Project area, and along the alternative pipeline route to LFC. The sediment properties and biota were tested for naturally occurring spatial trends and the presence of anthropogenic enrichment. Additionally, the interrelation between biological and physicochemical parameters was evaluated for possible toxicological affects. Results were compared to those of other regional studies to determine the degree to which the infaunal communities varied over time in the study area, and to determine whether the physicochemistry of the local benthic environment was representative of other areas within the Southern California Bight (SCB).⁵

3.1.1 Samples Analyzed

The assessment of the physical, chemical, and biological properties of seafloor sediments in the study region was based on an analysis of 113 sediment grab samples collected over the past 30 years at 47 sites and times (Figure 19, Table 3). Twenty-eight of these samples were collected at 14 stations on 30 January 2007 during the benthic leg of the offshore survey that was conducted in conjunction with the EIR for the proposed Project. These stations are designated with an “MRS” prefix. At each of these 14 stations, one sediment grab sample was subsampled for hydrocarbon and grain-size analyses, and the entire volume of another grab sample was sieved for infaunal organisms. For sample-tracking purposes, the subsamples earmarked for physicochemical analysis were designated with an “SC” prefix before the station number, to identify them as “*Sediment Chemistry*” samples, thereby distinguishing them from the infaunal samples, which were identified with the “MRS” prefix. The 14 benthic station numbers were consistent between the two sample sets.

⁵ The Southern California Bight (SCB) encompasses the body of water lying between Point Conception and the United States-Mexico border. The term “bight” is defined as bend in the coastline. The SCB is one of the most studied offshore areas of the United States.



Figure 19. Locations of the Sediment Sampling Sites

Table 3. Inventory of Sediment Samples Collected in the Study Region

Source	Station	Sample ID	Collection Date	Description	Replicate Grabs	Latitude	Longitude	Depth (m)	Shoreline Distance (km)	Low Seep Proximity (km)	High Seep Proximity (km)
Arco Coal Oil Point EIR	Arc01	Ar4S01	09/11/84	Station 1	3	34.38131	119.86067	63.3	2.91	0.13	0.26
	Arc02	Ar4S02	09/11/84	Station 2	3	34.38369	119.88379	66.1	2.52	0.04	0.10
	Arc03	Ar4S03	09/11/84	Station 3	3	34.38918	119.90141	63.1	2.74	0.54	1.11
	Arc04	Ar4S04	09/11/84	Station 4	3	34.39550	119.89336	54.7	1.72	0.25	0.89
	Arc05	Ar4S05	09/11/84	Station 5	3	34.39942	119.88354	43.4	0.84	0.00	0.10
	Arc06	Ar4S06	09/11/84	Station 6	3	34.39624	119.93632	68.9	4.11	1.16	4.37
		ArAS06	08/06/85	Station 6 August 1985	3						
		ArJS06	06/27/85	Station 6 July 1985	3						
	Arc07	Ar4S07	09/11/84	Station 7	3	34.40979	119.99331	68.3	4.18	6.54	9.73
	Arc08	Ar4S08	09/11/84	Station 8	3	34.41981	120.00721	59.3	3.61	8.14	11.40
	Arc09	Ar4S09	09/11/84	Station 9	3	34.36744	119.86207	78.7	4.38	0.74	0.85
	Arc10	Ar4S10	09/11/84	Station 10	3	34.37405	119.88355	73.6	3.57	0.94	1.15
	Arc11	Ar5S11	06/27/85	Station 11 Holly	3	34.38953	119.90576	63.2	3.01	0.94	1.50
	Arc12	Ar5S12	08/06/85	Station 12 Haven	3	34.39627	119.93089	66.8	3.77	0.70	3.92
Goleta Sanitary District	GSD1	GSDS1	10/06/05	Outfall Monitoring Station 1	5	34.39300	119.83800	49.9	1.34	2.25	0.77
	GSD2	GSDS2	10/06/05	Outfall Monitoring Station 2	5	34.40117	119.82517	31.4	1.62	3.68	2.12
	GSD3	GSDS3	10/06/05	Outfall Monitoring Station 3	5	34.40117	119.82350	31.2	1.67	3.74	2.27
	GSD4	GSDS4	10/06/05	Outfall Monitoring Station 4	5	34.40117	119.82200	31.1	1.67	3.79	2.38
	GSD5	GSDS5	10/06/05	Outfall Monitoring Station 5	5	34.40117	119.82167	31.1	1.67	3.79	2.38
	GSD6	GSDS6	10/06/05	Outfall Monitoring Station 6	5	34.40117	119.82217	31.1	1.67	3.79	2.38
Marine Research Specialists Ellwood Full Field EIR Marine Survey	MRS01	MRS01	01/30/07	Seep Station 1	2	34.40169	119.89302	26.7	1.25	0.03	0.68
	MRS02	MRS02	01/30/07	Along-Shore Station 2	2	34.45860	120.03975	5.4	0.52	12.76	15.54
	MRS03	MRS03	01/30/07	Along-Shore Station 3	2	34.43442	120.02278	56.8	2.56	10.07	13.13
	MRS04	MRS04	01/30/07	Along-Shore Station 4	2	34.41133	119.99408	68.0	4.08	6.72	10.02
	MRS05	MRS05	01/30/07	Along-Shore Station 5	2	34.39695	119.93567	68.7	4.01	1.15	4.35
	MRS06	MRS06	01/30/07	Holly Station 6	2	34.38777	119.90454	63.4	3.06	0.81	1.34
	MRS11	MRS11	01/30/07	Cross-Shore Station 11	2	34.42385	119.91633	6.2	0.55	1.93	3.80
	MRS12	MRS12	01/30/07	Cross-Shore Station 12	2	34.42020	119.91781	17.4	0.96	1.56	3.64
	MRS13	MRS13	01/30/07	Cross-Shore Station 13	2	34.41516	119.91813	31.3	1.43	1.04	3.37
	MRS14	MRS14	01/30/07	Cross-Shore Station 14	2	34.40873	119.91752	36.1	1.92	0.41	3.06
	MRS15	MRS15	01/30/07	Cross-Shore Station 15	2	34.40368	119.91575	53.7	2.30	0.32	2.79
	MRS16	MRS16	01/30/07	Cross-Shore Station 16	2	34.39573	119.91204	61.8	2.94	0.60	2.28
	MRS17	MRS17	01/30/07	EMT Station 17	2	34.40710	119.88815	17.7	0.54	0.63	0.68
	MRS18	MRS18	01/30/07	EMT Station 18	2	34.40719	119.89141	18.4	0.79	0.65	0.85

Source	Station	Sample ID	Collection Date	Description	Replicate Grabs	Latitude	Longitude	Depth (m)	Shoreline Distance (km)	Low Seep Proximity (km)	High Seep Proximity (km)
Southern California Coastal Water Research Project	B94S112	SCB4S112	8/18/1994	Bight'94 Station 112	1	34.41777	120.07648	78.8	4.70	14.27	17.45
	B94S136	SCB4S136	8/18/1994	Bight'94 Station 136	1	34.40985	119.94912	61.5	2.61	2.81	5.90
	B94S016	SCB4S16	7/19/1994	Bight'94 Station 16	1	34.45270	120.02815	31.7	0.69	11.63	14.28
	B94S038	SCB4S38	7/19/1994	Bight'94 Station 38	1	34.44420	120.06448	57.8	1.93	14.43	17.11
	B94S060	SCB4S60	8/18/1994	Bight'94 Station 60	1	34.43610	120.00448	47.1	1.95	8.94	11.60
	B98S2356	B98S2356	8/26/1998	Bight'98 Station 2356	1	34.44788	120.07345	48.7	1.36	14.93	18.03
	B98S2357	B98S2357	8/26/1998	Bight'98 Station 2357	1	34.40632	119.94079	61.6	3.10	1.97	5.10
	B98S2359	B98S2359	8/26/1998	Bight'98 Station 2359	1	34.39839	119.86476	38.8	1.06	0.69	0.86
	B98S2360	B98S2360	8/26/1998	Bight'98 Station 2360	1	34.39400	119.87538	51.3	1.35	0.00	0.00
	Ref5_30	Rf5SR5-3	8/7/1985	1985 30m Reference Station 5	1	34.45507	120.07390	33.4	0.56	15.63	18.27
	Ref5_60	Rf7SR5-6	6/3/1977	1977 60m Reference Station 5	1	34.43750	120.06720	64.8	2.59	14.47	17.16
		Rf5SR5-6	8/7/1985	1985 60m Reference Station 5	1						
	Ref6_60	Rf7SR6-6	6/3/1977	1977 60m Reference Station 6	1	34.40445	119.94670	62.7	3.22	2.33	5.57

3.1.2 Sample Collection

On 30 January 2007, the benthic sediment leg of the offshore survey was conducted. Ms. Bonnie Luke of MRS was the senior marine biologist responsible for the collection and offshore processing of the benthic samples. Sediment chemistry and benthic infaunal samples were collected using a chain-rigged Young grab whose design was modified from that of a Van Veen sediment sampler (Figure 20). The Young grab was equipped with a frame that enhanced the penetration, stability, and the proficiency of the grab in collecting a level, undisturbed sample. A stainless steel lip was also welded to the mouth of the jaw to improve the seal, which aids in sample retention during ascent. Two 25-kg weights were added to the grab frame to further facilitate penetration in the siltier sediments that were present farther offshore. The stainless-steel grab was coated with Dykor.[®] Dykor[®] has properties similar to Teflon[®] and improves the chemical inertness of the grab sampler. This limits contamination of the sediment chemistry samples.



Figure 20. Photograph of the Sediment Grab Sampler and Support Frame

Two 25-kg weights were added to the grab frame to further facilitate penetration in the siltier sediments that were present farther offshore. The stainless-steel grab was coated with Dykor.[®] Dykor[®] has properties similar to Teflon[®] and improves the chemical inertness of the grab sampler. This limits contamination of the sediment chemistry samples.

At each of the 14 benthic stations, the survey vessel was positioned over the target coordinates, and the sediment grab sampler was lowered over the starboard side using the overhead boom and deck winch. The descent speed of the grab was reduced as it approached the seafloor. The vessel position and “trip” time, namely, the time when the grab encountered the seafloor and the sample was collected, were accurately recorded. After sample retrieval, the vessel was repositioned over the target station location and the process was repeated until all two acceptable replicate samples had been acquired.

3.1.3 Chemistry Sample Processing

Collection of the sediment samples offshore complied with rigorous field-sampling protocols to avoid contamination. Prior to and throughout the offshore survey, the sampling equipment was thoroughly cleaned to eliminate the introduction of contaminants into the samples and to prevent cross-contamination between stations. Before the survey, the grab sampler and Dykor[®]-coated sediment scoops were washed with Alconox[®], deionized water, and 10 percent Hydrochloric Acid (HCl). During the survey, the grab and sampling utensils were washed with Alconox[®], rinsed with seawater, and subsequently decontaminated with deionized water, methanol, and 1 percent HCl prior to sampling at each station.

Surficial sediments for physicochemical analysis were collected from the upper 2 cm of a single grab sample recovered from each benthic station. Sufficient subsample volumes were collected

to provide material for QA/QC analyses. Samples were stored in the appropriate plastic containers and refrigerated at approximately 4°C prior until analysis. Chain-of-custody forms accompanied all sample shipments from the field and between laboratories.

3.1.4 Infaunal Sample Processing

At each of the 14 benthic stations, in addition to the sample collected for sediment physicochemistry, a replicate sediment grab sample was collected for the purposes of infaunal processing. However, in contrast to the chemistry subsampling, wherein only the first few centimeters of the sediments are of interest, the entire grab volume was processed for infaunal analysis. Also, at a few stations, multiple deployments of the grab sampler were required before an acceptable sediment sample was acquired. Acceptance criteria were based on penetration depth (exceeding 7 cm), surface condition (level), and overall sample integrity (undisturbed).

Samples extracted from the jaws of the grab were lightly washed, and elutriated onto a 1.0-mm mesh sieve as shown in Figure 21. The extracted material was then washed into a labeled 16-oz. jar and was preserved with 10 percent buffered formalin. After 48 hours, the formalin was rinsed from the samples on a 0.5-mm mesh sieve and the samples were transferred to 70 percent alcohol for processing, preservation, and storage. Samples were stained with a Rose Bengal solution to aid in sorting of the organisms into the following major taxonomic groups: annelida and nemertea, mollusca, crustacea, echinodermata, and miscellaneous phyla.

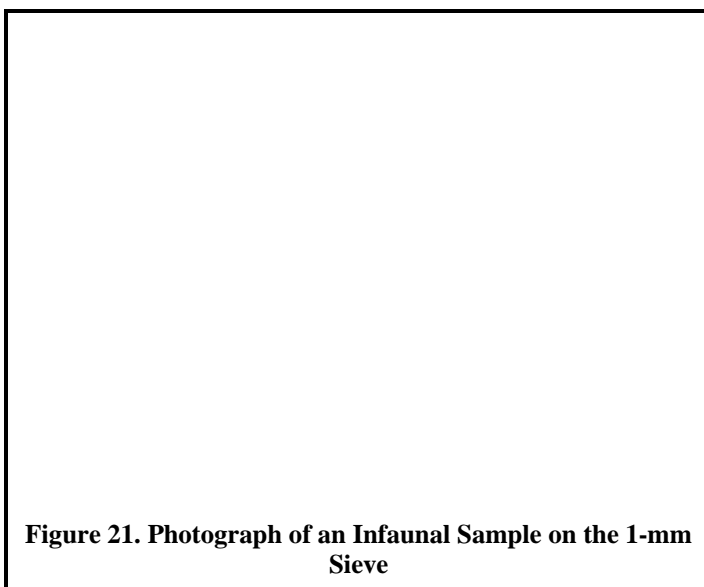


Figure 21. Photograph of an Infaunal Sample on the 1-mm Sieve

After sorting, the individual organisms were enumerated and identified to species level by one of two taxonomists who specialized in specific phyla. Dr. Kropp was responsible for mollusca, crustacea, and echinodermata specimens. He is a Senior Research Scientist at the Pacific Northwest National Laboratory, which is part of Battelle Marine Sciences Laboratory located in Sequim, Washington. He is a specialist with over 20 years of experience in benthic marine ecology, toxicology, and an expert on the systematics of crustaceans and mollusks. He has served as the principal investigator for or participated in marine environmental surveys in the tropical and boreal Pacific, off California, the Gulf of Mexico, along the Atlantic Coast of the United States, and in the Mediterranean. Dr. Kropp is a Research Associate with the Smithsonian Institution and a Research Affiliate of the University of Guam Marine Laboratory. He has authored or coauthored numerous journal publications and technical reports. He received a Ph.D. in Zoology from the University of Maryland in 1988, an M.S. in Biology from the University of Guam in 1982, and a B.S. in Zoology from San Diego State University in 1978.

Ms. Susan J. Williams of Ventura California was responsible for the enumeration and identification of the remaining taxa. Ms. Williams is an environmental scientist with over 30 years experience in ecological monitoring and assessment. She has a strong background in natural history and an excellent working knowledge of such varied communities as coastal sage scrub, coastal dunes, wetlands, and marine benthos. Ms. Williams also has training in hazardous materials management, including courses and seminars in CEQA, environmental auditing, and the fate of toxins in the environment. She has an extensive background in biological survey techniques and laboratory methodology. She has a B.S. and M.S. in Marine Biology from the California State University at Long Beach, and a post-graduate Certificate in Environmental Studies from the same institution. She has an instructor's credential for the California Community Colleges in Biological Sciences, Marine Sciences, and Ecology. She is a charter member of the Southern California Association of Marine Invertebrate Taxonomists and has acted as Assistant Curator for the Allan Hancock Foundation at the University of Southern California where she maintained a museum collection of marine animals and conducted independent research. Ms. Williams has published 13 manuscripts on subjects ranging from taxonomic works and ecological analyses to articles for the general public on environmental issues.

The pair of jaws on the grab sampler acquired sediments from a 0.1-m^2 area of the seafloor. At 0.0625 m^2 , the surface area covered by the grab sampler used in the 1984 and 1985 surveys conducted for the Arco Coal Oil Point Surveys was smaller than the 0.1 m^2 area covered by the sampler used in the other surveys, including this one. Prior to conducting the infaunal analyses, the counts reported for the Arco survey were scaled to be consistent with the organism densities reported for the other surveys. After scaling, there were 53,102 individual organisms representing 357 taxa that were used in the infaunal analysis. Of these, 39,537 organisms, or 74 percent were identified as one of 272 species.

3.1.5 Moisture Content

Moisture content and grain-size distribution are two important physical properties of marine sediments. Moisture content is a measure of the volume of interstitial water present in the sediment samples. While not an indicator of anthropogenic effects, it is an important parameter used in converting chemical concentrations measured in a wet sediment sample, to a dry-weight basis. Dry-weight concentrations allow a more direct comparison of contaminant levels associated with bulk sediments by eliminating variations in sample mass that arise because of arbitrary differences in water content. Also, as described below, moisture content is used, along with salinity measurements, to eliminate the bias introduced by salt content in grain-size determinations.

3.1.6 Grain-Size Analysis

The amount of silt and clay in seafloor sediments directly affects the composition of the resident infaunal community; although the precise mechanism for the relationship is rarely clear (Snelgrove & Butman, 1994). In addition, natural variation in trace-metal concentrations has been correlated with the fine-sediment fraction and, along with aluminum and iron, has been used to normalize metal concentrations to remove naturally occurring trends and reveal

anthropogenic influences (Dossis & Warren, 1980; Ackerman, Bergmann, & Schleichert, 1983; Horowitz & Elick, 1987).

Thus, without accurate measurement of the fine sediment fraction, variability in marine community composition or contaminant concentration could be erroneously ascribed to anthropogenic influences, when it may be the result of natural variation in the distribution of fine particulates instead. Because of the importance of fine sediments, the particle-size analysis was modified from the standard pipette method described by Plumb (1981) and Folk (1980). The refined procedure that was utilized produces significantly more accurate estimates of the fine grain-size fractions within marine benthic samples because it removes obvious inaccuracies that appear in the form of erroneous bimodal distributions, where clay fractions exceed silt fractions.

The standard pipette analysis method described by Plumb (1981) and Folk (1980) is normally only used when accurate estimates of the finest size fractions are needed. However, a series of inter-laboratory calibrations and experiments using method blanks, spikes, and other diagnostic procedures indicated that the standard procedure introduced bias in the fine-fraction measure (Marine Research Specialists, 1998). In response, a more refined method was developed to account for the presence of dissolved solids, namely, salt (Coats, Imamura, Fukuyama, Skalski, Kimura, & Steinbeck, 1999). Specifically, the weight of the solid content left after evaporation of the pipette extraction requires correction for dissolved salts. The refined procedure, which is described below, was applied to the 14 sediment samples collected in this field survey. It produced a significantly more accurate estimate of fine grain-size fraction than the standard procedure.

During wet-sieving of sediment samples, dissolved salts within the interstitial waters wash into the graduated cylinder used in the pipette analysis. The presence of these accumulated dissolved solids will increase the apparent weight of the fine fraction unless they are accounted for analytically. The corrected weight of the fine fraction (W_f) can be determined from salinity and moisture-content measurements, and is given by:

$$W_f = W_p - \frac{M \cdot S \cdot W_w}{1000}$$

where:

W_p = dry weight (mg) of the fine fraction after accounting for peptizing agent and pipette fraction,

M = moisture content (%) of the original sediment sample as collected in the field,

S = salinity (‰) within the interstitial water, and

W_w = wet weight (mg) of the sample used in the grain-size analysis.

The moisture content (M) was determined by drying a subsample from the original field sample. Salinity was measured by inserting a conductivity probe into the elutriate obtained from a grain-size subsample.

3.1.7 TPH Analysis

Sediment subsamples collected from replicate grab samples at the 14 benthic stations were analyzed at the temporary laboratory in Santa Barbara, California immediately following the

conclusion of the benthic leg of the offshore survey on 31 January. Concentrations of Total Petroleum Hydrocarbons (TPH) within the sediment samples were determined using the US EPA approved Method 9074 for Petroleum Hydrocarbons in a Soil Matrix by Turbidimetric Analysis as published in EPA SW-846 Test Methods. The method has a nominal detection limit of 10 mg/kg (parts-per-million or ppm). Prior to analysis, macrofauna and large remnants greater than 0.25 inches were removed, taking care to avoid contamination. All results were reported on an as-received (raw) basis, as shown in the laboratory datasheet (Figure 22), and on a dry-weight basis corrected for sample dilution.

3.2 PHYSICOCHEMICAL PROPERTIES

In contrast to the infaunal analyses, inferences concerning the physicochemical environment within the study region were largely derived from the sediment samples collected on 30 January 2007, rather than relying on a far larger database that includes historical data. As described below, the data reveal a seafloor environment near the proposed Project that is typical of uncontaminated nearshore areas within the SBC. In the along-shore direction, variation in grain size was minimal compared to the naturally occurring changes observed in the cross-shore direction. Specifically, the silt fraction increased steadily with distance from shore, and with increasing water depth.

3.2.1 Physical Properties

The grain-size fractions determined for each sediment subsample that was collected at the 14 benthic stations are summarized in Table 4. Analysis of these data lends insight into the geotechnical character of the seafloor sediments in the Project region. More detailed analysis of differences among the samples defines the inherent uncertainty in sample results, and identifies two outliers that resulted from problems during sample processing. For spatial differences whose amplitude exceeds the sampling uncertainty, the results lend insight into the physical processes that dominate within the benthic boundary layer at various locations within the study area.

Figure 22. Original Hydrocarbon Datasheet for the 14 Benthic Samples Collected on 31 January 2007

Table 4. Percent of Total Weight for each Grain-Size Fraction within Subsamples collected from Seafloor Sediments on 31 January 2007 as part of the Ellwood Marine Survey

Phi Size (φ)	-3.66 to -2	-2 to -1	-1 to 0	0 to 1	1 to 2	2 to 3	3 to 4	4 to 9	>9
Size (μm)	>4000	2000	1000	500	250	125	62.5	62.5 to 2	<2
Class	Sm Pebble	Gravel	Vry Crs Snd	Crs Sand	Med Snd	Fine Snd	Vry Fine Snd	Silt	Clay
SC01	0.00%	0.00%	0.03%	0.19%	1.36%	7.22%	66.32%	23.54%	1.33%
SC02	0.00%	0.00%	0.41%	1.02%	0.95%	2.77%	65.44%	27.00%	2.41%
SC03	0.00%	0.01%	2.04%	1.11%	1.21%	2.40%	36.06%	53.11%	4.07%
SC04	0.00%	0.22%	1.24%	1.68%	2.60%	6.37%	38.96%	39.90%	9.02%
SC04Dup ⁶	0.00%	0.47%	2.98%	1.16%	1.79%	4.44%	36.64%	42.59%	9.93%
SC05	0.00%	1.80%	5.44%	2.57%	2.00%	5.92%	26.17%	53.41%	2.69%
SC06	0.00%	1.12%	6.75%	3.25%	2.96%	20.75%	24.90%	28.62%	11.66%
SC11	0.00%	0.05%	1.15%	0.55%	1.19%	39.49%	45.55%	11.13%	0.89%
SC12	0.00%	0.04%	2.26%	1.50%	1.37%	11.91%	59.01%	21.25%	2.65%
SC13	0.00%	0.01%	2.40%	1.47%	1.30%	18.12%	33.21%	36.52%	6.99%
SC14	0.19%	0.15%	1.55%	0.82%	2.08%	34.77%	49.16%	10.69%	0.59%
SC15	0.16%	1.33%	8.62%	3.67%	2.40%	3.75%	21.07%	50.88%	8.12%
SC15Dup	5.76%	0.56%	3.69%	1.62%	1.91%	4.41%	19.05%	48.62%	14.38%
SC16	0.00%	2.93%	5.96%	3.39%	3.39%	14.29%	28.74%	28.88%	12.41%
SC16Dup	0.00%	1.96%	6.17%	2.52%	2.69%	9.88%	31.36%	33.16%	12.26%
SC17	0.24%	0.00%	0.46%	2.13%	4.42%	13.55%	31.87%	33.96%	13.36%
SC17Dup	0.00%	0.10%	4.77%	1.69%	1.50%	8.11%	31.37%	38.56%	13.91%
SC18	0.00%	0.00%	2.99%	1.47%	1.78%	35.45%	25.59%	22.55%	10.17%

Inherent Sampling Variability

Determination of the largest grain-size fractions is fraught with far greater uncertainty than that of sand and mud fractions. Because of this, the observed spatial differences in gravel and pebble fractions among samples cannot be considered reliable, whereas even small spatial differences in sand and mud fractions are well resolved. Subsamples of sediments from benthic grabs collected at each station were analyzed for their grain-size distribution. At four of the stations, duplicate analyses were conducted on separate subsamples to determine the sampling variability inherent in the determinations at a given station (Table 4). Determination of this inherent within-station variability is important because it dictates whether the perceived differences among stations can be considered significant. If the magnitude of the between-station (spatial) differences is comparable to that of the inherent within-station variability, then the perceived spatial differences are probably not reliably resolved. While this was the case for the largest size fractions, differences in the mud and sand fractions among the stations were clearly delineated by the analyses.

The percentage distribution of grain-size listed in Table 4 exhibits perceptible spatial differences among the sediment samples that were collected across the study area. However, duplicate analyses conducted on the same grab sample also exhibit some differences due to inherent

⁶ “Dup” lists the results of a duplicate analysis conducted on a separate subsample of sediment collected at particular station. Comparison with the results of the analysis conducted on the original subsample reflects the inherent (within-station) sampling variability in the grain-size analysis.

Figure 23. Cumulative Grain-Size Distribution of Duplicate Analyses a) with and b) without Coarse Fractions

sampling and analysis variability. In particular, the duplicate analysis conducted on the sediment chemistry sample collected at Station MRS15 (SC15Dup) contained an unusually large amount of pebble-sized material (5.76 percent) as compared to the original analysis conducted on a different subsample (0.16 percent in SC15). In fact, that subsample had more pebble-sized material than was found in any of the other subsamples.

These differences are visually apparent in the comparison of the cumulative size distributions shown in Figure 23. The disparity in coarse sand fractions between the original subsample (solid line) and the second subsample (dashed line), which is apparent in Figure 23a, is reduced significantly by exclusion of the coarse fraction (Figure 23b). The change is particularly apparent in the anomalous size distribution in the duplicated subsample from Station MRS15 (sample SC15 shown by the dashed red line in Figure 23a). Note that removal of the coarse fractions did not affect the somewhat anomalous sand distributions determined in the original subsamples at Stations MRS04 and MRS17 (samples SC04 and SC17 shown by the solid green and blue lines in Figure 23b). Those differences arose because some of the material in the subsamples was lost as a result of boil-over during digestion of organics using concentrated hydrogen peroxide.

Sample loss aside, why would the inherent variability in the coarse fraction be so much higher than for the sand and mud fractions? It is not because the weights of the duplicate and original subsamples were markedly different (Table 5). Moisture content was also similar between these samples, suggesting that the samples were properly homogenized prior to subsampling. Instead, the data indicates that the gravel and pebble-sized material is undersampled in the analysis of the subsamples. For example, the second (duplicate) subsample (SC15dup) analyzed at Station MRS15 happened to contain a single large pebble that accounted for almost 6 percent of the entire subsample weight.

The presence of pebble and gravel-sized particulates in the seafloor sediment samples arises from highly localized pockets of surficial shell hash that settles in the troughs of sand waves. In general, because of its patchy surficial distribution, the presence of pebble- and gravel-sized material is highly variable and does not accurately represent the variability in subsurface

Table 5. Weights used in the Grain-Size Analyses, Percent Summary for Major Size Classifications, and Moisture Content for All Sediment Subsamples

Phi Size (φ) Size (μm) Class	Dry Weight (grams)				Percentage Summary			
	Total	<-1	-1 to 4	>4	<-1	-1 to 4	>4	Moisture
		>2000	2000 to 62.5	<62.5	>2000	2000 to 62.5	<62.5	
		Coarse	Sand	Mud	Coarse	Sand	Mud	
SC01	109.254	0.000	82.076	27.178	0.00%	75.12%	24.88%	25.7%
SC02	111.701	0.000	78.848	32.853	0.00%	70.59%	29.41%	24.2%
SC03	76.972	0.006	32.957	44.009	0.01%	42.82%	57.18%	32.1%
SC04	99.238	0.220	50.465	48.553	0.22%	50.85%	48.93%	33.1%
SC04Dup	79.275	0.375	37.266	41.634	0.47%	47.01%	52.52%	32.8%
SC05	95.633	1.722	40.255	53.656	1.80%	42.09%	56.11%	37.2%
SC06	97.011	1.083	56.859	39.069	1.12%	58.61%	40.27%	34.1%
SC11	116.063	0.058	102.056	13.949	0.05%	87.93%	12.02%	23.8%
SC12	81.869	0.032	62.269	19.568	0.04%	76.06%	23.90%	30.5%
SC13	76.130	0.006	43.006	33.118	0.01%	56.49%	43.50%	35.8%
SC14	107.048	0.364	94.610	12.074	0.34%	88.38%	11.28%	26.7%
SC15	84.663	1.260	33.452	49.951	1.49%	39.51%	59.00%	42.3%
SC15Dup	72.560	4.586	22.261	45.713	6.32%	30.68%	63.00%	42.4%
SC16	92.506	2.708	51.598	38.200	2.93%	55.78%	41.29%	36.0%
SC16Dup	76.004	1.492	39.996	34.516	1.96%	52.62%	45.41%	39.7%
SC17	91.631	0.223	48.047	43.361	0.24%	52.44%	47.32%	38.3%
SC17Dup	72.618	0.073	34.446	38.099	0.10%	47.43%	52.46%	39.2%
SC18	77.334	0.000	52.029	25.305	0.00%	67.28%	32.72%	36.0%

sediments where the infauna reside. Because of this, the evaluation conducted in this report focuses on the sand and mud fractions. Similarly, because of sample loss during processing of the original subsamples at Stations MRS04 and MRS17, only the results from the analyses of the duplicate subsamples at those stations were used to evaluate the spatial variability in grain size throughout the study area, which is described below.

Grain-Size Characterization

Table 6 lists the summary parameters normally reported for grain-size distributions. Based on the discussion in the previous section, the results from less-reliable duplicate analyses are shown with strikethroughs. Statistical parameters such as mean particle size, standard deviation, and skewness, characterize sediment types by the well-recognized narrative descriptions that are listed in Table 7 on Page 42. These narrative descriptions are based on a comparison with a perfect log-normal distribution (Folk, 1980). Such comparisons work well if the grain-size distributions are unimodal, which was the case for all samples analyzed in the field survey. The most basic description is sediment type, which is determined by the relative amounts of gravel, sand, silt, and clay.

Table 6. Grain-Size Distributional Parameters

Sample	Mean (ϕ)	σ (ϕ)	Skewness	Mean (μm)	Percent Coarser than Listed Diameter (μm)				
					5%	16%	50%	84%	95%
SC01	3.75	0.852	0.39	74	151	109	80	47	12
SC02	3.93	0.951	0.54	66	126	99	76	37	8
SC03	4.75	1.668	0.46	37	164	94	53	10	3
SC04	4.93	2.379	0.56	33	294	111	64	5	1
SC04Dup	5.09	2.548	0.51	29	409	106	59	4	1
SC05	4.56	2.218	0.07	42	1291	139	52	11	4
SC06	4.55	3.205	0.42	43	1260	224	84	4	0
SC11	3.17	0.828	0.28	111	219	170	115	70	21
SC12	3.82	1.346	0.41	71	259	129	85	32	5
SC13	4.55	2.267	0.52	43	257	152	72	7	1
SC14	3.17	0.838	0.18	111	246	172	112	72	22
SC15	4.73	2.997	0.06	38	1371	264	43	5	1
SC15Dup	5.49	3.596	0.07	22	6653	150	31	2	0
SC16	4.62	3.357	0.38	41	1530	243	78	4	0
SC16Dup	4.82	3.240	0.39	35	1372	188	70	3	0
SC17	4.99	2.882	0.56	31	332	148	67	3	0
SC17Dup	5.19	3.089	0.44	27	984	126	58	3	0
SC18	4.29	2.618	0.68	51	300	183	107	7	0

Figure 24. Ternary Diagram of Grain-Size Properties with Coarse Fractions

Table 7. Narrative Classification of Grain-Size Distributions sorted by Water Depth

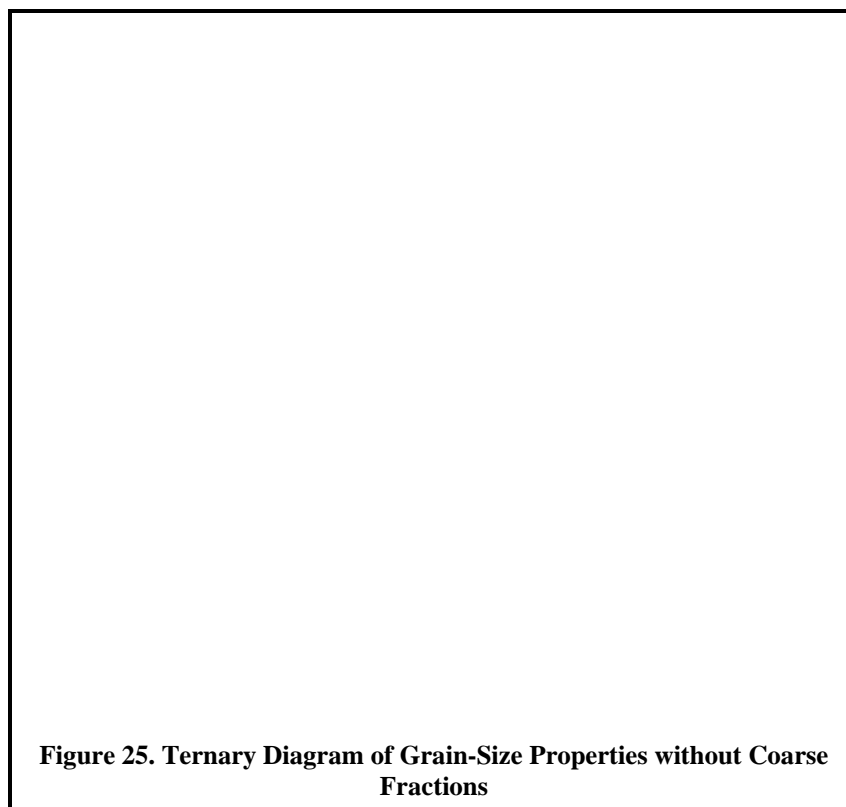
Sample	Depth (m)	Shoreline Distance (km)	Type	Sorting ⁷	Skewness ⁸
SC02	5.4	0.52	Silty Sand	Moderately Sorted	Strongly skewed toward more fines
SC11	6.2	0.55	Silty Sand	Moderately Sorted	Skewed toward more fines
SC12	17.4	0.96	Silty Sand	Poorly Sorted	Strongly skewed toward more fines
SC17	17.7	0.54	Silty Sand	Very Poorly Sorted	Strongly skewed toward more fines
SC17Dup	17.7	0.54	Sandy Silt	Very Poorly Sorted	Strongly skewed toward more fines
SC18	18.4	0.79	Silty Sand	Very Poorly Sorted	Strongly skewed toward more fines
SC01	26.7	1.25	Silty Sand	Moderately Sorted	Strongly skewed toward more fines
SC13	31.3	1.43	Silty Sand	Very Poorly Sorted	Strongly skewed toward more fines
SC14	36.1	1.92	Silty Sand	Moderately Sorted	Skewed toward more fines
SC15	53.7	2.30	Sandy Silt	Very Poorly Sorted	Near symmetrical
SC15Dup	53.7	2.30	Slightly Gravelly Sandy Mud	Very Poorly Sorted	Near symmetrical
SC03	56.8	2.56	Sandy Silt	Poorly Sorted	Strongly skewed toward more fines
SC16	61.8	2.94	Silty Sand	Very Poorly Sorted	Strongly skewed toward more fines
SC16Dup	61.8	2.94	Silty Sand	Very Poorly Sorted	Strongly skewed toward more fines
SC06	63.4	3.06	Silty Sand	Very Poorly Sorted	Strongly skewed toward more fines
SC04	68.0	4.08	Silty Sand	Very Poorly Sorted	Strongly skewed toward more fines
SC04Dup	68.0	4.08	Sandy Silt	Very Poorly Sorted	Strongly skewed toward more fines
SC05	68.7	4.01	Sandy Silt	Very Poorly Sorted	Near symmetrical

Sediment type can best be evaluated by the sample's position on a ternary diagram (Figure 24), which simultaneously displays the relative contribution of three size fractions. By virtue of their locations at the base of the triangle, none of the subsamples had a significant amount of gravel or coarser material, except for the duplicate subsample from Station 15 (SC15Dup). As described above, that subsample happened to contain a single large pebble, and consequently, it was classified in the "slightly gravelly" sediment type (Table 7). However, because sands and muds were the dominate size fractions, they made up the rest of the sediment-type designation.

Because the other subsamples consisted mostly of mud and sand, a second ternary diagram (Figure 25) can be used to further refine the dominate sediment type in the Project area. The diagram shows that the samples consisted largely of silts and sands, and the smallest size fraction (clay) constituted less than 15 percent of the sample weights. As a result, all were classified as silty sand or sandy silt, depending on whether more than half of the subsample consisted of sand-sized particles or silt-sized particles.

⁷ Narrative classifications of the degree of sorting is based on the standard deviation σ (ϕ) of the distribution as listed in Table 6 where moderately sorted distributions have $0.5 < \sigma < 1.0$, poorly sorted distributions have $1.0 < \sigma < 2.0$, and very poorly sorted distributions have $2.0 < \sigma$.

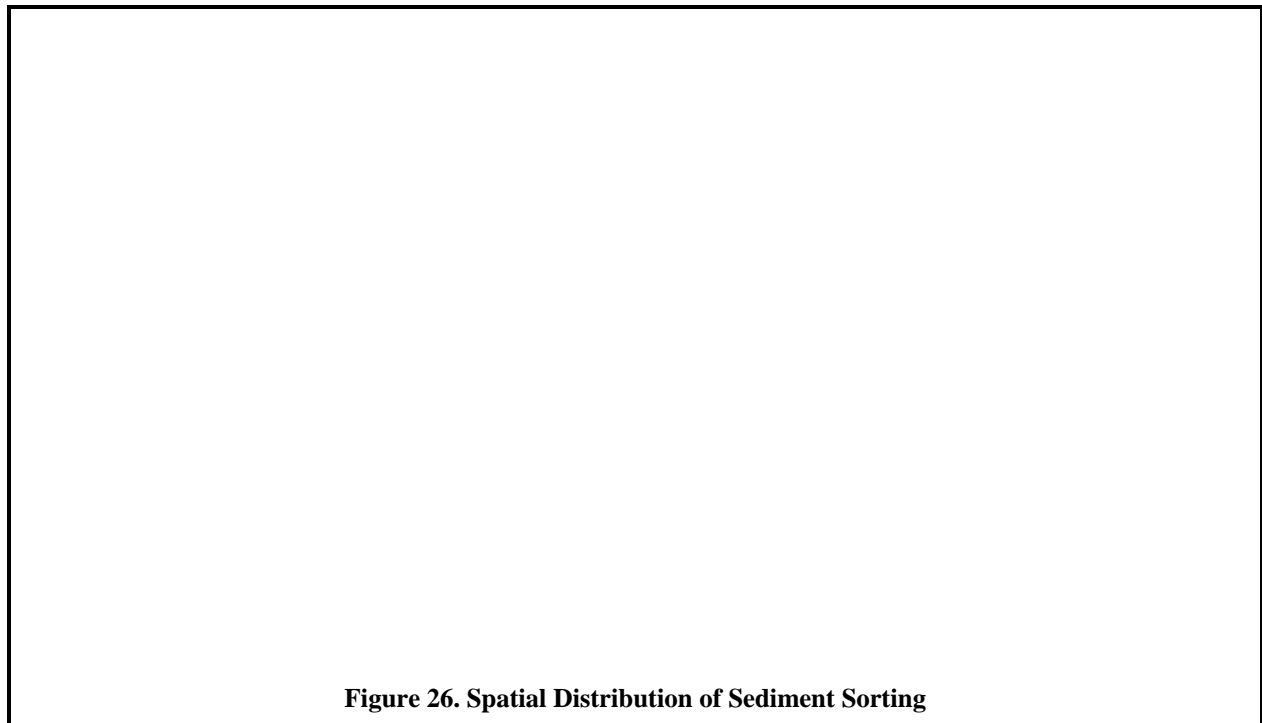
⁸ Narrative classifications are based on the skewness parameter listed in Table 6 where positive values indicate an excess of fines with nearly symmetrical distributions have $-0.1 < \text{skewness} < +0.1$, positively skewed distributions have $+0.1 < \text{skewness} < +0.3$, and strongly positively skewed distributions have $+0.3 < \text{skewness}$.



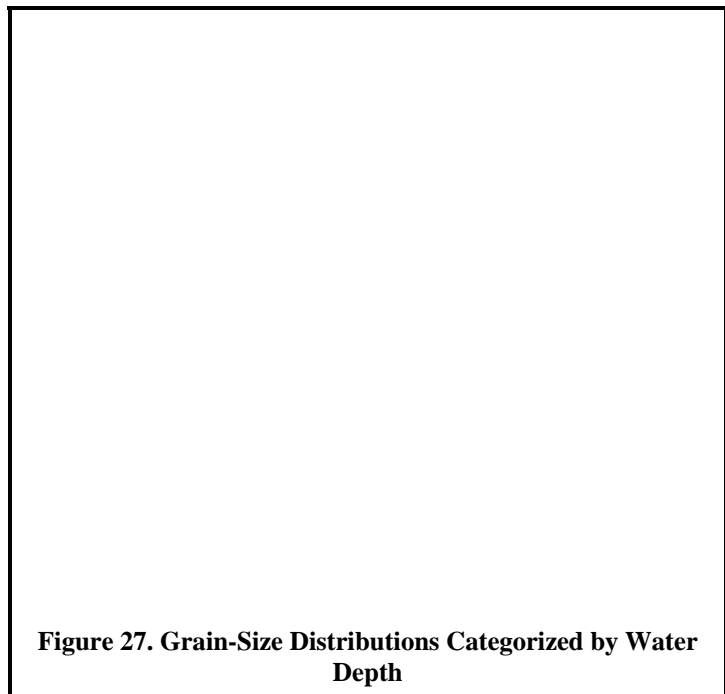
The narrative descriptions in Table 7 also characterize the spread (standard deviation) and asymmetry (skewness) of the observed grain-size distributions relative to the idealized log-normal distribution. These characteristics lend insight into the physical processes that originally determined the sediment distributions. Distributions that are skewed toward fine sediments tend to arise in depositional environments where the weak overlying flow field is incapable of winnowing the mud particulates from surficial sediments. Similarly, poorly sorted sediments, with large deviations from the mean, are found in quiescent environments where the sediments are not being regularly reworked and sorted into a single well-defined size class.

Cross-Shore and Seep Influences

The four smallest circles in Figure 26 indicate the sediments in samples SC01, SC02, SC11, and SC14 were moderately sorted. This level of sorting differed noticeably from the poor sorting found at the other ten benthic stations. The poor and very poor sorting found in the sediment samples collected at the other ten stations is indicative of an overlying benthic boundary layer where quiescent flow predominates. In contrast, the moderately sorted sediments found in the nearshore sediment samples (SC02 and SC11) were collected in water depths of less than 7 m. At that depth, strong oscillatory flow is occasionally generated near the seafloor by shoaling surface-gravity waves that are produced by passing winter storms. Over time, mechanical reworking of these nearshore sediments generally results in a more organized grain-size distribution that is dominated by fine and very fine sands.



Benthic samples collected at two other stations (SC01 and SC14) were also better sorted, despite their greater distance from shoreline. These samples were collected near natural seafloor seeps (Figure 26) where the energy associated with the seep discharge provided the sorting mechanism. In addition to enhanced sorting, both of these samples were also characterized by an unusually large amount of fine and very fine sand. As part of the original benthic sampling-station design, sample SC01 was intentionally collected very close to the Coal Oil Point Seep area east of the pipeline corridor (in Figure 26). As a result of its proximity to the seep area, that sample's grain-size distribution was somewhat unique among the four moderately sorted samples. Specifically, it had a noticeably greater fraction of medium and coarse sands compared to all other samples (dashed orange line in Figure 27), including the two nearshore samples (SC02 and SC11, shown by solid black lines). Steichen et al (1996)



also found that the surficial sediments surrounding hydrocarbon seeps tended to have an increased fraction of coarser grain sizes.

Although sediment sample SC14 was also influenced by seep processes, it was collected along the pipeline corridor in a location somewhat farther from an active seep area. As a result, its medium and coarse fractions of moderately sorted sediments were more comparable to those of the nearshore sediments than those of seep sample SC01. This is evident from the cross-shore trend in grain-size distributions along the pipeline corridor from Platform Holly to the EOF (Figure 28). The sand fractions on



Figure 28. Cross-Shore Grain-Size Distributions along the Pipeline Corridor between Platform Holly and the EOF

the right side of the figure split into two groups, with deep offshore samples (SC15, SC16, and SC06) having sand fractions approximately 15 percent lower than the seep (SC14) and nearshore stations (SC11, SC12, and SC13).

In contrast, the silt and clay fractions on the left of the figure exhibit a distinct cross-shore trend among the samples collected closer to shore, with the exception of seep sample SC14, which was out of step with the trend. Namely, clay-sized particles constituted less than one percent of the sample collected at the shallowest station (SC11, solid black line), but increased to three percent at the next deepest station (SC12, solid red line). The sample collected at Station MRS13 (sample SC13 shown by the blue line) had a clay fraction (eight percent) comparable to the deepest stations, while its elevated sand fraction (right side of the plot) remained comparable to the shallower stations. Even though the seep sediment sample SC14 (dashed orange line) was collected farther from shore than half the other samples, it had the lowest clay fraction of all the samples. Because of it was collected in a water depth of 40 m, processes other than wave-induced resuspension were responsible for removing fines from this sample. As described in subsequent sections of this report, however, the infaunal community within sediment sample SC14 was similar to the other seep sample SC01, indicating that the mechanics of seep discharge were responsible for winnowing clay and silt from both of these samples.

Insofar as seep proximity, sediment sample SC15 appears to have been collected closer (323 m) than SC14 (411 m) to the documented seep area that is centered on the pipeline corridor (Figure 26 on Page 44), yet the grain-size distribution in sample SC15 was very poorly sorted and consistent with other deep, non-seep sediment samples. The explanation for this is that the seep in question appears to no longer be active. The distribution of the seepage in this area was mapped by sonar in 1996. However, the location and volume of seep discharges have been shown to change significantly over time, with some active seeps disappearing entirely (Quigley et al 1999). The seep documented in 1996 at that location was not observed in the high-resolution bathymetry collected as part of this offshore survey. Instead, it is likely that the more-

recently mapped seep, designated Holoil Seep, may have influenced the sediments in sample SC14 (Leifer, Boles, Luyendyk, & Clark, 2004).

Along-Shore Trends

Because there are few known active seeps located along the alternative pipeline route, grain-size distributions within samples collected along that transect were dictated largely by water depth and distance from shore. Samples collected offshore of Las Flores Canyon (SC02, SC03, and SC04) traverse the inner continental shelf. With increasing distance from the shoreline, they exhibit a steady decrease in grain-size sorting, which is reflected by the steepness of the distribution function at its inflection point (Figure 29). Thus the cross-shore decrease in sorting arises from increasing clay fractions and decreasing sand fractions with increasing depth.

Figure 29. Grain-Size Distributions along the Alternative Pipeline Corridor between Platform Holly and LFC

The shallowest sample was collected at Station SC02, only 520 m from the shoreline in a water depth of 5.4 m (black line in Figure 29). Accordingly, it had moderately sorted, very fine sediments that were comparable to the nearshore sample SC11 collected along the existing pipeline corridor. Station SC03 was located farther offshore (2.56 km) in greater water depth (56.8 m) and where sediments were more poorly sorted with increased fine fractions and reduced sand fractions (brown line). The remaining samples (SC04, SC05, SC06, and SC16) were all collected in water depths comparable to Platform Holly, where sediments were very poorly sorted with high silt fractions. Spatial variability in sediment-size distributions among the six samples that were collected more than 2 km from shore in water depths exceeding 50 m was small compared to the variability among the nearshore and seep samples.

Moisture Variability

The moisture content of the benthic sediment samples was positively correlated with the mud fraction (Figure 30, Table 5 on Page 40). Consequently, samples SC01, SC02,

Figure 30. Relationship between Sediment Sample Moisture and Mud Fraction

SC11, and SC14 had the lowest moisture content by virtue of their silt and clay deficiencies. However, higher moisture content in muddier samples is counterintuitive because one would expect smaller porewater volumes in compact fine sediments due to their smaller interstices. In practice however, the greater porosity in the sandier samples results in less water retention when the grab sampler is raised out of the water and positioned on the survey vessel. Thus, prior to collection of the sediment samples used in the analysis, more water drained out of the sandier samples. As a result, the reported moisture contents do not accurately reflect *in situ* conditions and do not directly lend insight into seafloor sediment conditions, such as compaction. Nevertheless, quantifying the moisture content specific to the samples themselves is vital for accurately determining other physicochemical properties. In particular, determination of dry-weight chemical concentrations and the dissolved solids (salt) content used in grain-size analyses are dependent on the sample's moisture content, not the *in situ* moisture.

3.2.2 Chemical Properties

Total petroleum hydrocarbon (TPH) concentrations were measured within subsamples of seafloor sediments that were collected during the benthic leg of the marine-resource survey, and are regularly measured during the annual offshore monitoring program for the Goleta Sanitary District's (GSD) effluent discharge (Table 8, Figure 31). The GSD benthic stations are located approximately 5 km east of the survey area, on the other side of Coal Oil Point (Figure 19 on Page 30). The GSD TPH concentrations reported in the table were measured in samples collected in 2005 (Aquatic Bioassay & Consulting Laboratories, Inc., 2006). The raw instrumental responses recorded for MRS benthic subsamples (Figure 22 on Page 37) were converted to bulk concentrations, dry weight concentrations, and dry concentrations normalized to the mud fraction.

Table 8. Sediment Hydrocarbon Concentrations and Related Sediment Properties Offshore Ellwood and Goleta

Sample	Depth (m)	Distance (km)			Concentration				
		Shore	Seep	High Seep	Moisture (%)	Mud (%)	TPH Bulk (mg/kg)	TPH Dry (mg/kg-dry)	TPH Normalized (mg/kg-mud)
SC01	26.7	1.3	0.03	0.68	25.7	24.9	278	374	1503
SC02	5.4	0.5	12.76	15.54	24.2	29.4	473	624	2122
SC03	56.8	2.6	10.07	13.13	32.1	57.2	290	427	747
SC04	68.0	4.1	6.72	10.02	32.9	52.5	398	593	1129
SC05	68.7	4.0	1.15	4.35	37.2	56.1	217	345	615
SC06	63.4	3.1	0.81	1.34	34.1	40.3	202	306	760
SC11	6.2	0.6	1.93	3.80	23.8	12.0	491	644	5358
SC12	17.4	1.0	1.56	3.64	30.5	23.9	335	482	2017
SC13	31.3	1.4	1.04	3.37	35.8	43.5	637	992	2280
SC14	36.1	1.9	0.41	3.06	26.7	11.3	377	515	4566
SC15	53.7	2.3	0.32	2.79	42.4	59.0	129	224	380
SC16	61.8	2.9	0.60	2.28	37.9	45.4	112	180	396
SC17	17.7	0.5	0.63	0.68	38.7	52.5	229	374	713
SC18	18.4	0.8	0.65	0.85	36.0	32.7	160	250	764
GSD S1	49.9	1.3	2.25	0.77	—	39.8	—	703	1768
GSD S2	31.4	1.6	3.68	2.12	—	48.4	—	675	1395
GSD S3	31.2	1.7	3.74	2.27	—	23.3	—	401	1720
GSD S4	31.1	1.7	3.79	2.38	—	28.1	—	709	2521
GSD S5	31.1	1.7	3.79	2.38	—	47.7	—	320	671
GSD S6	31.1	1.7	3.79	2.38	—	24.9	—	405	1625



Table 8 compares these various forms of TPH concentrations with spatial parameters that may have an influence on the concentrations, namely, water depth, shoreline distance, and distance to documented seeps. Both the distance to the outer margin of the seep, and the closest-approach distance from seep areas that are associated with high discharge rates (purple and red shading in Figure 31) are of import. The table also compares TPH concentrations with potentially influential physical properties of sediments, namely, moisture content and mud fraction.

Two conclusions follow from an analysis of the sediment TPH concentrations. First, TPH concentrations throughout the study area, including the GSD discharge location, were high compared to most other open coastal regions offshore California. Second, the measured TPH concentrations bore no apparent relationship to water depth, shoreline distance, seep proximity, moisture content, or mud fraction. Thus, seep hydrocarbons are pervasive throughout the seafloor sediments in the region, but are somewhat patchy in their distribution. As discussed in the following section, the infaunal communities in the sediment samples with elevated TPH were fundamentally different from those of the other stations, indicating that the perceived differences in concentrations were well-resolved by the sampling program, and were not due to random sampling error.

The TPH concentrations measured during the benthic leg of the marine-resource survey, and those measured near the GSD outfall to the east, all exceeded 180 mg/kg-dry, and in one sample (SC13) approached 1000 mg/kg-dry. TPH concentrations this high are rarely found in sediments along the open coastal reaches of California, except in areas where natural hydrocarbon seeps occur. For example, along the central California coastline, sediment TPH concentrations are rarely detected above a method detection limit (MDL) of 10 mg/kg. In 80 seafloor sediment samples collected over the last decade in Estero Bay, which is located 130 km (80 miles) north of the study area, only five samples exceeded the MDL (Marine Research Specialists, 2007). The

highest TPH measured was 46 mg/kg-dry, an order-of-magnitude lower than the average concentrations measured offshore Ellwood (477 mg/kg-dry).

Oceanic dispersion processes normally distribute sediment contaminants so that concentrations increase with proximity to the seafloor source. In addition, contaminant concentrations, particularly trace metals, tend to naturally increase with increasing mud fractions because binding sites are more plentiful due to the greater available surface area per unit volume. However, neither of these trends was apparent in the TPH database (Table 8). Specifically, linear regression of TPH concentrations against seep proximity, shoreline distance, water depth, or mud content did not reveal a statistically significant correlation at the 95-percent confidence level ($p > 0.24$).⁹ The lack of a relationship indicates that normalization of TPH concentrations by the mud fraction, shown in the last column of the table, does not serve to measurably reduce inherent variability among the samples.

The patchy distribution of the measured TPH concentrations is visually apparent in Figure 31. The highest TPH concentration, 992 mg/kg-dry in sample SC13, was not found in the sample (SC14) that had a coarse, well-sorted grain-size distribution indicative of reworking by seep processes. In addition, sample SC01, collected within 30 m of a known seep, had a TPH concentration (278 mg/kg-dry) that was well below the average for the area. Finally, the sediment samples collected along the deeper sections of the pipeline corridor (SC15, SC16, SC06) had some of the lowest TPH concentrations (≤ 202 mg/kg-dry) while samples collected at sites more distant from the seep field, along the alternative pipeline corridor (SC02, SC03, SC04), had higher concentrations (≥ 290 mg/kg-dry).

The patchiness of the TPH distributions within the sediments throughout the study area suggests that hydrocarbons from seep discharges are randomly deposited. This is consistent with findings concerning the distribution of tarballs along California beaches, namely, that hydrocarbons from seeps within the Santa Barbara Channel are dispersed over large distances by ocean currents and winds (Hostettler, Rosenbauer, Lorenson, & Dougherty, 2004). For example, during and after the offshore survey, a series of winter storms dispersed seep hydrocarbons along beaches as far north as Monterey Bay (Hostettler, 2007).

3.3 BENTHIC INFAUNAL BIOLOGY

It is important to characterize benthic infauna as part of any marine resource assessment because they are the organisms most likely to be impacted by marine construction as part of the proposed Project or the offshore pipeline alternative. Also, infauna living within the surficial sediments act as sensitive sentinels for the presence existing anthropogenic impacts. In particular, they serve as indicators of existing marine pollution because they have limited mobility and cannot easily escape exposure to contaminants in their environment. The presence of existing, impaired benthic conditions in the Project area is important to document, not only because they are part of the baseline characterization, but because contaminants that reside within the sediments could be resuspended into the water column by construction activities, where they could be spread and become more bioavailable to marine organisms.

⁹ The “ p ” value reflects the likelihood that a measured trend is due to chance alone, and the smaller the p -value the more statistically significant is the relationship. Thus, a p -value of 0.05 (5%) coincides with the 95% confidence level and reflects a 5% risk that the difference is not significant, but due to chance alone.

Benthic infauna are particularly useful for identifying the presence of marine pollution because of their well-defined response to contaminants. Many laboratory toxicity bioassays and field studies have documented which species are more sensitive to pollutant stresses, as well as those that are tolerant and opportunistically populate impaired environments in the absence of competition from sensitive organisms. Changes in relative abundance of these taxa can imply the presence of degraded environmental conditions. Thus, infaunal community structure is often more diagnostically important than total population levels. However, quantifying and analyzing benthic community structure is complex; the use of multivariate statistical techniques significantly enhances the historical reliance on univariate properties such as organism density and species diversity.

Benthic infauna are also important indicators of marine pollution because of where they reside. Contaminants discharged into marine waters are preferentially associated with particulates, which ultimately settle and accumulate on the seafloor. Because infauna reside within seafloor sediments, they are closer to this source of pollution. Also, infauna occupy a relatively low trophic level within the marine food chain. They are relatively sessile within surficial sediments, making them a major food source for the more mobile benthic epifauna, such as crabs, which are, in turn, consumed by demersal finfish and marine mammals. Additionally, many infauna are filter feeders that may bioaccumulate contaminants to detectable levels even when standard chemical assays of seawater samples are unable to detect low-level contamination. These contaminants can be biomagnified as they are passed up the food chain to higher trophic levels.

In recognition of infauna's role as a sensitive and important detector of marine pollution, most marine monitoring programs require regular assessments of the overall health of the benthic community. Infaunal assessments also address the COP requirement that indigenous marine biota not be degraded. Mechanical disturbance of seafloor sediments caused by trenching of cross-shore water pipelines and power cables could impact infauna to a limited extent. Additionally, any accidentally spilled oil could impinge on the nearshore benthos, affecting both subtidal and intertidal infauna. If spilled from a subsea pipeline, oil could also locally impact infauna in the area surrounding the breach.

3.3.1 Univariate Analyses

Determination of whether adverse biological conditions exist within the study region involves assessing whether the existing benthic environment supports a balanced indigenous population (BIP) of shellfish, fish, and wildlife. A BIP is an ecological community which exhibits characteristics similar to those of nearby, healthy communities existing under comparable, but unpolluted, environmental conditions. Certain biological characteristics of the community examined in an evaluation of a BIP including species composition, abundance, biomass, dominance, and diversity; spatial and temporal distributions; trophic structure; and the presence or absence of indicator species. Most marine environmental assessment programs determine the presence of a BIP using data based solely on the infaunal organisms that live with sediments surrounding a potential pollutant source. In evaluating a BIP, infauna have an important advantage over other marine organisms, such as marine mammals or finfish. Infauna are relatively easy to collect in numbers large enough for reliable statistical testing, and they do not move over large areas, so their response is site specific.

Pollution affects marine ecosystems by changing the number and type of benthic organisms found in the sediments. Consequently, subtle changes in community composition are not always readily apparent in the large volume of raw data generated by field surveys. With more than 53,000 individual organisms representing 367 individual taxa that have been collected in the region, global assessments of the infaunal community are challenging. These data must be summarized into concise parameters that are indicative of existing environmental conditions, and their variation in time and space. Biodiversity is a common indicator of the well-being of ecological systems, and forms the cornerstone of most impact assessment studies. Unfortunately, biodiversity is difficult to define quantitatively.

One of the difficulties is that diversity has two major components: species richness and evenness. For example, two samples may have the same number of species and individuals, namely, the same richness. However, one sample may have most of its organisms concentrated into only a few species (uneven), while the second sample has abundance evenly distributed among the species. The diversity index would be higher for the second sample. Thus, species richness measures the variety (number) of species, while evenness measures the distribution (abundance) of individuals among the species (Magurran, 1988). Healthy ecosystems are thought to be both rich in species and evenly distributed with respect to individuals among those species. Although no single measure can accurately represent changes in both evenness and richness along a pollution gradient, many indices attempt to do so. The Shannon Diversity Index (H') is the most widely used diversity index because it exhibits some degree of sensitivity to both evenness and richness.

Typically, diversity and other infaunal indices are determined within individual samples and their variation among the samples is examined for trends potentially related to environmental gradients. To that end, standard biological community indices were determined from the abundance data in the 99 infaunal samples examined as part of this study (Table 9). However, these indices only reflect the diversity within a local area at a particular time (α -diversity). In contrast, pollution and other stresses tend to induce marked changes in community composition between samples that are widely separated spatially and temporally, which is measured by β -diversity (Smith, Gibson, Brown-Leger, & Grassle, 1979). Thus, analysis of individual measures of α -diversity within samples is not well-suited to an infaunal dataset containing moderate levels of β -diversity (heterogeneity), such as in the dataset considered here. Compositional differences among the 99 samples examined as part of this analysis were moderately large, as demonstrated by a Whittaker (1972) β -diversity of 3.2.¹⁰

There are other limitations associated with the traditional community indices listed in Table 9. Most diversity indices are poorly suited for describing potential impacts to infaunal communities because they lack biological meaning, show little correlation with environmental quality, are difficult to interpret ecologically, and often result in ambiguous or biased estimates of diversity (Goodman, 1975; Washington, 1984; Green, 1979). As a result, many indices are not recommended for routine inclusion in benthic monitoring programs (U.S. Environmental Protection Agency, 1987).

¹⁰ β_w measures the ratio of the total number of species in the dataset to the average number species in the samples, minus 1. If $\beta_w=0$, then all the samples have the same number of species. $\beta_w=3.2$ indicates that the database had over four-times as many species as the average individual sample.

Despite all of these reservations, a large number of marine benthic studies have routinely reported the standard infaunal community indices for decades, and relied on them in their examinations of temporal and spatial trends. This historical record of univariate analyses provides a useful backdrop for comparison of the infaunal data examined in this study. Although multivariate techniques are somewhat better suited to the evaluation of datasets with high β -diversity, univariate statistics generally confirm the multivariate results presented in the following subsection.

Organism Density

Table 9 reports infaunal parameters determined for a specific point in time at 44 benthic sites. These results were based on an analysis of 99 sediment grab samples collected over the past 30 years. One of the sites, Ref5_60 was sampled on two separate occasions, once in 1977, and again in 1985. Another site, Arc06, was sampled three times, so indices are reported for 47 individual instances at a total of 44 sites in Table 9. In addition, multiple indices determined from individual replicate grab samples collected during 20 of these sampling occasions in the GSD and Arco databases were averaged to compute a single index for each sampling location and time. Data based on counts, such as the number of individuals or species, were log-transformed prior to averaging. Transformations of abundance and other types of data prior to analysis were performed to make the variables more biologically meaningful, conform to a statistical distribution (usually Gaussian), achieve additivity, and stabilize variance (homoscedasticity).

The “*Total Organisms*” column in Table 9 lists the average abundance of all infaunal taxa within a 0.1 m surface area of the seafloor. The 53,102 individual infaunal organisms represent 357 infaunal taxa. Motile epifaunal taxa were excluded from the database. Additionally, most of the community indices are based only upon those organisms identified to species level. Because of their size, or because the specimens were damaged, only approximately 39,537 organisms, or 74 percent of the original subset, were identified as one of the 272 species. Their abundances are listed in the column entitled “*Identified Organisms*.” The next two columns list the total number of species, and the ratio of the number of identified organisms to the total number of species. While this provides a crude measure of α -diversity within each sample, the other indices provide more stable measures of diversity because they account for differences in the frequency distributions of abundance and species.

Organism density ranged across more than an order of magnitude, with all of the GSD samples containing strikingly higher densities (Figure 32). Although the distribution on the map suggests a spatial difference, the increased infaunal densities found in GSD samples arose because populations in 2005, when the GSD samples used in the analysis were collected, were markedly higher than historical levels (Figure 33 on Page 56). Prior to 2004, average numbers of individuals remained steady, with densities in the range of those reported in the other studies described in this report.

Table 9. Average Infaunal Community Indices

Source	Station	Sample ID	Total Organisms	Identified Organisms	Number of Species	Organisms per Species	Diversity (H')	Brillouin Index (h)	Dominance (C')	Dominance (75%)	Species Richness (d)	Evenness (J')
Arco Coal Oil Point EIR	Arc01	Ar4S01	126	76	24	3.20	2.79	2.39	0.10	13	5.39	0.88
	Arc02	Ar4S02	161	117	33	3.62	3.00	2.62	0.09	15	6.82	0.86
	Arc03	Ar4S03	243	160	30	5.32	2.69	2.43	0.13	10	5.81	0.79
	Arc04	Ar4S04	231	172	42	4.13	3.21	2.88	0.07	17	7.95	0.86
	Arc05	Ar4S05	311	244	56	4.37	3.55	3.22	0.05	24	10.06	0.88
	Arc06	Ar4S06	204	146	34	4.23	2.91	2.59	0.11	13	6.79	0.82
		ArAS06	272	234	38	6.16	2.99	2.75	0.08	12	6.84	0.82
		ArJS06	144	115	24	4.96	2.57	2.28	0.13	8	4.85	0.81
	Arc07	Ar4S07	177	119	34	3.58	3.31	2.91	0.05	17	6.97	0.94
	Arc08	Ar4S08	156	111	29	3.84	2.87	2.52	0.11	13	5.99	0.85
	Arc09	Ar4S09	84	61	15	4.13	2.15	1.84	0.21	7	3.52	0.79
	Arc10	Ar4S10	190	129	27	4.91	2.25	1.99	0.26	8	5.43	0.68
Goleta Sanitary District	Arc11	Ar5S11	310	284	39	7.42	2.86	2.65	0.10	11	6.66	0.78
	Arc12	Ar5S12	206	177	34	5.25	2.77	2.51	0.11	10	6.37	0.79
	GSD1	GSDS1	1227	819	117	7.05	3.70	3.49	0.06	25	17.33	0.78
	GSD2	GSDS2	1287	921	85	10.99	2.76	2.63	0.18	10	12.34	0.62
	GSD3	GSDS3	1487	1113	114	9.82	3.17	3.01	0.15	17	16.13	0.67
	GSD4	GSDS4	1105	866	97	9.01	2.78	2.62	0.22	13	14.16	0.61
Marine Research Specialists Ellwood Full Field EIR Marine Survey	GSD5	GSDS5	1217	950	115	8.30	3.13	2.96	0.17	20	16.63	0.66
	GSD6	GSDS6	1120	858	107	8.01	3.08	2.90	0.18	19	15.76	0.66
	MRS01	MRS01	108	71	28	2.54	2.80	2.36	0.11	11	6.33	0.84
	MRS02	MRS02	284	143	50	2.86	3.44	3.01	0.05	19	9.87	0.88
	MRS03	MRS03	239	176	54	3.26	3.62	3.22	0.04	23	10.25	0.91
	MRS04	MRS04	171	144	40	3.60	2.96	2.61	0.10	12	7.85	0.80
	MRS05	MRS05	110	80	30	2.67	3.03	2.58	0.07	14	6.62	0.89
	MRS06	MRS06	94	72	32	2.25	3.14	2.63	0.06	16	7.25	0.91
	MRS11	MRS11	135	66	33	2.00	3.30	2.73	0.05	17	7.64	0.94
	MRS12	MRS12	204	99	44	2.25	3.54	3.01	0.04	21	9.36	0.94
	MRS13	MRS13	286	200	61	3.28	3.79	3.38	0.03	26	11.32	0.92
	MRS14	MRS14	233	176	36	4.89	2.58	2.31	0.17	10	6.77	0.72
	MRS15	MRS15	163	122	34	3.59	2.91	2.57	0.09	10	6.87	0.83
	MRS16	MRS16	99	72	38	1.89	3.48	2.88	0.04	20	8.65	0.96
	MRS17	MRS17	134	101	39	2.59	3.31	2.84	0.05	16	8.23	0.90
	MRS18	MRS18	90	66	30	2.20	3.11	2.60	0.06	14	6.92	0.92

Source	Station	Sample ID	Total Organisms	Identified Organisms	Number of Species	Organisms per Species	Diversity (H')	Brillouin Index (h)	Dominance (C')	Dominance (75%)	Species Richness (d)	Evenness (J')
Southern California Coastal Water Research Project	B94S112	SCB4S112	409	255	66	3.86	3.50	3.17	0.06	22	11.73	0.84
	B94S136	SCB4S136	399	276	56	4.93	3.39	3.11	0.05	16	9.79	0.84
	B94S016	SCB4S16	555	423	91	4.65	3.96	3.65	0.03	30	14.88	0.88
	B94S038	SCB4S38	542	399	82	4.87	3.79	3.50	0.04	26	13.52	0.86
	B94S060	SCB4S60	547	399	82	4.87	3.92	3.62	0.03	29	13.52	0.89
	B98S2356	B98S2356	523	371	92	4.03	3.87	3.54	0.04	30	15.38	0.86
	B98S2357	B98S2357	173	111	32	3.47	3.04	2.67	0.07	13	6.58	0.88
	B98S2359	B98S2359	442	367	71	5.17	3.55	3.28	0.05	22	11.85	0.83
	B98S2360	B98S2360	174	134	44	3.05	3.26	2.86	0.06	17	8.78	0.86
	Ref5_30	Rf5SR5-3	169	119	50	2.38	3.49	3.00	0.05	22	10.25	0.89
	Ref5_60	Rf7SR5-6	316	270	36	7.50	2.31	2.13	0.21	6	6.25	0.65
		Rf5SR5-6	313	223	55	4.05	3.32	2.99	0.07	19	9.99	0.83
	Ref6_60	Rf7SR6-6	223	179	37	4.84	2.70	2.43	0.15	11	6.94	0.75

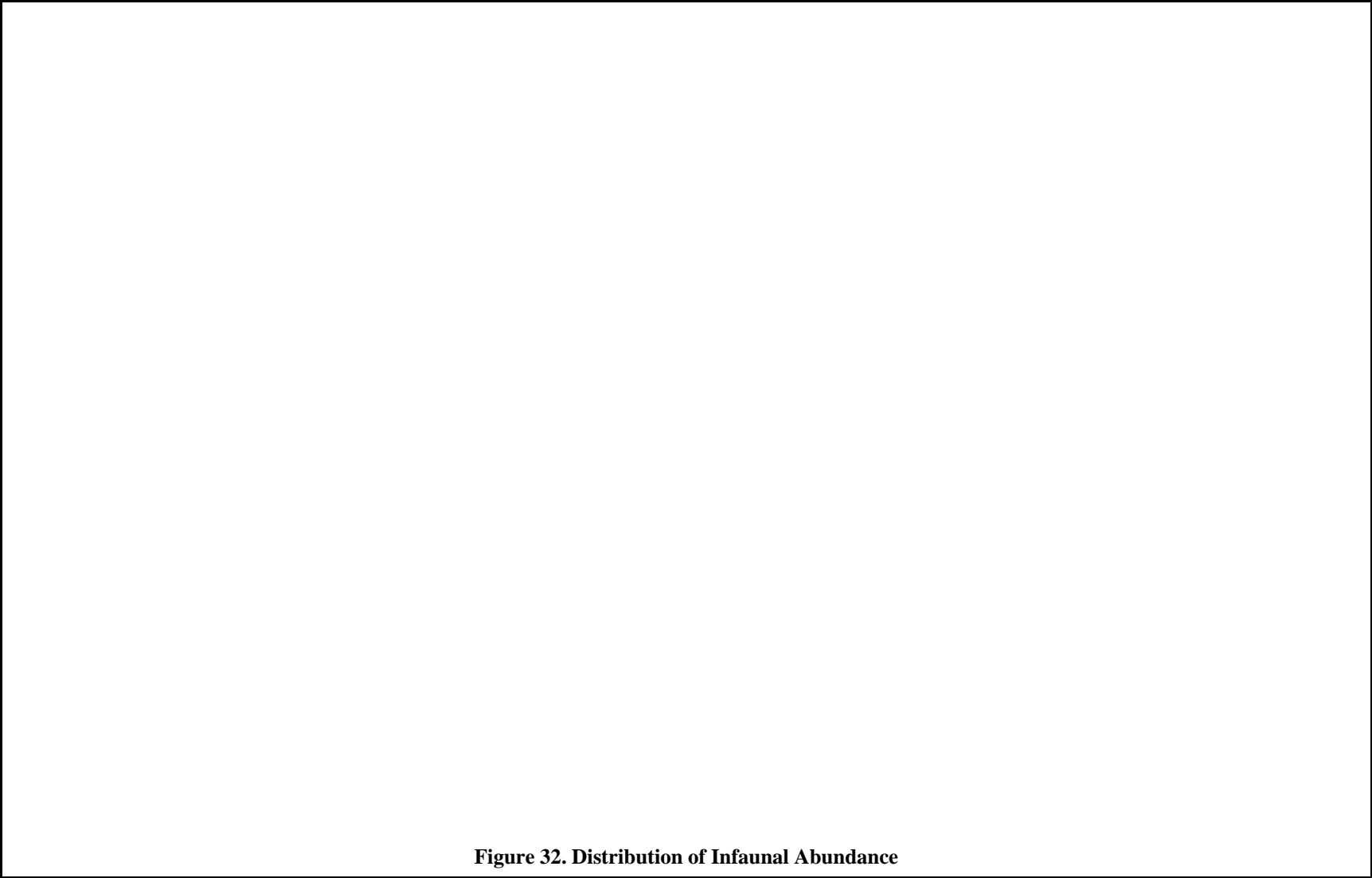
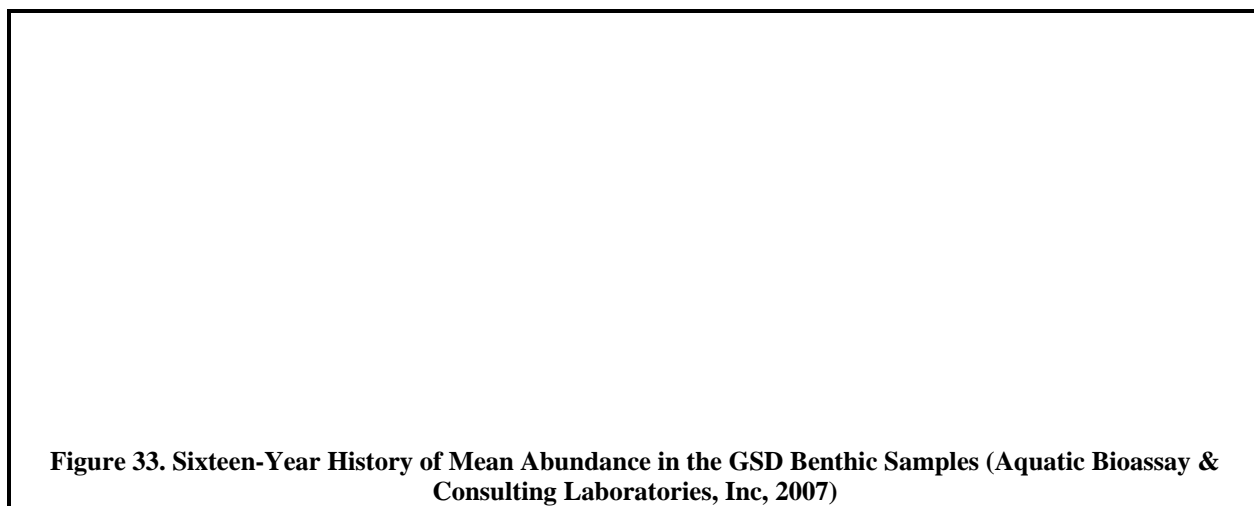


Figure 32. Distribution of Infaunal Abundance



It is not known whether the GSD infaunal densities continued to be high into 2007, when the MRS Ellwood samples were collected, but the data suggests that the anomalously high GSD densities highlighted on the map for 2005 did not continue into the winter of 2007, and that the difference that is apparent on the map was largely due to temporal rather than spatial variability. As discussed below, the observed population increase was not reflected by an increase in diversity. Instead, the increase was largely due to high recruitment of the cirratulid polychaete *Monticellina* spp., as well as other taxa during 2004, after which populations remained high into 2005, when *Monticellina* spp. represented 31 percent of the organisms collected (Aquatic Bioassay & Consulting Laboratories, Inc., 2006).

Species Diversity

The Shannon diversity index (H') (Shannon & Weaver, 1949) is one of the most common diversity indices used in ecological assessments. It measures the relative distribution of individual organisms among the species present in the sample. H' increases for broader distributions of individuals among species. If all individuals are of one species then H' is 0.00. If each individual organism is a separate species then H' is determined by the logarithm of the total number of organisms collected. For other distributions, the diversity index is given by:

$$H' = - \sum_{j=1}^S \left[\left(\frac{n_j}{N} \right) \ln \left(\frac{n_j}{N} \right) \right]; \text{ where: } S = \text{total number of species, } n_j = \text{number of individuals in the } j^{\text{th}}$$

species, N = total number of individuals, and \ln = natural logarithm (base e).

Some studies have found a decrease in this index in response to pollutant stress in benthic communities. However, this index is ambiguous because it depends on how evenly the organisms are distributed among the species. Consequently, a statistically significant reduction in this index can occur in the absence of anthropogenic (human-induced) stresses. The value of the Shannon index usually falls between 1.5 and 3.5, and only rarely surpasses 4.5 (Margalef, 1972). Table 9 shows that approximately 20 percent of the samples had a diversity exceeding 3.5. However, there was no clear spatial pattern associated with the distribution of diversity within the database. Accordingly, the high abundances found in the GSD samples in 2005 were

tempered by an increased number of species, and the resulting diversity in those samples was comparable to the rest of the database.

When randomness in the sample cannot be guaranteed, then the Brillouin index (h) is a more appropriate measure of diversity (Pielou, 1977). It is calculated using the formula:

$$h = \frac{\ln(N!) - \sum_{j=1}^S [\ln(n_j!)]}{N}$$

The Brillouin index gives a similar measure of diversity as the Shannon

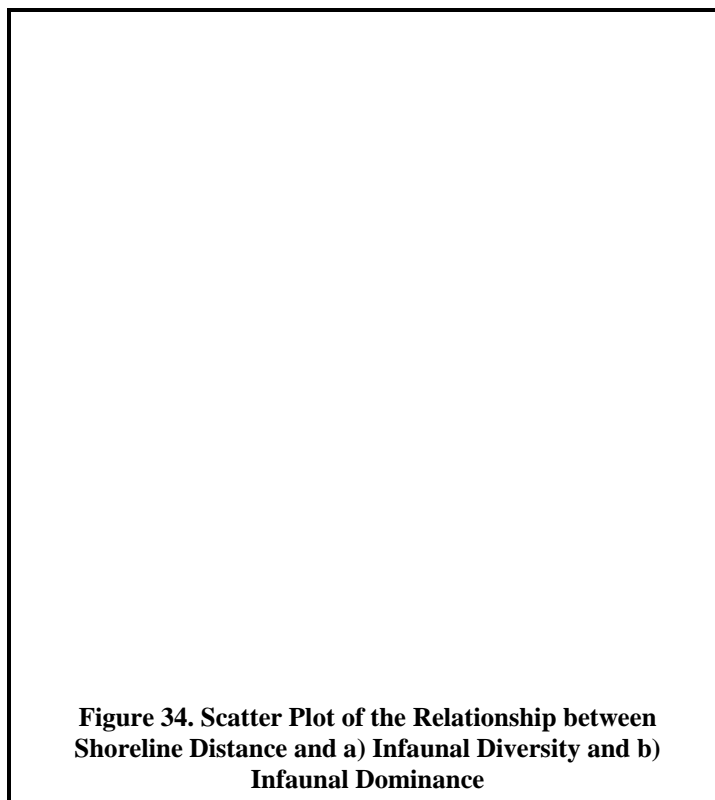
index when applied to the same data, although it produces a slightly lower value. In contrast to the Shannon index, however, the Brillouin index will vary between samples although the number of species and their proportional abundance remain the same. Because of its dependence on sample size and the increased complexity of its computation, the Brillouin index is more rarely used than the Shannon index. Table 9 shows that although the Brillouin index was smaller in magnitude, it ranked the samples in nearly the same order as the Shannon index with regard to diversity.

Diversity tended to decrease with increasing distance from the shoreline among the samples analyzed in the study region (Figure 34a). Although there was substantial scatter among the data, the linear correlation was statistically significant ($p < 0.001$).

Species Evenness

The Pielou evenness index (J') (Pielou, 1977) measures how evenly the individual organisms are distributed among the species present in the sample. J' increases for more even distributions of individuals among species. If all individuals belong to a single species, then J' is indeterminate. If each species is represented by a single organism, then J' will be equal to 1.00. For other distributions, the evenness index is given by: $J' = \frac{H'}{\ln S}$;

where: S = total number of species, and H' = Shannon-Wiener diversity index. Because this index is derived from the Shannon-Wiener diversity index (H'), it is subject to the same limitations. This index ranged between 0.61 and 0.96 in the database. In general, the MRS samples collected in 2007 had the most even distribution of abundance across species. Eight of the fourteen samples had an evenness index exceeding 0.9.



Species Dominance

Dominance indices increase with decreasing diversity and are heavily weighted toward the most common species in a sample. The best known of these measures is Simpson's index (C') (Simpson, 1949; Wittaker, 1965). It is related to other diversity and evenness indices, but increases with increasing proportions of individuals associated with a few species. If all individuals are of one species, then C' is maximized and is equal to the maximum dominance of 1.00. If individual organisms are evenly distributed among species ($J'=1.00$), then C' asymptotically approaches 0.00 with increasing numbers of individuals. The Simpson dominance

measure is given by: $C' = \sum_{j=1}^S \left(\frac{n_j}{N} \right)^2$ but for finite communities, the unbiased form is:

$$C' = \sum_{j=1}^S \left(\frac{n_j(n_j - 1)}{N(N - 1)} \right) \text{ (Magurran, 1988). In contrast to evenness and diversity, no clear pattern of}$$

Simpson's dominance emerged with respect to location or study in Table 9.

An unrelated measure of dominance has been ascribed to Swartz et al. (1985). The Swartz dominance index (Sw) is defined as the minimum number of species that account for 75 percent of all individual organisms collected in a sample. In this dominance measure, species are first ranked by the number of individual organisms before establishing the cumulative percent equal to or exceeding 75 percent. This is an inverse measure because higher dominance is reflected in a lower number of species accounting for 75 percent of the individual organisms. Despite this, it is not subject to many of the limitations that plague the other univariate indices. It is a non-parametric measure that does not assume an underlying distribution of individuals among species.

Because it is a more robust measure of dominance, the cross-shore trend in Sw revealed that the decrease in diversity with increasing shoreline distance was partially related to an increase in species dominance (Figure 34b). Despite the scatter in the data, this cross-shore trend was statistically significant ($p < 0.001$). It demonstrates that the cross-shore diversity decrease was not solely due to a decrease in the number of species (species richness). Instead, the diversity trend was also affected by an increase in the dominance of some taxa.

Species Richness

The Margalef species richness index (d) (Margalef, 1951) measures the number of species in a sample relative to the number of individual organisms. d strongly increases for increasing numbers of species and increases only logarithmically for decreasing numbers of individuals. If only one species is present then d is 0.00. For other distributions, the richness index is given by:

$$d = \frac{S - 1}{\ln N}. \text{ Its applicability to biological communities is dependent on whether specimens are log-}$$

normally distributed among the species in a given sample. Such an assumption is not globally applicable to benthic marine communities, and without testing each data set, this richness index is of questionable value. Its undue dependence on the number of species is reflected in Table 9 where the increased numbers of species that were found in the GSD samples caused those six samples to have a higher reported richness index than most other samples in the database.

3.3.2 Multivariate Analyses

The multivariate complexity of infaunal abundance data makes analysis and summary challenging. Application of standard statistical methods is often inadequate for many reasons. Individual benthic samples can contain many species, each of which is enumerated separately. Other samples can contain a completely different suite of organisms. In this analysis, the resulting data matrix consisted of counts for 357 species in 99 samples. Analyzing this complex matrix for potential differences among samples by comparing differences in individual species is intractable, not just because of the number of species, but because pairs of samples may have few or no species in common. In response to these challenges, onshore landscape ecologists have, over the last 50 years, developed specialized multivariate analysis tools. These analysis techniques are highly effective at extracting the dominant patterns from complex species-sample databases. The multivariate techniques employed exploit redundancies (correlations) in the abundance of individual species among the samples, and compress the data into the most meaningful patterns.

Unfortunately, the dominant patterns extracted from the species-sample hyperspace are presented in ordination diagrams that can be difficult to grasp intuitively, at least initially (See, for example Figure 37 on Page 65). This is largely because the diagram's axes do not represent distances in physical dimensions. Instead, the locations of the points within the diagram characterize the composition of the community within individual benthic samples. The distance between a pair of points measures the degree of difference in the species compositions contained within those samples. Widely separated points have very dissimilar infaunal communities, namely, few species in common, and differences in the abundance of those species that are common between the samples. In contrast, points that lie close to one another have communities where the abundance of individual species within the respective samples is very similar.

In addition, horizontal separations characterize a difference in species composition that fundamentally departs from differences in community composition along the vertical axis. Often, changes along the two axes coincide with different environmental gradients in the samples. For example, differences in water depth of the sample may account for the observed differences in community composition along the horizontal axis, while differences in grain-size or proximity to contaminant exposure may correlate with the sample separation along the vertical axis.

Inherent Sampling Variability

As with the other field measurements, it is crucial to determine the inherent sampling variability associated with the individual field measurements. Variability among repeated replicate grab samples collected from an individual station at a particular time lends insight into the inherent uncertainty of values reported for each station. This within-sample variability is fundamental for testing hypothesis concerning the significance of perceived differences between samples collected at different locations. If the inherent sampling variability is statistically larger than the observed difference between the two stations, then the spatial difference cannot be considered significant.

A dendrogram (tree diagram) produced from the multivariate species database provides a convenient graphical means for determining the relative magnitudes of within-site and between-

site infaunal variability among the samples (Figure 35 and Figure 36). Testing the relative degree of difference among the 99 individual samples indicates whether differences among replicates collected at a given site and time are smaller than the differences between the sites, indicating that spatial differences are large enough to be reliably resolved, even in the presence of inherent sampling uncertainty. Dendrograms display the relative similarity among samples, or groups of samples, using a branched diagram similar to the branches on a tree. Sample pairs that are similar coalesce into a branch toward the left on the percent-information-remaining axis (Figure 35). The horizontal information axis at the top of the dendrogram reflects the amount of information (variability) that is left in the sample-species matrix after two samples are combined. Combining samples with relatively similar species composition results in a minimal loss of information (variability) in the original species-sample matrix. As more samples, or other groups, are added to each branch, the differences in the communities associated with each group become increasingly larger, and combining these groups results in a more significant loss in the information.

The dendrogram demonstrates that the replicate grabs collected from an individual site contained communities that were usually more similar to one another, than to the communities present at adjacent stations. Individual replicates are color- and symbol-coded by site. Strong replicate groupings are particularly evident within the samples collected by the GSD in 2005 (Figure 36). They collected five replicate benthic grabs (designated R1 through R5) at six sites (GSDS1 through GSDS6). The relationship among these 30 samples is shown in the lower portion of the dendrogram. At four of the six sites, all five replicates collected at each station exhibited greater fidelity with each other, than with stations in very close proximity. Figure 19 on Page 30 shows that the GSD stations were located east of the Project area and, except for Station 1 (GSDS1), all were located in close proximity to the wastewater outfall. Even the difference between the infauna at Stations GSDS4 and GSDS5, which are only separated by a few decameters, could be distinguished among their replicate samples.

A statistical analysis of variance (ANOVA) in the multivariate dataset confirms that the within-station similarity of all the GSD replicate samples was far greater than expected by chance ($p < 0.003$). The p -value cited here, and throughout this section, is the probability that the measured difference between groups (sites) would have occurred by chance alone. It is determined by comparing the magnitude of the difference between sites, and the scatter in the replicate samples collected at a particular site. If the scatter in replicate samples is large compared to the difference in sites, then the site difference is more likely to be an artifact of chance alone, rather than a real spatial difference. Generally, differences in groups are considered statistically significant when p -values are less than 0.05, which corresponds to a 5 percent (1-in-20) probability that the difference occurred by chance alone. The observed infaunal differences among the six GSD sites are very unlikely (0.3 percent) to have occurred by chance.

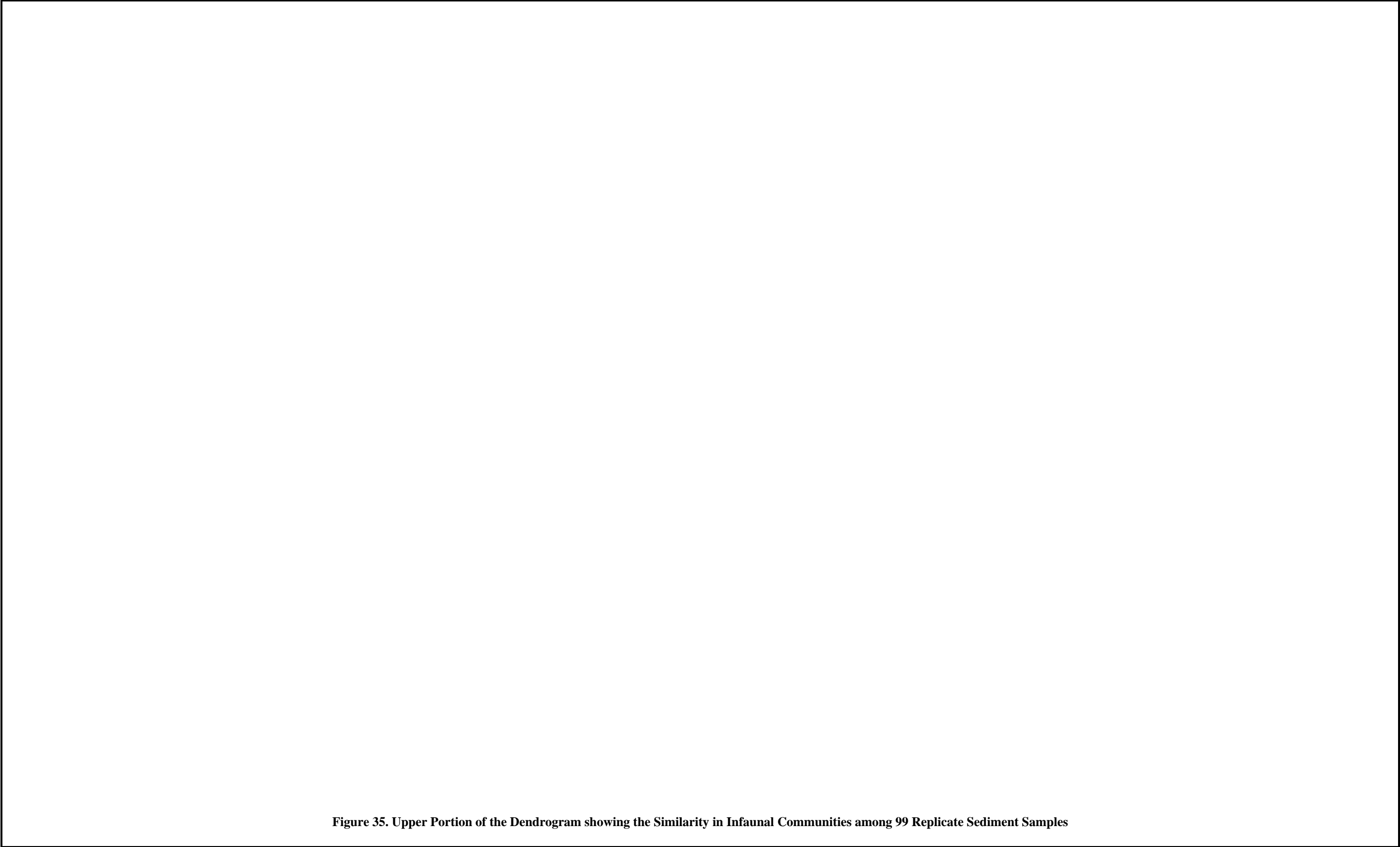


Figure 36. Lower Portion of the Dendrogram showing the Similarity in Infaunal Communities among 99 Replicate Sediment Samples

ANOVA is complicated to apply in multivariate hyperspace. Consequently, a Multi-Response Permutation Procedure (MRPP) (Mielke P. , 1984; Mielke & Bery, 2007) was also applied using PCOrd software (McCune & Grace, 2002) and a Sørensen (Bray-Curtis) distance measure (Sørensen, 1948). The chance-corrected within-site agreement was very high ($A=0.59$) for the analysis of the GSD replicates. If all the replicates from a particular site contained identical species, then the agreement would be perfect ($A=1$). An agreement of $A>0.3$ is considered high for most ecological datasets. The probability that the difference between each pair of GSD samples was due to chance was low for all pairs of samples ($p<0.0018$), although the probability for the difference between Stations GSD5 and GSD6 was slightly higher ($p=0.0026$). This finding is consistent with the dendrogram in Figure 36, which shows that some of the replicates from these two stations did not always cluster first with the other replicates from the same station.

Forty-two replicate benthic samples were also collected throughout the Project area in 1984 and 1985 as part of the Arco Coal Oil Point Project (Chambers Group, 1987). In the case of that survey, three replicate grab samples were collected at each station. Those samples, designated by the prefix "AR," are clustered near the top of the dendrogram in Figure 35. As in the case of the GSD samples, the Arco replicate samples generally exhibited the highest fidelity with other replicate samples from the same station. Not surprisingly, an MRPP applied to the entirety of the Arco data shows a very low likelihood ($p<0.001$) that the observed replicate clustering would occur by chance, especially considering the within-site agreement ($A=0.76$).

Grab samples from two sites, Stations Ar4S01 and Ar4S02, exhibited a reduced amount of fidelity with other replicate samples collected at the same site. Those samples were collected close to the outskirts of natural seeps west of the Project area (Figure 19 on Page 30). Slight differences in the location of the grabs relative to the seep, and strong gradients in the infauna surrounding the seep, probably resulted in larger-than-normal variability in the communities among those replicate samples. Three of the pair-wise comparisons that included those sites had high probabilities ($p>0.05$) that the observed differences were due to chance because of low within-site agreement ($A<0.2$).

The rest of the samples shown in the dendrogram in Figure 35 represent single grab samples collected at a particular site at a particular time. They are listed in dark blue and lend no insight into the within-station variability, although the dendrogram does indicate whether they have an affinity for any of the replicate samples from the Arco and GSD surveys, which they do not. This includes the 14 samples collected during the 2007 offshore marine-resource survey conducted as part of this EIR (Stations MRS01 through MRS06, and MRS11 through MRS14). They also include 13 samples collected as part of several regional studies conducted under the auspices of the Southern California Coastal Water Research Project (SCCWRP, 2008). Data from the MRS samples and these additional studies both cluster in the center of the dendrogram.

This analysis of replicate samples demonstrates that infaunal differences among the sites were generally larger than the within-site variability determined from replicate grabs. The statistical analyses indicate that spatial gradients or temporal trends identified in the infaunal communities within this database are likely to be reliably delineated, and are not due to random sampling error.

Temporal Changes

The benthic surveys included in the infaunal database span three decades, allowing the capture of large fluctuations in the infaunal community that occurred offshore the Ellwood coast. Specifically, multivariate analyses show that the infaunal community in the benthic samples collected as part of the Arco Coal Oil Point EIR in 1984 (Chambers Group, 1987) was significantly different from that of the GSD samples collected in 2005 (Aquatic Bioassay & Consulting Laboratories, Inc, 2007), and that both of these datasets differed from the samples collected in 2007 as part of the Ellwood Full Field EIR. However, these differences were not always apparent in the univariate statistics listed in Table 9. As described previously, the increased abundance in the GSD samples was due to a large recruitment event between 2003 and 2004, which resulted in higher-than-normal infaunal populations during 2005, when the GSD samples that were used in this analysis were collected. However, the difference between average diversity (H') in the GSD samples and other samples was no larger than what would be expected by chance alone ($p=0.42$). This would seem to suggest that the increase in abundance was unrelated to fundamental changes in the structure of the infaunal community; however, multivariate analysis demonstrated otherwise.

The dendrogram (Figure 35 and Figure 36) reflects profound differences in the infaunal communities among the three principal datasets. For example, all of the Arco samples clustered together except Station 5 (Ar4S05). All three replicates collected at that station, which was the shallowest Arco station and was located in the middle of the Coal Oil Point Seep area (Figure 19 on Page 30), had infaunal communities that were more similar to the communities found within the MRS samples than the other Arco samples. Except for the samples collected at that station, all of the Arco grab samples formed a cluster at the top of the dendrogram. The group of Arco samples coalesced with the group of non-GSD samples in the middle of the dendrogram, but only after 90 percent of the variability (information) in community structure had been explained by clustering within each of these two major sample groups. The last two branches to coalesce in the dendrogram were between this combined group and the group of GSD samples. Thus, the infaunal community within the GSD samples was least like any of the other sediment samples.

The ordination diagram (Figure 37) further quantifies the global differences in the community structure among these three major groups. The points characterize the community structure within a composite of all the replicate grab samples collected at an individual site at a particular time. The distance between points reflects the degree of dissimilarity in the community structure between the composite samples. Vertical separations reflect infaunal differences that are fundamentally different from horizontal separations, because the axes are 98.6 percent orthogonal (uncorrelated and unrelated). The horizontal axis represents 44.1 percent of the variability of the variability in the original 346-dimensional species hyperspace. The vertical axis represents an additional 34.5 percent and together, the two-dimensional ordination describes nearly 80 percent of the infaunal structure in the original database.

Figure 37. Ordination of Benthic Infaunal Samples

All ordinations conducted as part of this study, including the one shown in Figure 37, were based on a non-metric multidimensional scaling (NMS) (Mather, 1976; Kruskal, 1964) of Sørensen distance. This is the same distance metric that was used to measure infaunal dissimilarity in the dendrogram and the MRPP discussed above. The optimal solution was determined from 250 runs with random starting coordinates stepping down from six dimensions. The stress of the NMS result is an inverse measure of fit to the data. The two-dimensional solution was selected because it exhibited a marked reduction in stress from a one-dimensional solution (34.7) to the two-dimensional solution (13.9), but only modest reductions for subsequent dimensions (8.9, 7.1, 5.7, and 4.8, for three through six dimensions). 250 Monte Carlo randomization tests demonstrated that the probability that the stress associated with two-dimensional solution could have occurred by chance was less than 0.4 percent ($p < 0.004$). The stability of the optimal solution was determined from an examination of stress at each iteration, which stabilized at 40 iterations and exhibited little variation through the final, 60th iteration. This indicates that the solution's dimensionality was not too high, and that multiple, localized minima were not associated with the global stress minimum determined in the optimal solution.

The resulting ordination diagram (Figure 37) shows all of the GSD samples clustering tightly together along the vertical axis in a location that is well separated from most other samples, particularly the Arco and MRS samples, which separate along the horizontal axis. Because the separations among the three major groups occurred along different axes, they represent different infaunal trends. For example, the trend that distinguishes the Arco and MRS samples from one another along the horizontal axis is completely different from the trend reflected by the separation of the GSD samples along the vertical axis.

Additionally, in contrast to the GSD samples, the cloud of points associated with samples from the Arco and MRS surveys scattered over a much larger area of the diagram. This indicates that the infaunal variability among the samples within each of these two groups was much larger than the variability among the GSD samples. This is expected given that the GSD samples were separated by less than 1.5 km, while the Arco and MRS samples covered an along-shore distance of 15 km, and encompassed a much broader range in water depth and seep proximity.

Despite the scatter in the Arco and MRS points in the ordination diagram, each grouping was well resolved and quite independent of the other two major groups. This is demonstrated by an MRPP which showed a very high chance-corrected, within-group agreement ($A=0.49$). The probability that a similar degree of grouping would occur by chance was extremely low ($p < 0.00004$).

The wide separation in ordination space indicates that the infaunal communities collected in the three surveys were highly dissimilar. Indicator species analysis (Dufrêne & Legendre, 1977) identifies which taxa were primarily responsible for the observed differences. The 45,000 specimens collected in the three surveys were separated into 349 taxa. Many of these taxa were common to all surveys in comparable abundance, however, some were not. These indicator species differentiated the infaunal communities collected during the three surveys.

Table 10. Five most Indicative Taxa of the Three Major Benthic Surveys

GSD		Arco		MRS	
Taxon	IV	Taxon	IV	Taxon	IV
<i>Monticellina</i> spp.	98.4	<i>Glyceria capitata</i>	65.2	<i>Erichthonius brasiliensis</i>	50.6
<i>Chaetozone hedgpethi</i>	96.7	<i>Prionospio dubia</i>	62.2	<i>Byblis millsii</i>	40.4
<i>Polycirrus californicus</i>	95.5	<i>Paramage scutata</i>	50.7	<i>Tellina modesta</i>	31.5
<i>Petaloclymene pacifica</i>	94.8	<i>Gymnonereis crosslandi</i>	46.1	<i>Ampelisca cristata</i>	28.8
<i>Aphelochoeta petersenae</i>	90.0	<i>Amphiodia</i> spp.	45.6	<i>Eupolymnia heterobranchia</i>	28.0

Table 10 lists the five taxa that were most strongly associated with the samples from each of the three surveys. The indicator value (IV) can range from zero, indicating no relationship to the sample group, to 100, where the taxon has perfect fidelity within that group of samples. Group fidelity is determined both by the relative abundance of that taxon within the group, and by its frequency of occurrence in the samples of a particular group relative to the dataset as a whole. Perfect group fidelity occurs when a taxon only occurs within the samples of a particular group (100 percent relative abundance), and the taxon occurs within all the samples of that group (100 percent relative frequency). All of the IVs listed in Table 10 were higher than expected by chance alone ($p < 0.0026$), but the taxa indicative of the GSD survey were almost always present in high abundance in all of the GSD samples, while generally being absent from samples collected in the other surveys. As a result, they had much higher IV's.

The high fidelity of the polychaete worm, *Monticellina* spp., in the GSD samples is particularly noteworthy. Not only were unidentified specimens of the genus *Monticellina* near to being perfectly indicative of GSD samples (IV=98.4), but specimens of two of its identifiable species, *M. siblina* and *M. cryptica* also had extremely high IVs (>78). *Monticellina* populations exploded in 2004, and it were largely responsible for the markedly higher total infaunal populations observed in the GSD samples collected in 2004, 2005, and 2006 (Figure 33 on Page 56). In 2005, *Monticellina* species constituted 31 percent of all the organisms collected by the GSD (2006).

Although the cause of the extraordinarily high *Monticellina* recruitment in 2004 remains unknown, it was only partially responsible for the marked difference in the GSD samples identified in the ordination analysis. As shown in Table 10, there were a number of other taxa that were closely identified with the GSD samples. Had the 2004 recruitment of *Monticellina* been restricted to that taxon alone, then the Shannon diversity index (H') listed in Table 9 would have reflected the marked difference in the community structure in the GSD samples. Namely, an increased presence of *Monticellina* spp. relative to other taxa would have resulted in reduced diversity (H' and h), decreased evenness (J') and richness (d), and increased dominance (C' and C_{75}) in the GSD indices. In fact, the only indices that indicated a significant difference in the GSD indices that was consistent with an increased abundance of an isolated species was a decreased evenness and an increased dominance ($p<0.0001$).

The samples collected in other surveys did not have strong indicator taxa (IV<66). This suggests that the unusual character of the GSD samples was largely due to an increase in the GSD indicator taxa listed in Table 10, rather than a relative absence of taxa that were prevalent in the other surveys. The typical signature of environmental gradients is a more balanced change in taxa, with both increases in some taxa, and decreases in others. Consequently, the observed difference in the GSD samples was probably related to temporal changes in the infaunal community throughout the region, rather than a spatial gradient related to the location of the GSD samples in the eastern portion of the survey region.

In addition, the large observed difference in the infauna identified in the three surveys was not an artifact of changes in taxonomic identification of individual species over time. Taxonomists periodically reclassify and rename species to provide a better match to the taxonomic hierarchy as more information is gathered about the characteristics of a particular class of organisms. However, such reclassifications can be problematic for benthic environmental assessments when those assessments are based purely on temporal changes in the populations of individual species. For example, a change in the name of an important indicator species could be misinterpreted as a temporal change in the infaunal community. Such was not the case for the database analyzed in this study, however.

Typically, taxonomic reclassification involves changes in the name of a particular species within a particular genus. On rare occasions, entire genera are reclassified. Changes at the family level are even rarer. To evaluate whether taxonomic reclassification was responsible for the observed infaunal differences in the three major surveys, an ordination analysis was conducted on the dataset after aggregating taxa to family, or lower taxonomic levels. Although this results in a significant loss in taxonomic discrimination, it largely eliminates the influence of temporal artifacts introduced by taxonomic reclassification.

The ordination of taxonomic aggregates was almost identical to the ordination shown in Figure 37, although the variability represented by the ordination (78.7 percent) was slightly reduced by the loss in taxonomic discrimination from the original analysis (80 percent). The horizontal axis, which distinguishes between the Arco and MRS samples, only represented only 29.3 percent in the aggregate analysis, versus 44.1 percent in the ordination of the higher taxonomic levels. However, the vertical axis, which isolated the GSD samples, accounted for much more (49.3 percent) of the variability among major taxonomic groups than the original analysis (34.5 percent), probably because marginal distinctions among similar species, such as within the *Monticellina* genus, were lumped together. In any regard, the separation among the three groups of samples was well resolved. This was confirmed by an MRPP which showed a very high chance-corrected, within-group agreement ($A=0.43$) and an extremely low probability that a similar degree of grouping would occur by chance ($p < 0.00002$). The distinction between the MRS and GSD samples was less pronounced than the difference with Arco samples, probably because those two sample sets were collected within only a few years of one another.



Figure 38. Dendrogram Displaying the Relationship Among Infaunal Communities in Sediment Samples Collected from the Same Site on Four Different Occasions.

However, marked changes in community structure may have occurred in as little as one year. Arco Station 6 was sampled in 1984 (Ar4S06) and twice in 1985 (ArJS06 and ArAS06 in Table 3 on Page 31). The MRS survey revisited the same site in 2007 (MRS05 in Figure 19 on Page 30). An MRPP shows that the within-group agreement was high ($A=0.53$) and the observed differences in the communities among the four sampling occasions were not likely to have been due to chance alone ($p < 0.025$). Figure 38 shows that largest difference was between the MRS and Arco samples because they spanned the longest time period. In their analysis of the Arco samples, Chambers Group (1987) ascribed most of the difference between the 1984 and 1985 samples to an increase in two of the Arco indicator taxa (*Paramage scutata* and *Gymnonereis crosslandi*) listed in Table 10. However, more rigorous multivariate analysis shows that the increase in the populations of these polychaetes occurred between the two surveys in 1985, which were only one month apart, rather than between the 1984 and 1985 sampling. This indicates that short-term seasonal changes may be just as large as interannual differences. However, the change in the infaunal community that occurred at this location in the two decades between the MRS and Arco surveys overwhelmed both the seasonal and interannual changes observed in the Arco database. For instance, no *P. scutata* specimens were found in the MRS05 sample.



Environmental Factors

To focus attention on spatial rather than temporal differences in the infaunal communities, a multivariate analysis was performed on the subset of data consisting of the MRS samples. As discussed above, the infaunal community differed markedly among the data sets due to temporal variation, and combining them confounds the interpretation of any potential spatial gradients at a given time. Analysis of the MRS data provides a recent synoptic assessment of spatial variability throughout the study area.

The ordination joint plot shown in Figure 39 definitively divides the infaunal communities within the MRS samples into three groups that are delineated by environmental factors. The joint plot provides a visual interpretation of the differences in the infaunal communities found in the fourteen samples collected in 2007 as part of the marine-resource survey conducted for the Ellwood Full Field EIR. It simultaneously displays the infaunal differences (by the distances between sample points) and the environmental variables that are correlated with those differences (shown as arrows or vectors). The arrows point toward those samples most closely associated with particular environmental factors. An MRPP performed on the three groups

indicates that the within-group infaunal community agreement was high ($A=0.59$), with a very low likelihood that the groupings would have occurred randomly by chance alone ($p<0.004$).

Grain Size, Sorting, and Water Depth

The strongest difference in infaunal communities among the samples was differentiated along the vertical axis. The associated change in community structure represented by the differences along the vertical axis constituted a large proportion (90.6 percent) of the overall variability in the MRS infaunal dataset. Four interrelated environmental variables correlated with the distribution of two groups of samples along this axis. The communities found within deep offshore stations (05, 06, 15, and 16) and within the EMT (17 and 18) were all very similar. This group was typified by greater water depth, and a grain-size distribution with a high percentage of fines, a greater degree of sorting, and a reduced median grain size. Although Stations 17 and 18 contained infaunal communities that were similar to the stations located in water depths exceeding 50 m, those two stations were located in shallow water (18 m) within the EMT (Figure 19 on Page 30). Nevertheless, they had very poorly sorted sediments more typical of deep-water environments, and their infaunal communities were correspondingly similar. This suggests that the differences in infaunal community were better correlated with grain-size sorting than water depth. This is confirmed by the longer length of the sorting vector in Figure 39.

Figure 26 on Page 44 indicates why the EMT area, which is located comparatively close to shore, did not have coarser, better-sorted sediments like most of the other inshore stations. The increased fines found in that nearshore area probably result from the more quiescent, depositional conditions that prevail there due to the protection afforded by nearby Coal Oil Point. Regardless of the reason for the difference, the ordination shows that the infaunal community in that nearshore area was more closely affiliated with the community found in fine-grained sediments offshore. This supports the idea that the infaunal community is controlled more by sediment conditions, than by water depth or distance from shore.

The infaunal communities found at shallow nearshore stations (02, 11, and 12; Figure 26 on Page 44), and near seeps (Stations 01 and 14) were also very similar, and were diametrically opposed to the group of stations characterized by very poor grain-size sorting (Figure 39). This group had a higher median grain size and an attendant moderate sorting expected the effects of energetic reworking of surficial sediments from shoaling waves or the ejection of seep gasses (Table 7 on Page 42).

Statistical analysis of the joint plots confirms that grain-size sorting, rather than location or depth, provides the strongest correlation with differences in community structure between the two groups that separate along the vertical axis. A Mantel (1967) test measured the correlation between ecological distances, as represented by the ordination, and spatial distances, as represented by the difference in the location of the samples in UTM coordinates. If there was a strong relationship between the geodetic proximity of samples and their community structure, it would be evident in the Mantel test. Instead, a randomization (Monte Carlo) permutation found that the correlation between the spatial and infaunal distance matrices was almost non-existent (standard Mantel statistic= $r=-0.03$) and that the probability that such a correlation could occur by chance was high ($p=0.41$). Conversely, the correlation between sorting and the two groups along the vertical axis was high ($r=0.73$), with a low likelihood that the relationship occurred by chance ($p=0.001$).

Hydrocarbons

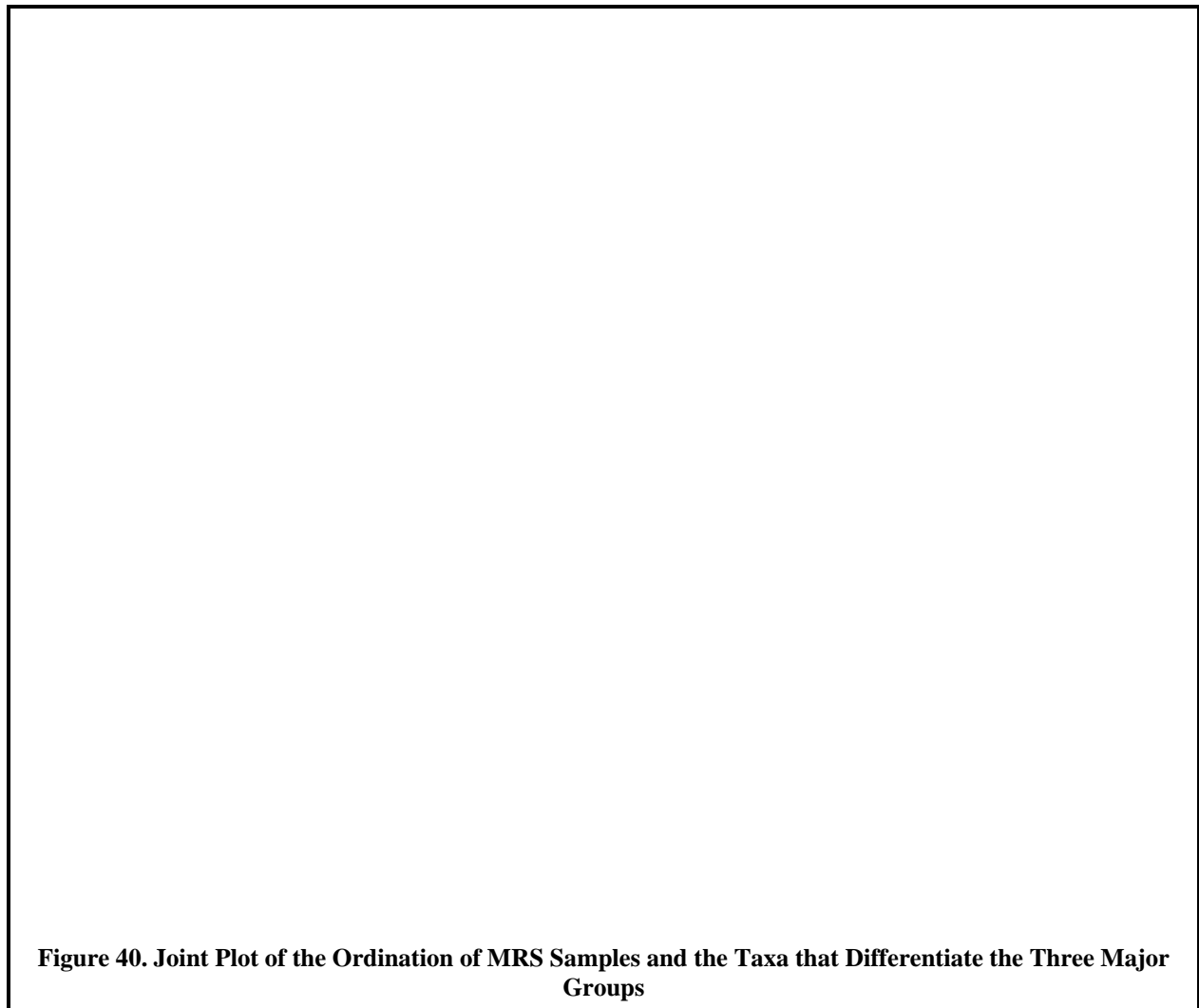
The infaunal community at the remaining stations (03, 04, and 13) was fundamentally different from that of the other stations. Moreover, although these samples represented only a small proportion (2.9 percent) of the overall variability, the difference in the community was completely independent (100 percent orthogonal) of the vertical variation in infauna along the vertical axis. Thus, the unusual character of the infaunal community within these samples was not associated with sediment properties or water depth. Instead, as indicated in the joint plot (Figure 39), the infauna at these stations were strongly correlated with increased concentrations of hydrocarbons (TPH; $r=0.23$; $p=.026$).

The relationship between TPH and infauna was unexpected. As discussed in Section 3.2.1, TPH concentrations were elevated throughout the study area, but the distribution of samples with slightly higher TPH concentrations bore no relationship to seep proximity. Stations 03 and 04 in particular, were far removed from the location of known seeps, yet they contained higher TPH concentrations than intervening stations located much closer to known seeps (Figure 31 on Page 48). This suggested that the dispersion of hydrocarbons was random, or that the observed difference in TPH concentrations among stations was potentially due to random sampling error. However, identifiable differences in the infauna at the three widely separated mid-depth stations provide independent confirmation that the elevated TPH concentrations within sediments were well resolved, and that they were responsible for the observed differences in the structure of the infaunal community. The processes that influenced the TPH distribution, and the associated differences in infaunal characteristics, are not readily apparent from the data collected in this study. However, the covariance in these disparate datasets demonstrates that the observed spatial variability in TPH does exist, and that it affects the marine biota.

The joint plot (Figure 39) also suggests that the infaunal community collected at Station 04 had attributes similar to both the hydrocarbon group and the fine-sediment group. However, including it in the fine-sediment grouping resulted in a slightly lower, within-group agreement (0.55) than the agreement (0.59) found with the grouping shown in the joint plot. Moreover, the sediments from Station 04 contained comparatively elevated hydrocarbon concentrations (Figure 31 on Page 48), suggesting that this station belongs in the hydrocarbon group with Stations 03 and 13, and to some extent Station 02.

Influential Taxa

The ordination analysis also reveals which taxa differentiate the infaunal communities within each of the three groups of stations. Figure 40 depicts how variation in the abundance of 26 individual taxa within the 14 individual samples correlates with the two ordination axes. As with the joint plot of environmental variables, the length of the taxon vectors is determined by the total (r^2) correlation, and the direction is determined by the relative strength of the correlation with each axis. Thus, the length of an arrow for an individual taxon reflects how strongly it participated in differentiating the samples among the three groups. The arrows point toward samples which have a comparatively elevated abundance of that taxon.



The taxa that differentiated the three MRS sample groups (Figure 40) were not the same as those that differentiated temporal changes in the infaunal communities among the entire dataset, which included the historical samples (Table 10 on Page 66). The 26 taxa shown in the joint plot were selected because they exhibited the largest overall correlations, with r^2 exceeding 0.5. Thus, out of the 206 taxa included in the ordination, the ones shown on the joint plot were most responsible for differentiating the infaunal communities among the three groups. Accordingly, they also usually had large, statistically significant ($p < 0.05$) indicator values. Statistically significant indicator values (IVs) for the group toward which a particular taxon's arrow points, are listed in parenthesis after that taxon's name.

In contrast to the other two station groupings, three of the six taxa associated with the fine-sediment station group shown at the bottom of the ordination diagram, did not have IVs listed, and those that did, had generally lower IVs than indicator taxa in other groups. This was because these taxa did not exhibit a high degree of fidelity with all the stations in the fine-sediment group. The diversity among the indicator taxa for this group is also reflected in the wider angular

spread of the arrows compared to arrows that point toward the other groups. Finally, the samples associated with this group were more widely distributed in the ordination diagram than the other two groups, indicating a greater infaunal dissimilarity among the samples of that group. The overall weaker taxonomic affiliation associated with this group probably arose because the samples were spread across a larger depth range where infaunal communities within samples 17 and 18, collected within the relatively shallow (<20 m) EMT loading zone, were grouped with samples collected near Platform Holly, with depths exceeding 50 m.

As with the data analyzed here, Maurer et al (1999) found that differences in infaunal assemblages throughout the Southern California Bight correlated with sediment grain-size properties and water depth. However, that study related the infaunal assemblages to trophic guilds distinguished by the feeding strategies used by the organisms. In contrast, the indicator taxa that differentiate the coarser and finer sediment infaunal assemblages in Figure 40 do not separate cleanly into the expected trophic guilds.

Finer offshore sediments often support burrowing deposit feeders while coarse-grained nearshore sediments tend to be populated by opportunistic filter feeders. However, of the six taxa that differentiated the finer sediment group, only the bamboo worm, *Maldane sarsi*, and the parchment tube worm, *Amphicteis scaphobranchiata*, are considered deposit feeders. Moreover, the increased presence of these worms in the fine sediment group maybe less related to their feeding strategy than to the fact that they live in tubes buried within the sediments (Nowell & Jumars, 1984). Thus, these worms were probably relatively absent from coarser-grained sediments because it is more difficult for the tubes to survive in harsher sedimentary environments that are constantly being mechanically reworked by oscillatory currents from shoaling surface gravity waves, and from energetic seep discharges. The four other species indicative of the fine-sediment group include the clamworms, *Gymnonereis crosslandi* and *Glycera nana*, which are both surface raptorial detritus feeders, phoronid horseshoe worms, which are tube-building suspension feeders, and the small carnivorous gammarid amphipod, *Heterophoxus affinis*.

The samples containing higher hydrocarbon concentrations were easily differentiated from the other two groups of samples by their unique infaunal community. Samples from the seep Stations 01 and 14 were not included in this group because they did not contain elevated hydrocarbon concentrations, and because their infauna were far more similar to samples containing coarser sediments, than to sediments containing elevated hydrocarbon concentrations. As discussed in Section 3.2.2, this lack of correlation between seep proximity and elevated hydrocarbon concentration is likely due to the patchy nature of the hydrocarbon distribution throughout the northern Santa Barbara Channel.

Insofar as the seep infaunal community, Spies & Davis (1979) found little difference between the infaunal community at the Isla Vista seep site and an adjacent nearshore site within the study area, although densities of organisms were higher at the seep sites. In a more recent broader evaluation of seeps within the study area, Steichen et al (1996) found that the density of nematodes was higher in seep sediments while all other major taxa were negatively correlated with hydrocarbon concentration. They ascribe the difference in the findings of these two seep studies to the difference in sampling scale. Steichen et al (1996) sampled localized, heavily oiled areas where infaunal densities were reduced by toxic effects. In contrast, Spies & Davis (1979)

sampled areas adjacent to areas with especially elevated hydrocarbons, where bacterial decomposition of hydrocarbons provided an organically enriched food source. Although Figure 40 shows that nematodes (nemata) were an indicator taxon of seep sites, as well as other coarser grain-size samples, they were not associated with the samples with elevated hydrocarbons.

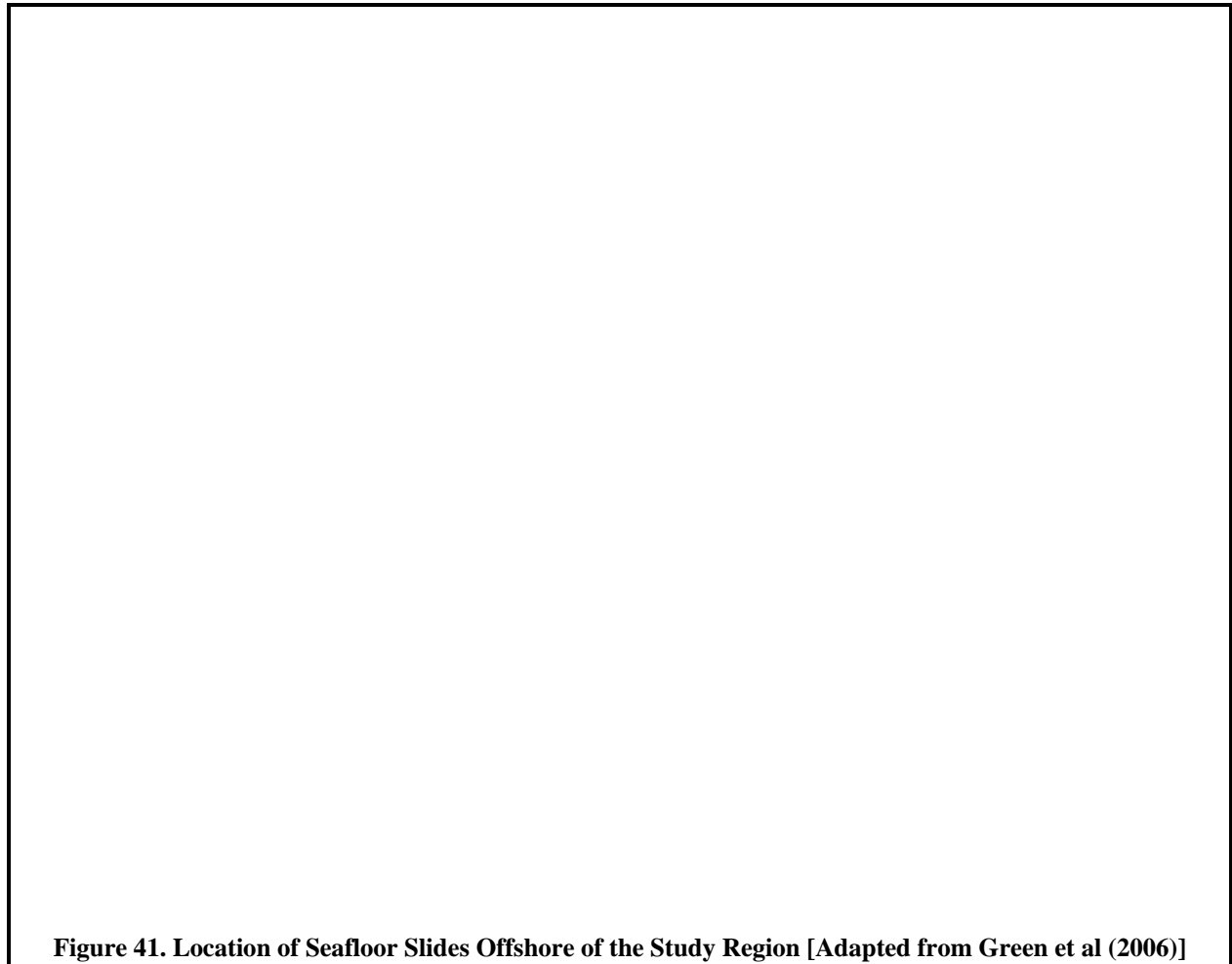
Levin et al (2000) summarized infaunal studies conducted in seep environments and identified taxa that are indicative of seep sites. Most of these taxa, such as *Capitella* sp., are pre-adapted to organic-rich, reducing environments. However, the taxa that differentiated the elevated hydrocarbon group in Figure 40 were neither seep taxa, nor were they particularly indicative of a disturbed environment. This suggests that it was the elevated hydrocarbon concentrations alone that distinguished the sediment communities at Station 03, 04, and 13, rather than any direct association with other unique aspects of seep environments, including mechanical disturbance or a reducing environment. Nevertheless, changes in infaunal communities after sustained exposure to elevated hydrocarbon concentrations are typical of environmental stressors in general (Gray, 1979). Namely, opportunistic, pollution-tolerant taxa, such as *Capitella* sp., increase in abundance at the expense of more sensitive species. Because none of the indicator taxa associated with the three elevated-hydrocarbon samples is considered to be particularly tolerant to pollution, hydrocarbon levels were probably only elevated enough to cause subtle, but still discernable changes in the infaunal communities within those samples.

4.0 SEAFLOOR FEATURES

The investigation of seafloor features was an important component of the marine-resource survey because such features can represent marine resources of cultural, biological, or geological (geohazard) significance. Because much of the seafloor in the vicinity of the Ellwood survey area is flat and covered by deep, soft sediments, the presence of an occasional hard-substrate feature, whether natural or man-made, is often accompanied by marked increases in populations of sensitive filter-feeding epifauna, finfish, and kelp. Moreover, most of the isolated seafloor features found in water depths greater than 15 m are of anthropogenic origin and, therefore, require some level of review to assess their cultural or archaeological significance.

Finally, the presence of geohazards, such as active seeps, folded rock features, or slope failures may require rerouting of seafloor pipelines, or, if widespread, preclude of their installation altogether. A variety of geohazards are known to occur in localized areas of the northern Santa Barbara Channel. For example, both seeps and reef features were observed in the high-resolution bathymetry collected as part of this survey. However, none of the identified features are so extensive that they would preclude installation of a cross-shore power line, or an alternative offshore pipeline to LFC.

Similarly, just offshore of the study area are the remnants of a major seafloor landslide known as the Goleta slide (Greene, et al., 2006). The headwall of this steep escarpment is located approximately 2 km from the alternative pipeline route, which is shown in blue in Figure 41. As such, it is probably too distant to represent a major geohazard that would preclude installation of seafloor lines as part of the proposed Project or its alternatives. Nevertheless, the high-resolution bathymetric surveys conducted by other investigators reveal cracks in the sediment propagating eastward along the slope from the Gaviota slide's headwall (Figure 41). These and other features



associated with the slides attest to the dynamic nature of the seafloor in the northern Santa Barbara Channel.

As part of the offshore marine-resource survey, seafloor features within the study area were identified and investigated with swath bathymetry, a fathometer, a magnetometer, and an ROV. Seafloor features of potential interest were identified from the bathymetric data. These data were screened and prioritized for their potential environmental significance. High priority targets were further investigated with a narrow-beam dual-frequency fathometer to further define the character and hardness of the targets. When warranted, ROV deployment was attempted, and the feature was directly examined with an imaging sonar, and was photodocumented with high-resolution still and video imagery. The magnetometer was deployed only during the bathymetric portion of the survey along the alternative pipeline corridor. No significant magnetic anomalies were identified in that record.

4.1 INVENTORY

The high-resolution bathymetric survey covered a 14 km² survey area (Figure 42). To maintain a consistent level of overlap, the distance between tracklines decreased with decreasing water depth. For water depths exceeding 20 m within the existing pipeline corridor, tracklines were run

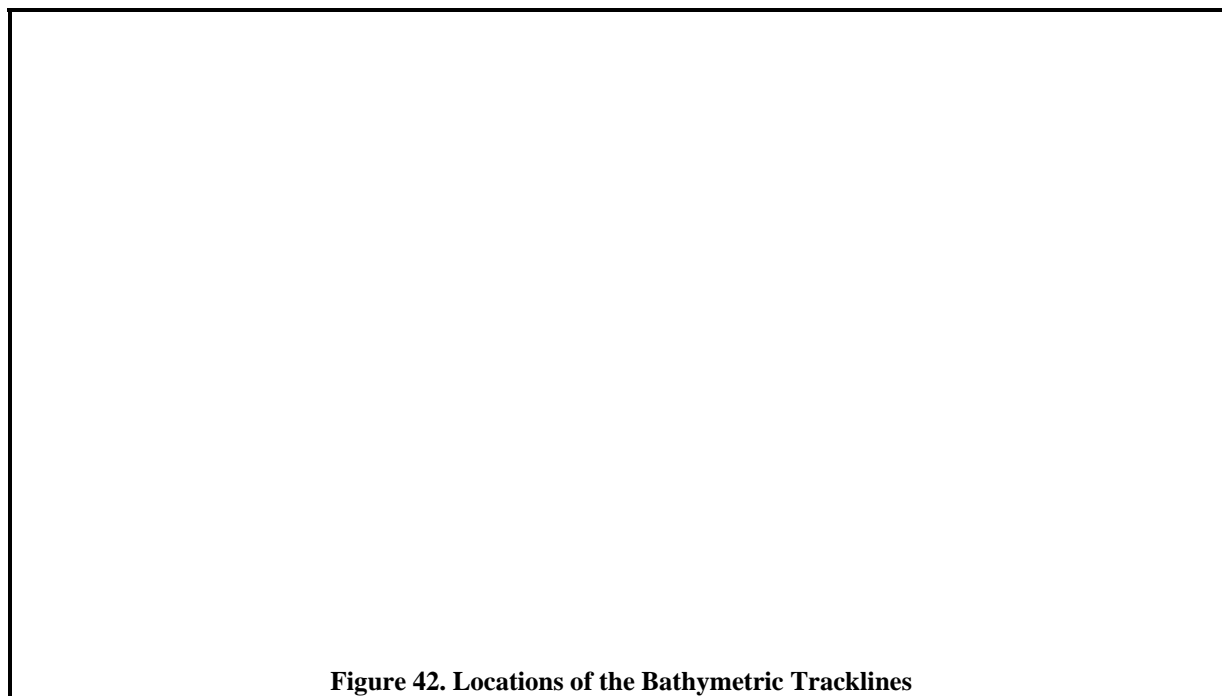


Figure 42. Locations of the Bathymetric Tracklines

perpendicular to the corridor. For shallower areas, tracklines paralleled isobaths and a tie-line was run along the transition zone to ensure uninterrupted seafloor coverage. Within the alternative pipeline corridor, tracklines were more widely spaced than within the existing corridor and the EMT loading zone. Consequently, data overlap was only approximately 50 percent along the alternative corridor, as opposed the nominal 100 percent overlap in the area of the proposed Project. Only some small nearshore areas within the northern portion of the existing pipeline corridor were not surveyed due the presence of dense canopies of kelp which would entangle equipment, impeding performance and negatively affecting data quality. In total, the 167 tracklines captured reliable bathymetric data along 211 km of linear tracklines. Depths ranged from 5 m to 75 m.

A comprehensive initial screening of all bathymetric data in its original full resolution format led to the identification of 592 localized acoustic signatures to be further screened in the analysis. The lateral dimensions of the features ranged in size from one meter to 510 m. The smallest features were generally found to be crab pots, while the largest features were associated with low-lying areas of rocky reef. Relief heights ranged from 0.5 m to 22 m, although the largest relief heights were artifacts of acoustic reflections from seep bubbles, kelp stands, or lines extending upward from abandoned crab pots. Twenty-five of the features were depressions, or seafloor scars.

Upon further evaluation of the 592 of the features, 42 percent were determined to be crab or lobster pots, or other fishing-related gear. Over 18 percent of the features were identified as other forms of anthropogenic debris of minimal significance because of their size or distance from areas of likely disturbance from the proposed Project. Of biological interest were the natural and artificial reefs that were associated with 6 percent of the features identified in the screening study. The remaining 11 percent of the acoustic targets were associated with known natural seep

discharges, and seafloor equipment, such as the EMT mooring gear and LFC produced-water outfalls.

4.2 ANTHROPOGENIC DEBRIS

As noted above, most of the seafloor features with small lateral dimensions that were identified in the bathymetric data were crab, lobster, or fish traps and pots. Of the 592 seafloor features of potential interest, 252 were determined to be seafloor traps. Many of these determinations were confirmed by visual observation of the surface buoys associated with such traps, and by observation of a line in the vicinity of the seafloor target, which was typically offset in the downstream direction by the prevailing flow field. For the most part, however, the determinations were made from the unique acoustic signature displayed by the traps and their associated retrieval lines.

Most of the traps identified in the bathymetric data were lost or abandoned, and no longer had the associated surface buoy that is used to mark and retrieve traps. Nevertheless, many had portions of the retrieval lines still attached to the traps, and the small amount of air in the lines often caused them to drift above the seafloor. Air is a strong acoustic reflector, and the lines appear as very narrow features (<1 m) extending well above the seafloor, but that are connected to a seafloor feature of slightly larger lateral dimension (1 m), namely, the trap. The large number of pots and traps observed in the study area attests to the intensity of the active crab and lobster fishery in the study area.

Another 107 small seafloor features were identified as discarded equipment, mechanical parts, pieces of pipe, lost cargo, and other debris of human origin. This material occurred randomly throughout the survey area, and was often distinctly linear or circular in shape, had small relief and limited lateral dimension (<5 m), and usually presented a strong acoustic reflection indicating hardness. Because of the small size and likely modern origin of this material, these targets were not thought to be of biological or cultural significance.

4.3 SEAFLOOR EQUIPMENT

Actively used seafloor equipment, pipelines, mooring gear, and outfalls comprised was another class of seafloor features identified in the bathymetric database. For example, the existing cross-shore pipelines near the LFC and EOF were delineated in the bathymetric data. Within the EMT, the bathymetric data delineated the configuration and location of the mooring gear and the crude-oil loading line used by the Barge *Jovalan* (Figure 43). This information helps with the assessment of potential impacts from the equipment's intended removal as part of the proposed Project. Specifically, the length and orientation of each mooring's anchor chain, and the location of the anchor can be gauged relative to their proximity to Shane Seep, and the nearshore rock reef that lies shoreward of Mooring #4.

4.4 NATURAL AND ARTIFICIAL REEFS

The character, location, and extent of rocky reef habitat were also delineated as part of the seafloor survey. Rocky reef habitats are important because, in shallow water, they support sensitive kelp beds, while in deep water, they provide a comparatively uncommon substrate for epifaunal organisms to thrive on. Although the 37 reef structures identified in the survey did not

account for a large proportion of the overall number of identified seafloor features, the area covered by these features was significantly larger than the amount of seafloor covered by other seafloor features. There were three major areas of where natural rock outcrops were observed in the bathymetric data. One set was located in very shallow water (<10 m) in the eastern portion of the EMT loading zone (Figure 43). This reef complex is located offshore of Sands Beach near the mouth of the Devereux Slough on the western side of Coal Oil Point. Aerial photographs document only limited amounts of patchily distributed kelp attached to the hard-substrate features delineated by the multibeam survey data. However, larger stands of kelp exist immediately to the southeast, closer to Coal Oil Point.



Figure 43. Swath Bathymetric Images of a) the Locations of Seafloor Features within the EMT Mooring Area, and b) the Acoustic Signature of the Shane Seep

An area of exposed rocky substrate in deep water (65 m) was identified along an alternative offshore pipeline route (Figure 44). However, its presence does not preclude installation of an offshore pipeline for several reasons. First, the reef structure was patchy, and the image shows that the two major outcrop areas captured in the bathymetric survey did not extend all the way across the swath of seafloor that was surveyed. Thus, if need be, a pipeline could conceivably be routed around the reef areas. Second, an entirely different corridor for the alternative offshore pipeline route could be selected that obviates the need for localized rerouting around this particular structure. The survey along the selected corridor was performed to see if there were any widespread environmental impediments to an offshore pipeline alternative. This particular route was selected because it coincided with the route proposed as part of the Arco Coal Oil Point Project (Chambers Group, 1987). Third, the vertical extent of the rocky outcrops at this location were generally limited to less than 2 m. Deep water, low-relief, rocky reefs tend to support epifauna that are more tolerant to turbidity and mechanical disturbance than organisms residing on high-relief structures (Hardin, Toal, Parr, Wilde, & Dorsey, 1994). Consequently, pipelaying activities in the vicinity of these reefs would be of a reduced concern from a marine resource standpoint.



Figure 44. Multibeam Image of Offshore Rocky Reef Structure along the Alternative Pipeline Corridor



Figure 45. Pier Debris Adjacent to the Pipeline Landing near the EOF



Figure 46. Kelp Stands Associated with Pier Debris Adjacent to the Pipeline Landing near the EOF

The third natural reef area identified during the field survey was located along the shoreline just east of the present pipeline landing area near the EOF. This is an area where an extensive complex of artificial reefs were created by the debris left after old oil piers were demolished (Figure 45). However, the natural reef, a portion of which is apparent in the lower right of the bathymetric image, extended beyond the offshore reach of the historical piers. Although low in elevation and close to shore, this natural reef complex supports substantial kelp stands as seen in an aerial photograph (Figure 46). This natural reef complex extends westward in water depths between 10 m and 15 m and consists of a low rock shelf that is generally less than 1 m in elevation.

The localized, artificial reef complexes and associated kelp stands near the EOF landing were produced by the remnants of numerous oil piers that lined this section of coast during the early 20th century. The origins of this artificial reef complex are apparent from the close correspondence between the high-resolution bathymetric image, the locations of the piers in the NOAA obstructions database, and the pier shapes and locations in a historic photographs of the area (Figure 45). Finally, the distribution of kelp seen in aerial imagery closely matches the pier shapes and locations (Figure 46).

4.5 SEEPS

The study area is within a prolific region of natural hydrocarbon seeps and some of these seeps are apparent in the bathymetric dataset (Figure 47). The most intense seepage is distributed along

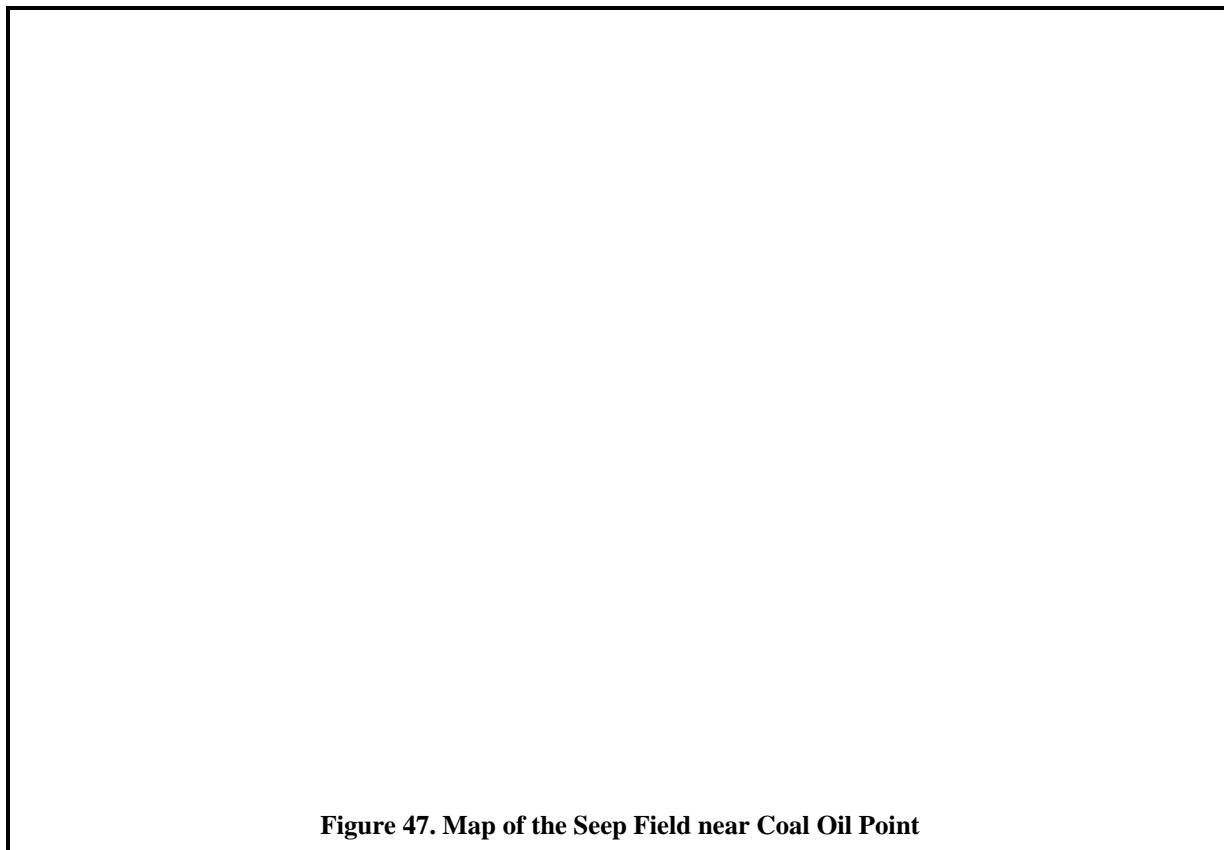


Figure 47. Map of the Seep Field near Coal Oil Point

the axes of three major, faulted anticlines. The Holoil and Sea Dog Seeps are located near the existing pipeline route between Platform Holly and the EOF. In addition, one well-studied seep, the Shane Seep, is located within the offshore EMT mooring area, and has been active since 1960 (Figure 43b on Page 78). It lies in a water depth of 22 m where strong upwelling flows of 0.3 m/s are driven by the rising seep bubbles. Because of the high acoustic reflectivity of gas bubbles, the rising plume from the seep is readily apparent in the bathymetric imagery.

5.0 BIBLIOGRAPHY

- Ackerman, R., Bergmann, M., & Schleichert, G. (1983). Monitoring heavy metals in coastal and estuarine sediments – a question of grain size: < 20µm versus < 60 µm. *Environmental Technology Letters* , 4, 317-328.
- Aquatic Bioassay & Consulting Laboratories, Inc. (2007). *Goleta Sanitary District 2006 Annual Monitoring Report*.
- Aquatic Bioassay & Consulting Laboratories, Inc. (2006). *Goleta Sanitary District 2005 Annual Monitoring Report*.
- Auad, G., & Henderschott, M. (1997). The low-frequency transport in the Santa Barbara Channel: description and forcing. *Continental Shelf Research* , 17 (7), 779- 802.
- Auad, G., Hendershott, M., & Winant, C. (1999). Mass and heat balances in the Santa Barbara Channel: estimation, description and forcing. *Progress in Oceanography* , 43 (1), 111-155.
- Beckenbach, E. H. (2004). Surface Circulation in the Santa Barbara Channel: An Application of High Frequency Radar for Descriptive Physical Oceanography in the Coastal Zone. *A Dissertation submitted in partial satisfaction of the requirements for the degree Doctor of Philosophy in Marine Science* . University of California Santa Barbara.
- Breaker, L. W. (2003). A curious relationship between the winds and currents at the western entrance of the Santa Barbara Channel. *Journal of Geophysical Research* , 108 (C5), 3132.
- Chambers Group. (1987). *EIR/EIS Proposed Arco Coal Oil Point Project*. Prepared for California State Lands Commission, Santa Barbara County, U.S. Army corps of Engineers Los Angeles District.
- Coats, D., Imamura, E., Fukuyama, A., Skalski, J., Kimura, S., & Steinbeck, J. (1999). *Monitoring of Biological Recovery of Prince William Sound Intertidal Sites Impacted by the Exxon Valdez Oil Spill: 1997 Biological Monitoring Survey*. NOAA Hazardous Materials Response and Assessment Division, 7600 Sand Point Way NE, Seattle, WA 98115. Edited By: G. Shigenaka, R. Hoff, and A. Mearns.
- Cudaback, C., Washburn, L., & Dever, E. (2005). Subtidal inner-shelf circulation near Point Conception, California. *J. Geophys. Res* , 110 (C10), C10007.

- Dever, E., & Winant, C. (2002). The evolution and depth structure of shelf and slope temperatures and velocities during the 1987-1998 El Niño near Pt. Conception, California. *Progress in Oceanography*, 54, 77-103.
- Dever, E., Hendershott, M., & Winant, C. (1998). Statistical Aspects of Surface Drifter Observations of Circulation in the Santa Barbara Channel. *Journal of Geophysical Research-Oceans*, 103 (C11), 24781-24797.
- Dever, E., Johnson, W. R., Wang, D.-P., Winant, C., & Oey, L.-Y. (2004). A Model of the Near-Surface Circulation of the Santa Barbara Channel: Comparison with Observations and Dynamical Interpretations. *Journal of Physical Oceanography*, 34 (1), 23-43.
- Dorman, C., & Winant, C. (2000). The Structure and Variability of the Marine Atmosphere around the Santa Barbara Channel. *Monthly Weather Review*, 128, 261-282.
- Dossis, P., & Warren, L. (1980). Distribution of heavy metals between the minerals and organic debris in a contaminated marine sediment. In R. Baker (Ed.), *Contaminants and Sediments, Vol. 1: Fate and transport, case studies, modeling toxicity* (pp. 119-139). Ann Arbor, Michigan: Ann Arbor Science.
- Dufrêne, M., & Legendre, P. (1977). Species assemblages and indicator species: the need for a flexible asymmetrical approach. *Ecological Monographs*, 67, 345-366.
- Folk, R. (1980). *Petrology of Sedimentary Rocks*. Austin, TX: Herpmill Publishing Co.
- Goodman, E. (1975). The theory of diversity-stability relationships in ecology. *Q. Rev. Biol.*, 50, 237-266.
- Gray, J. (1979). Pollution-induced changes in populations. *Phil. Trans. R. Soc. Lond.*, 286, 545-561.
- Green, R. (1979). *Sampling design and statistical methods for environmental biologists*. New York, NY: John Wiley & Sons, Inc.
- Greene, H., Murai, L., Watts, P., Maher, N., Fisher, M., Paull, C., et al. (2006). Submarine landslides in the Santa Barbara Channel as potential tsunami sources. *Natural Hazards and Earth System Sciences*, 6 (1), 63-88.
- Hardin, D. D., Toal, J., Parr, T., Wilde, P., & Dorsey, K. (1994). Spatial variation in hard-bottom epifauna in the Santa Maria Basin, California: the importance of physical factors. *Marine Environmental Research*, 37 (2), 165-193.
- Harms, S., & Winant, C. (1998). Characteristic patterns of the circulation in the Santa Barbara Channel. *Journal of geophysical research*, 103 (C2), 3041-3065.
- Hendershott, M., & Winant, C. (1996). The circulation of the Santa Barbara Channel. *Oceanography*, 9 (2), 114-121.
- Horowitz, A., & Elick, K. (1987). The relation of stream sediment surface area, grain size, and trace element chemistry. *Applied Geochemistry*, 2, 437-445.
- Hostettler, F. (2007, May). *Tar Balls Washed Onto Central California Beaches by Storms*. (U. S. Department of the Interior, U.S. Geological Survey) Retrieved February 17, 2008,

- from Sound Waves Montly Newsletter: Coastal Science & Research News from Across the USGS: <http://soundwaves.usgs.gov/2007/05/research2.html>
- Hostettler, F., Rosenbauer, R., Lorenson, T., & Dougherty, J. (2004). Geochemical characterization of tarbells along the California coast, part I - Shallow seepage impacting the Santa Barbara Channel Islands, Santa Cruz, Santa Rosa, and San Miguel. *Organic Geochemistry* , 35 (6), 725-746.
- Kruskal, J. (1964). Non-metric multidimensional scaling: a numerical method. *Psychoenetrিকা* , 29, 1-27.
- Leifer, I., Boles, J., Luyendyk, B., & Clark, J. (2004). Transient discharges from marine hydrocarbon seeps: spatial and temporal variability. *Environmental Geology* , 46, 1038-1052.
- Leifer, I., Clark, J., & Chen, R. (2000). Modifications of the local environment by a natural marine hydrocarbon seep. *Geophys. Res. Lett* , 27, 3711-3714.
- Levin, L., James, D., Martin, C., Rathburn, A., Harris, L., & Michener, R. (2000). Do methane seeps support distinct macrofaunal assemblages? Observations on community structure and nutrition from the northern California slope and shelf. *Mar. Ecol. Progr. Ser.* , 208, 21-39.
- Magurran, A. (1988). *Ecological diversity and its measurement*. Cambridge: University Press.
- Mantel, N. (1967). The detection of disease clustering and a generalized regression approach. *Cancer Research* , 27, 209-220.
- Margalef, R. (1951). Diversidad de especies en las comunidades naturales. *Publ. Inst. Biol. Aplic.* , 9, 5-27.
- Margalef, R. (1972). Homage to Evelyn Hutchinson, or why is there an upper limit to diversity. *Trans. Connect. Acad. Arts Sci.* , 44, 211-235.
- Marine Research Specialists. (1998). *ity of Morro Bay and Cayucos Sanitary District, Offshore Monitoring and Reporting Program, Semiannual Benthic Sampling, October 1997*. Prepared for the City of Morro Bay, Morro Bay, CA.
- Marine Research Specialists. (2007). *Offshore Monitoring and Reporting Program, 2006 Annual Report, Prepared for the City of Morro Bay and Cayucos Sanitary District, February 2004*. Morro Bay, California.
- Mather, P. (1976). *Computational Methods of Multivariate Analysis in Physical Geography*. London: J. Wiley and Sons.
- Maurer, D., Nguyen, H., Robertson, G., & Gerlinger, T. (1999). The Infaunal Trophic Index (ITI): Its Suitability For Marine Environmental Monitoring. *Ecological Applications* , 9 (2), 699-713.
- McCune, B., & Grace, J. (2002). *Analysis of Ecological Communities*. Gleneden Beach, OR: MjM Software Design.

- Mielke, P. (1984). Meteorological applications of permutation techniques based on distance functions. In P. Krishnaiah, & P. Sen (Eds.), *Handbook of statistics* (Vol. 4, pp. 813-830). The Hague, The Netherlands: Elsevier Science.
- Mielke, P. W., & Bery, K. J. (2007). *Permutation methods: a distance function approach* (2nd ed.). New York: Springer-Verlag.
- Nowell, A., & Jumars, P. (1984). Flow environments of aquatic benthos. *Ann. Rev. Ecol. Syst.*, 15, 303-328.
- Oey, L., Wang, D., Hayward, T., Winant, C., & Hendershott, M. (2001). "Upwelling" and "cyclonic" regimes of the near-surface circulation in the Santa Barbara Channel. *Journal of Geophysical Research-Oceans*, 106 (C5), 9213-9222.
- Pielou, E. (1977). *Mathematical ecology*. New York, NY: John Wiley and Sons.
- Plumb, R. J. (1981). *Procedures for handling and chemical analysis of sediment and water samples*. Vicksburg, Miss.: U.S. Army Corps of Engineer Waterway Experiment Stations.
- Quigley, D., Hornafius, J., Luyendyk, B., Francis, R., Clark, J., & Washburn, L. (1999). Decrease in Natural Marine Hydrocarbon Seepage Near Coal Oil Point, California, Associated with Offshore Oil Production. *Geology*, 27 (11), 1047-1050.
- SCBPPFCT. (1995). *Field Operation Manual for Marine Water-Column, Benthic, and Trawl monitoring in Southern California. August 22, 1995*. Southern California Bight Pilot Project Field Coordination Team.
- SCCWRP. (2008). *The Southern California Coastal Water Research Project*. Retrieved from <http://www.sccwrp.org/>
- Sea-Bird Electronics, Inc. (1993). *SBE 13/22/23/30 Dissolved Oxygen Sensor Calibration and Deployment. Application Note No. 13-1, rev B, Revised April 1993*.
- Sea-Bird Electronics, Inc. (1989). *Calculation of M and B Coefficients for the Sea-Tech Transmissometer. Application Note No. 7, Revised September 1989*.
- Shannon, C., & Weaver, W. (1949). *The mathematical theory of communication*. Urbana, IL: Univ. of Illinois Press.
- Simpson, E. (1949). Measurement of diversity. *Nature*, 163, 688.
- Smith, W., Gibson, V., Brown-Leger, L., & Grassle, J. (1979). Diversity as an indicator of pollution: cautionary results from microcosm experiments. In J. F. Grassle, G. Patil, W. Smith, & C. Tallie (Eds.), *Ecological diversity in theory and practice* (pp. 269-277). Fairland, MD: International Cooperative Publishing House.
- Snelgrove, P., & Butman, C. (1994). Animal-Sediment Relationships Revisited: Cause Versus Effect. *Oceanography and Marine Biology: an Annual Review*, 32, 111-177.
- Sørensen, T. (1948). A method of establishing groups of equal amplitude in plant sociology based on similarity of species content. *Biologiske Skrifter*, 5, 1-34.

- Spies, R., & Davis, P. (1979). The infaunal benthos of a natural oil seep in the Santa Barbara Channel. *Mar. Biol.* , 50, 227—237.
- State Water Resources Control Board. (2006). *2005 California Ocean Plan, Water Quality Control Plan Ocean Waters of California Effective February 14th, 2006*.
- Steichen, D. J., Holbrook, S., & Osenberg, C. (1996). Distribution and abundance of benthic and demersal macrofauna within a natural hydrocarbon seep. *Marine Ecology Progress Series* , 138, 71-82.
- Swartz, R., Schultz, D., Ditsworth, G., DeBen, W., & Cole, F. (1985). Sediment toxicity, contamination, and macrobenthic communities near a large sewage outfall. In T. Boyle (Ed.), *Validation and Predictability of Laboratory Methods for Assessing the Fate and Effects of Contaminants in Aquatic Ecosystems* (pp. 152-175). Philadelphia, PA: American Society for Testing and Materials.
- U.S. Environmental Protection Agency. (1987). *Recommended Biological Indices for 301(h) Monitoring Programs*.
- Washington, H. (1984). Diversity, biotic and similarity indices. A review with special relevance to aquatic ecosystems. *Water Res.* , 18, 653-694.
- Wittaker, R. (1965). Dominance and diversity in land plant communities. *Science* , 147, 250-260.